2021-06-28

# Esterification of Octanoic Acid over Solid Acid Catalysts Derived from Petroleum Coke

Schemberger Schafranski, Annelisa

UNIVERSITY OF CALGARY

# Esterification of Octanoic Acid over Solid Acid Catalysts Derived from Petroleum Coke

by

Annelisa Schemberger Schafranski

A THESIS

SUBMITTED TO THE FACULTY OF GRADUATE STUDIES

IN PARTIAL FULFILMENT OF THE REQUIREMENTS FOR THE

DEGREE OF MASTER OF SCIENCE

GRADUATE PROGRAM IN CHEMICAL ENGINEERING

CALGARY, ALBERTA

JUNE, 2021

ABSTRACT

Petroleum coke (petcoke) is a solid waste of the oil industry, with limited use due to its high sulfur content (> 6.5 wt%) and other impurities. As a carbon-rich, abundant and inexpensive material, petcoke is a potential resource for carbon-based catalysts. Esterification is a broad, important class of reactions for which carbon-based catalysts have been investigated and applied successfully. The treatment of petcoke (functionalization) with different conditions of temperature, time, and types of acid incorporates surface groups, which are the active sites for the reaction.

This study tested the catalytic performance of acid-modified petcoke samples over a model reaction: esterification of octanoic acid with methanol. A commercial catalyst, Amberlyst-15, was used for comparison. The effect of various parameters was evaluated, including stirring speed (200 - 800 rpm), temperature (40 - 80 °C), catalyst loading (1 - 4.5 wt%), and methanol-to-acid molar ratio (40:1 - 10:1). The selectivity of all catalysts was 100% towards the ester yield, with no byproducts from the reaction.

The method for the evaluation of catalyst activities was based on kinetic parameters and turnover frequency. The catalytic activity of acidic petcoke samples was comparable to the commercial catalyst in terms of conversion with time at the same reaction conditions, and even higher on a per acid site basis. Based on those results, acid-modified petcoke is a prospective material for catalyzing esterification reactions.

Different properties arise from the treatment of petcoke with strong acids. The number of strong acid sites, overall acid strength as well as the surface hydrophobicity all influence the catalytic performance for the esterification reaction. Leaching of active sites was problematic and resulted in almost complete deactivation of the petcoke-derived catalysts. An appropriate balance in the

surface hydrophobicity/hydrophilicity and a strong attachment of the active sites to the petcoke surface are required for stability.

ACKNOWLEDGEMENTS

First and foremost, I would like to thank God Almighty, without whom nothing is possible.

I owe my deepest gratitude to my supervisor Dr. Josephine M. Hill, for the unique opportunity of joining her research group. I am grateful for her patience, encouragement, and guidance throughout my learning process. Her continuous optimism and meaningful assistance were crucial for me to make such progress. Without them, this research and thesis may not have been completed. I would like to acknowledge the Natural Sciences and Engineering Research Council (NSERC) for operating funds for my research project as well.

I would also like to thank the examination committee members: Dr. Hector De La Hoz Siegler and Dr. Jinguang Hu, for dedicating their time and expertise to this important step of my graduate program. Thanks to Suha Abusalim and Arthur de Vera for helping me with administrative matters and the Department of Chemical & Petroleum Engineering for the provided support. Moreover, I am thankful to Dr. Éverton F. Zanoelo from the Federal University of Parana (Brazil), P.Eng. Gustavo Nunes and P.Eng. Braz M. Zanutto from Petrobras (Brazil) for believing in my work and supporting my application for the University of Calgary.

I am thankful to have worked and learned from all the current and past members of the Laboratory for Environmental Catalytic Applications (LECA): Dr. Ingrid Motta, Dr. Jingfeng Wu, Dr. Senthil Venkatesan, Dr. Tiago Coelho, Dr. Ye Xiao, Ahmed Abdelaziz, Ana Carlotto, Javier Mora, Robert Levi Pryde, Sip Chen Liew, Yoni Nederstigt; special thanks to Dr. Francisco Javier Lopez Tenllado for his contribution in several steps of my research, and Dr. Qing Huang for her cooperation on providing materials for this research to happen.

I am so grateful for my family. My parents have always been the best example of kindness and perseverance throughout my life. Thank you for giving me the opportunities and experiences that have made me who I am and for giving me the strength to follow my dreams, even if that meant living far from home in another country. Thanks to my sister for always being there for me as a bosom friend. I would also like to extend my gratitude to my friends and relatives, who helped me in many treasured ways. I cannot list all the names here, but you are always on my mind.

Finally, to my loving husband, Vitor. Thank you for always being by my side, supporting my decisions, encouraging me to pursue my goals, and making the journey easier. His patience, love, and care were essential when I doubted myself during these two years of research challenges and many uncertainties regarding our lives. I cannot thank you enough, as this achievement would not be possible without you.

# DEDICATION

*This thesis is dedicated to Vitor, the most supportive and loving husband.*

TABLE OF CONTENTS

LIST OF TABLES

LIST OF FIGURES AND ILLUSTRATIONS

LIST OF SYMBOLS, ABBREVIATIONS, AND NOMENCLATURE

| Acronym | Definition |
|---|---|
| $B^+$ | Brønsted acid sites |
| DBT | Dibenzothiophene |
| GC–FID | Gas Chromatography with a Flame Ionization Detector |
| $L^+$ | Lewis acid sites |
| PC | Petcoke, petroleum coke |
| PTFE | Polytetrafluoroethylene |
| rpm | Rotations per minute |
| TPA | 12-Tungstophosphoric acid |
| TOF | Turnover frequency |
| XPS | X-ray photoelectron spectroscopy |

| Symbol | Definition |
|---|---|
| $A$ | Pre-exponential factor ($min^{-1}$) |
| $A_i$ | Peak area of analyte |
| $A_{st}$ | Peak area of internal standard |
| $C_{A0}$ | Initial concentration of octanoic acid (mmol/mL) |
| $CC$ | Calibration curve |
| $C_i$ | Concentration of reagent, product, or solute in solution (mol/mL) |
| $C_{NaOH}$ | Molarity of titer (mmol/mL) |
| $D_{AB}$ | Diffusivity of the limiting reactant in the solvent ($m^2/s$) |
| $D_{eff}$ | Effective diffusivity inside the catalyst particle ($m^2/s$) |
| $d_p$ | Diameter of catalyst particle (m) |
| $E_a$ | Apparent activation energy of reaction (J/mol·K) |
| $g$ | Gravitational acceleration ($m/s^2$) |
| $[H^+]$ | Strong acidity of the catalyst (mmol/g) |
| $k$ | Pseudo-first-order rate constant ($min^{-1}$) |
| $k_c$ | Mass transfer coefficient (m/s) |
| $K_e$ | Equilibrium constant |
| $k_i$ | Rate constant of forward or reverse reaction ($min^{-1}$) |
| $m_c$ | Mass of catalyst (g) |
| $m_{c,eq}$ | Equivalent mass of catalyst for titration (g) |
| $m_E$ | Mass of ester, actual or theoretical (g) |
| $m_i$ | Mass of analyte in solution (g) |
| $MR$ | Mears criterion |
| $m_{st}$ | Mass of internal standard in solution (g) |
| $n$ | Number of samples |
| $N_A$ | Number of moles of octanoic acid (mol) |
| $N_{A0}$ | Initial number of moles of octanoic acid (mol) |
| $N_E$ | Amount of ester produced (mmol) |
| $N_{SC}$ | Schmidt number |
| $R$ | Universal gas constant (8.314 J/mol·K) |
| $R^2$ | Coefficient of determination |

| | |
|---|---|
| $-r_A$ | Reaction rate per unit volume (mol/mL·min) |
| $-r'_A$ | Reaction rate per unit mass of catalyst (mol/g-cat·s) |
| $-r''_A$ | Reaction rate per area of catalyst surface (mol/m$^2$·s) |
| $R_f$ | Response factor of GC |
| $r_p$ | Radius of catalyst particle (m) |
| $-r_s$ | Reaction rate on the catalyst surface |
| $s$ | Sample standard deviation |
| $S$ | Selectivity (%) |
| $T$ | Temperature (K) |
| $t$ | Time (s, min, or h) |
| $U$ | Superficial velocity of the fluid |
| $V$ | Volume of the reaction solution (mL) |
| $V_i$ | Molar volume of component i at normal boiling point (m$^3$/kmol) |
| $V_{NaOH}$ | Volume of sodium hydroxide solution (mL) |
| $WP$ | Weisz-Prater criterion |
| $x$ | Conversion of octanoic acid (%) |
| $\bar{X}$ | Mean value |
| $x_e$ | Equilibrium conversion of limiting reagent |
| $X_i$ | Sample value |
| $Y$ | Ester yield (%) |
| $\Delta G_f^o$ | Gibbs free energy of formation (J/mol) |
| $\Delta G_r^o$ | Gibbs free energy of reaction (J/mol) |
| $\Delta H_f^o$ | Standard enthalpy of formation (J/mol) |
| $\Delta H_r^o$ | Standard enthalpy of reaction (J/mol) |
| $\Delta H_{vap,i}$ | Enthalpy of vaporization of component i at normal boiling point (J/kmol) |
| $\Delta\rho$ | Absolute differential density of catalyst and solution (kg/m$^3$) |
| $\eta$ | Effectiveness factor |
| $\theta$ | Alcohol-to-acid molar ratio |
| $\lambda$ | Ratio ‘radius of solute molecule (nm)’/‘pore radius (nm)’ |
| $\mu_B$ | Viscosity of solvent (Pa·s) |
| $\mu_s$ | Viscosity of solution (Pa·s) |
| $\nu$ | Kinematic viscosity (m$^2$/s) |
| $v_i$ | Stoichiometric coefficient |
| $\rho_c$ | Density of catalyst (kg/m$^3$) |
| $\rho_s$ | Density of solution (kg/m$^3$) |
| $\varphi$ | Thiele modulus |

# Chapter One: INTRODUCTION

## 1.1 Overview

Petroleum coke (petcoke) is a low-value byproduct from the refining of crude oil [1]. It has been stockpiled as a solid waste of the oil industry over many years, accounting for millions of tonnes per year worldwide [2]. Petcoke has limited applications as fuel for boilers, anodes for the smelting industry, and cement manufacture due to its high sulfur content (> 6.5 wt%) and other impurities [3]. It is also a source of pollutants, including aromatics compounds and volatile compounds [4]. However, as petcoke is a carbon-rich, abundant and inexpensive material, it is a potential resource for carbon-based catalysts [5]. Activation treatment of petcoke is the typical initial stage, followed by a functionalization, a step in which surface groups are incorporated [6]. Functionalized carbon has been used for many reactions, including esterification, transesterification, hydration, hydrolysis, hydrogenation, photocatalysis, electrocatalysis, dehydration, and dehydrogenation of alcohols [7], [8].

Esterification, in particular, is an important class of reaction in organic synthesis [9]. Its products, esters, are present in several daily and industrial applications, such as solvents, fragrances, pharmaceuticals, plasticizers, flavors, pesticides, herbicides, biofuels, and other intermediates [10]–[12]. Many esters are important intermediates for the petrochemical industry, being produced through reactive distillation [13]. Another example is that esters derived from lactic acid are promising green-substituents for toxic halogenated compounds derived from the petroleum industry, widely used as solvents for several applications [14], [15]. In the last decades, special attention has been given to the esterification of free fatty acids for biodiesel production [16], resulting from searching for alternative energies in the current scenario. The reduction of total acid

number (TAN) of crude oil by esterification of naphthenic acids is another important application of this class of reaction [17].

The heterogeneous esterification reaction is preferable to homogeneous reactions or supercritical technologies because of recyclability, lower waste generation, and lower energy consumption [18]. Thereby, considering all those advantages, including the high content of carbon in petcoke, esterification reaction is a potential field for the application of petcoke-derived catalysts. There are only a few investigations in the literature, however, about this implementation.

Liu *et al.* [19] reported a good performance for esterification of petcoke materials, chemically activated at 800 °C in the presence of KOH, with a subsequent acid treatment with ammonium heptamolybdate and activation by carbothermal hydrogen reduction up to 900 °C. Wu *et al.* [20] also reported high activity and reusability of petcoke-derived materials, previously activated with KOH at 800 °C, followed by sulfonation. Xiao & Hill [21] investigated the performance of sulfonated petcoke samples without previous activation, which showed comparable activities for esterification to the typically used homogeneous catalyst, sulfuric acid. Despite the reported results of petcoke materials over esterification reactions, there is no baseline for comparison between them in terms of activity. Therefore, the development of a proper method for analysis of functionalized petcoke-derived materials concerning turnover frequency is an opportunity for the current study.

### 1.2 Objectives

This thesis aims to provide a better understanding of how to test and compare the catalytic activity of solid-acid catalysts prepared from petcoke for esterification reactions. The experimental setup and data collection were improved, and the effect of various parameters (including temperature,

alcohol-to-acid (molar) ratio, stirring speed, and loading of catalyst) on the reaction rate was determined. Two main topics were examined in this thesis:

- method limitations: evaluation of the influence of various parameters on kinetics results and assumptions for this study;
- performance of acid-modified petcoke in comparison to a standard catalyst over a model esterification reaction, evaluation of required properties of materials – selectivity, activity, and stability – and analysis of the influence of acidic, structural, and physical features.

### 1.3 Thesis Organization

There are five remaining chapters in this thesis. Chapter Two provides background information and a literature review on the fundamentals of esterification, solid acid catalysts, kinetic model, and thermodynamics related to this reaction. Chapter Three describes the methodology for activity measurement, stability test, determination of kinetic parameters, and sources of error. Chapter Four describes the method limitations for the kinetic analysis of the next chapter, including preliminary tests, reactor setup, data collection and analysis, transfer limitations, and equilibrium conversion. In Chapter Five, kinetic parameters of an esterification model reaction catalyzed by acid-modified petcoke are presented in comparison to a standard catalyst. Moreover, the chapter includes the assessment of the activity and stability of petcoke-derived catalysts, and an analysis of the acidity of those catalysts. Chapter Six presents the conclusions and recommendations for this thesis. The block diagram below, Figure 1-1, represents the primary outcomes from experiments and results presented in Chapters Four and Five.

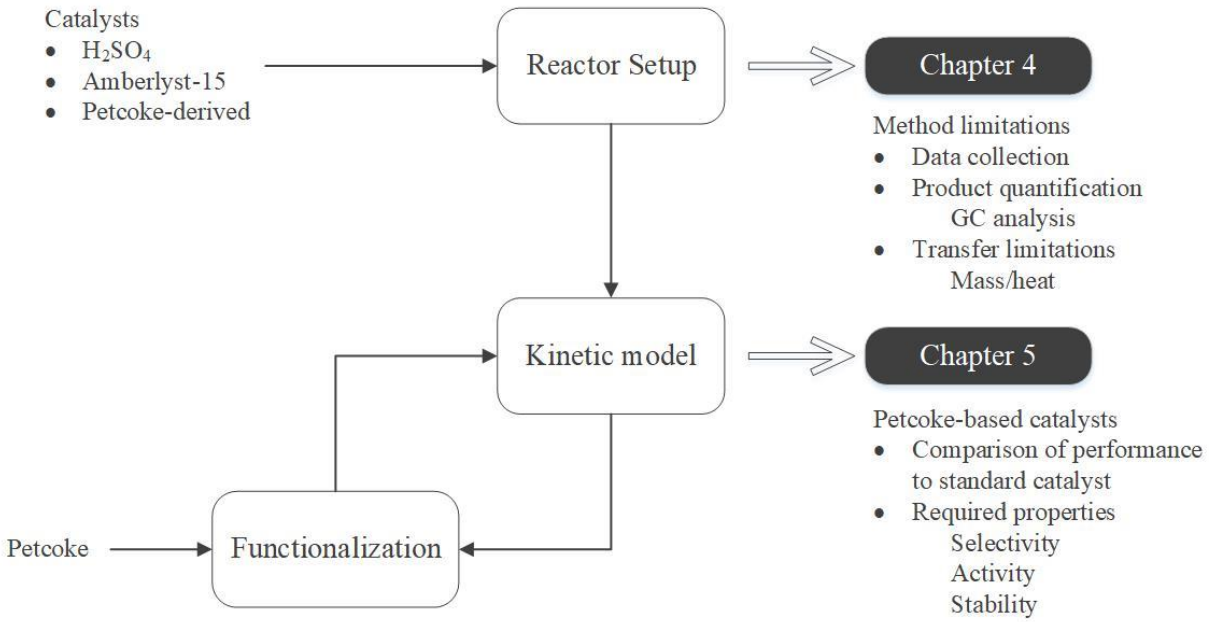


Figure 1-1. Block diagram of outcomes from Chapters 4 and 5.

Chapter Two: LITERATURE REVIEW

## 2.1 Esterification Reaction

Also known as Fischer esterification, these reversible reactions condense a carboxylic acid and an alcohol to produce an ester and water, Equation 1. Hydrolysis is the reverse reaction. An acid medium is necessary to promote the reaction: the presence of either a homogenous or a heterogeneous acid catalyst [22].

$$R_1OOH + HOR_2 \xrightleftharpoons{H^+} R_1OOR_2 + H_2O \qquad 1$$

Esterification reactions are typically carried out at low/mild temperatures (< 260 °C, to minimize thermal decomposition) and low pressures (even vacuum in the case of a homogeneous reaction, < 5 kPa) [13]. Most researchers, however, generally focus on optimizing reaction conditions for ambient pressures and temperatures not higher than 80 °C, because of the thermal stability limitations of some catalysts, such as ion exchange resins [23]. Even lower temperatures are used for biological catalysts (enzymes) [24]–[26]. Therefore, more efficient catalysts have been the primary focus of research. Considering that the catalytic activity stems from the interaction of several parameters, different modifications on the materials have been tested to provide better catalytic properties.

## 2.2 Catalytic Esterification

In the absence of a catalyst, esterification is restricted to a low reaction rate (as low as $1 \times 10^{-7}$ mol/mL·min), depending on the autoprotolysis of the carboxylic acid (self-catalyzed reagent) [15], [22], [27]. Therefore, the utilization of external acid catalysts (homogeneous or heterogeneous) is common, including biological catalysis [28]. The use of homogeneous catalysts,

such as sulfuric acid or hydrochloric acid, is widely reported in the literature [13], [29]–[32]. There is a particular interest in heterogeneous catalysis, however, due to the recyclability after the reaction, no need for neutralization, easier separation, minimal waste generation, little corrosion, and lower energy consumption (no additional operations of neutralization and purification), and lower environmental pollution for recovery compared with homogeneous catalysts [32]–[36]. The challenge is reaching equivalent efficiency in terms of activity as the homogeneous catalysts, and stability for reuse [20], [37]. The homogeneous catalyst sulfuric acid ($H_2SO_4$), for example, is composed almost entirely of active species for catalysis, which explains its greater activity [38]. Solid acid catalysts generally become less active when reused. The deactivation is mainly caused by the leaching of active sites into the reaction media, adsorption of water formed during the reaction, and deposition of organic compounds on the catalyst surface [38], [39].

### *2.2.1 Solid acid catalysts*

Researchers have been investigating the use of potential solid acids for esterification. An example is Nafion-H, an ion exchange resin and the oldest heterogeneous catalyst applied for this reaction [29]. Many other solid acid catalysts have been developed, which have advantages and disadvantages, depending on the reaction conditions.

Solid acid catalysts are normally described in terms of the acidity, i.e., concentration of functional groups, strength and nature (Brønsted/ Lewis), and support morphology, i.e., surface area and porosity [40]. Among others, the types of solid acids include ion exchange resins [41]–[43], zeolite [44], [45], mesoporous silica [46], [47], sulfonated-zirconia [48]–[50], and niobic acid [51], [52], which will be briefly described next, followed by a review of carbon-based solid acid catalysts.

Ion exchange resins are sulfonated crosslinked polystyrene [13]. They are common catalysts for liquid-phase esterification with more than 60 years of application in the industry [13]. Their behavior in different reaction compositions is governed by their polymeric nature [53]. The catalytic activity normally depends on swelling in a polar medium [54], which makes the acid sites (sulfonic groups) readily available to the reactants [54]. The deficient thermal resistance, however, prevents its use over 120 °C [33]. Also, the stability of ion exchange resins is relatively low. The presence of water promotes the dissociation of sulfonic acid groups in the solution, deactivating the polymer [13].

Zeolites are crystalline aluminosilicates interlinked by oxygen atoms [53]. They show good resistance at elevated temperatures due to the pretreatment (> 500 °C) [55]. The synthesis bases on the desired catalytic properties: acid strength distribution, hydrophobicity, and pore size, leading to modifications on the acid exchange level, framework Si/Al ratio, and crystalline structure, respectively [55]. The high performance of zeolites is mostly due to the strength of Brønsted sites prepared within a certain range of acidity [33]. Zeolites act as molecular sieves, adsorbing some molecules selectively for reaction, while excluding others [53].

Mesoporous silica is a composite matrix with pore diameters in the range of 2 - 50 nm, in which the pore size can be fine-tuning, as in zeolites [53]. They are semi-crystalline materials, however, because of amorphous pore walls [53]. Pure mesoporous silica has low activity, acidity, and thermal stability due to the neutral framework (Si) [56]. Thus, the activity, stability, and selectivity depend on the incorporation of acid sites, metal atoms or Brønsted acids, within the catalyst framework [53].

Sulfated zirconia ($SO_4^{2-}/ZrO_2$) generally shows good catalytic activity, selectivity, reusability, and thermal stability [33], [40]. Zirconia occurs as three polymorph phases: monoclinic, tetragonal, and cubic, with the tetragonal phase being the most active [13]. The catalytic activity and selectivity are related to the following properties: mesoporosity, formation of tetragonal phase, and optimum ratio Brønsted/Lewis acid sites [33], [57]. The leaching of sulfate species is observed with treatments above 850 °C and in an aqueous medium [53].

Niobic acid (hydrated niobium oxide, $Nb_2O_5 \cdot nH_2O$) is another inorganic solid Brønsted acid [58], which shows great performance due to a high acid strength, even in the presence of water [33]. Nevertheless, the strong acidity decreases severely with heat treatment above 520 °C [59].

Carbon-based catalysts were described by Konwar *et al.* [60] as highly active and economically attractive catalysts for esterification, among other solid acid materials. As reported in the literature, carbon-based catalysts can achieve high catalytic performance compared to other solid acid catalysts, being ca. 60 - 80% as active as concentrated sulfuric acid, under the same reaction conditions [61]–[64].

### *2.2.2 Carbon-based catalysts*

Carbon materials have been extensively studied for the catalysis of esterification reactions, as they might be prepared from a wide range of low-cost carbonaceous sources [19], [65]–[68]. Carbon-derived catalysts typically offer good operational stability, mechanical properties, chemical inertness, thermal conductivities, low densities, easy accessibility and surface functionalization, and surface hydrophobicity [63], [69]–[71].

Carbon materials have a broad pore-size distribution, from microporous (< 2 nm) to macroporous (> 50 nm) [70]. The mesoporosity (2 nm < pore size < 50 nm) favors diffusion, facilitating the contact of reactants with the active sites (internal and external sulfonic groups) [66]. Porous carbon can be easily prepared by incomplete carbonization, showing adequate pore size (2 - 6 nm) for use as a support [20]. The surface area of carbon materials also shows a large range, from < 2 $m^2/g$ (amorphous carbon) [64], [72] up to 3000 $m^2/g$ (biomass-derived microporous activated carbon) [70].

Most carbon-based catalysts reported in the literature have sulfonic (-$SO_3H$), carboxylic (-COOH), and phenolic hydroxyl (-OH) functional groups attached to the surface, with varied acid densities [73]. In this case, the esterification is catalyzed by the sulfonic groups [20], [74]–[76], which work as strong Brønsted acid sites (proton donors) in the reaction mechanism [8]. Sulfonic groups linked by strong hydrogen bonds are responsible for a stronger acidity due to the mutual electron-withdrawal [58]. The other functional groups, -COOH and (phenolic) -OH, also contribute to a significant fraction of the total acidity [68].

Although -COOH and -OH (also Brønsted acid sites) have weak acidities to catalyze the esterification, they might contribute to the catalytic activity in some cases [67]. By improving the hydrophilicity of the carbon material through the strong affinity of -COOH and -OH with the polar moiety of the reactants, those weak acid groups act as anchoring sites and enhance the access of reactant molecules to the material surface [75], [77]. Solid acids with hydrophilic surfaces, however, show a decrease in the reaction rate when a significant amount of water is present in the reaction system [78]. Water hinders the reactants from interacting with the active sites effectively by forming a layer over the hydrophilic species [64][79]. Thus, the hydrophobic surface of the

material helps keep the acid strength stable when water is present by preventing the hydration of functional groups [68].

*2.2.3 Petcoke-derived catalysts*

The raw petcoke properties depend mainly on the type and conditions of the coking process (delayed *versus* fluid coking) and the feedstock composition [3]. Petcoke is generally a microporous material though, as determined by the characterization analysis with $CO_2$ adsorption [3]. Table 2-1 lists the typical composition and properties of petcoke.

Table 2-1. Characterization analysis of petcoke. Adapted from J. M. Hill, A. Karimi, M. Malekshahian, Characterization, gasification, activation, and potential uses for the millions of tonnes of petroleum coke produced in Canada each year, *Can. J. Chem. Eng*, 92, 1618-1626 [3]. 

| | **Fluid coke** | **Delayed coke** |
|---|---|---|
| Quantitative analysis (%)* | | |
| Moisture | 1.3 | 0.3 |
| Ash | 2.0 | 3.7 |
| Volatile | 6.9 | 15 |
| Fixed carbon | 91 | 82 |
| Elemental analysis (%)* | | |
| Carbon, C | 84 | 84 |
| Hydrogen, H | 1.9 | 3.8 |
| Nitrogen, N | 2.2 | 1.8 |
| Sulfur, S | 7.5 | 6.5 |
| Oxygen, O | 4.8 | 3.8 |
| Surface area - $N_2$, BET ($m^2/g$) | 20 | 1.9 |
| Surface area - $CO_2$, DR ($m^2/g$) | 300 | 110 |

*Due to the standard errors (less than ± 1 wt% for the quantitative analysis, and less than ± 0.5 wt% for the elemental analysis), the values do not add up to 100%.

Several metals are present in petcoke, especially Si and Al, including small amounts of Fe, Ca, Ti, K, Na, Mg, and P [3]. The high concentration of sulfur is one drawback of using petcoke as fuel, which leads to environmental problems and severe fouling and corrosion on the heat transfer tubes [80]–[82]. The sulfur in petcoke is presented mostly in organic forms, as stable compounds such as thiophene, requiring high temperatures for removal (> 1100 °C) [83], [84]. For the application in solid acid catalysts, however, petcoke has the advantage of not requiring previous desulfurization.

The typical synthesis process to prepare materials from petcoke starts with a thermochemical treatment. This step is carried out at activation temperatures in the range 450 - 900 °C [19] during short times (2 h or less), with co-activation agents as KOH [85], to result in developed pores and surface area for use as a support or as a catalyst, itself. Nevertheless, Xiao & Hill [21] demonstrated successful synthesis of petcoke-derived catalysts without previous activation.

The next step is the functionalization of the material. Oxidizing acids, like sulfuric acid and nitric acid, are employed in a wet chemical treatment that normally results in a high degree of functionalization [86]. Sulfuric acid (concentrated or fuming) incorporates -$SO_3H$ on the material surface, while oxygen-containing groups (-COOH and phenolic -OH) are also generated by the oxidation of aliphatic $CH_3$/$CH_2$ [78]. Besides those groups, nitric acid is also responsible for incorporating some nitrogen hetero doping [87].

### 2.3 Kinetics

The reaction order and kinetic model can not be generalized for this class of reactions since different conditions are employed for each reaction over the range of one (formic acid) to twenty carbon atoms (arachnid acid) – aliphatic to aromatics – or more.

Therefore, in terms of the kinetic model, esterification reactions generally fall into one of the following: pseudo-homogeneous, Eley-Rideal, and Langmuir-Hinshelwood (L-H) [15], [88], depending on the reaction mechanism over the catalyst; and first or second order, according to the molar ratio of reagents.

The overall rate is expressed by the reversible model, Equation 2, depending on the concentration of all compounds in solution.

$$-r = k_1 C_A C_B - k_2 C_C C_D \qquad 2$$

where $-r$ is the rate of reaction (mol/mL·min); $C_A$ and $C_B$ are the concentrations (mol/mL) of carboxylic acid and alcohol, $C_C$ and $C_D$ are the concentrations of ester and water (mol/mL); and $k_i$ is the rate constant for the forward (1) and reverse (2) reaction ($min^{-1}$).

The pseudo-homogeneous first-order reaction model is the most recurrent kinetic model applied for esterification reactions [18], [89], especially when a molar excess alcohol (usually > 10:1) is provided for the reaction [31], [54], [88]. For the first-order reaction, alcohol is provided in excess, which holds its concentration almost constant, and the forward rate depends only on the acid concentration. Thus, the rate of reaction can be estimated by Equation 3 for the beginning of reaction – when the concentration of products is not relevant [90].

$$-r = k_1 C_A C_B = k C_A \qquad 3$$

where $k$ is the pseudo-first-order rate constant ($min^{-1}$). When the alcohol-to-acid molar ratio is equal to 1:1, however, the rate depends on the concentration of both reagents. Thus, the second-order model can be used to fit the reaction data at the beginning of the reaction: $-r = k_1 C_A C_B$. Still, some authors prefer to use this model even using excess alcohol [91], [92].

The equilibrium rate constant ($K_e$) can be determined experimentally according to Equation 4:

$$K_e = \frac{k_1}{k_2} = \frac{x_e^2}{(\theta - x_e)(1 - x_e)} \qquad 4$$

where $\theta$ is the alcohol-to-acid molar ratio; and $x_e$ is the equilibrium conversion of carboxylic acid (dimensionless). The term $x$ represents the conversion of the limiting reagent (A) during the reaction and is given by the ratio between moles of A reacted and moles of A fed.

Esterification reactions can be catalyzed over either Brønsted or Lewis acid sites [64]. In the Eley-Rideal model, a common mechanism in catalysis by solid acids, only one reactant bonds to the catalytic groups (normally the more polar), while the other combines with it [13]. Figure 2-1 illustrates this mechanism over a Lewis acid site ($L^+$). The carbonyl oxygen of free fatty acid interacts with the acidic site of the catalyst producing a carbocation. The nucleophilic attack of alcohol to the carbocation forms a tetrahedral intermediate, eliminating a water molecule to form a molecule of ester [93].

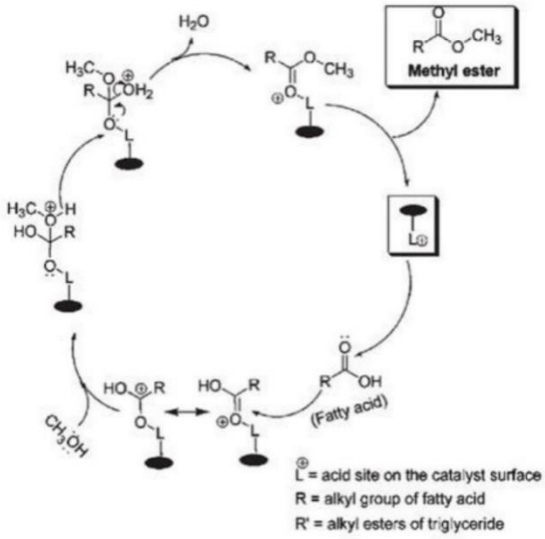


Figure 2-1. Schematic of esterification catalyzed by Lewis acid sites ($L^+$) of TPA catalyst. Adapted from M. G. Kulkarni, R. Gopinath, L. C. Meher, A. K. Dalai, *Green Chem.*, 2006, 8, 1056-1062 [93], with permission from The Royal Society of Chemistry.

The Langmuir-Hinshelwood model is also reported by some studies related to esterification [15], [94], when both reactants are highly polar and bond strongly to the catalytic group [13]. In this case, the reagents carboxylic acid and alcohol may adsorb on either Brønsted or Lewis acid sites of the catalyst. The mechanism of adsorption on Brønsted acid sites ($B^+$) is illustrated in Figure 2-2. A Brønsted acid protonates the hydroxyl group of alcohol; meanwhile, the carboxylic acid is also protonated on an adjacent site forming the carbocation. The nucleophile is produced by deprotonation of the alcohol, followed by an attack to the carbocation. A tetrahedral intermediate is generated, followed by the ester formation after water elimination [88].

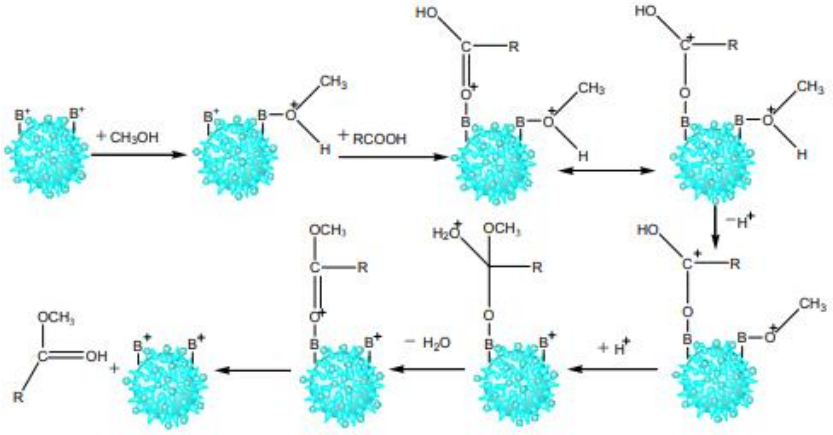


Figure 2-2. Dual-site mechanism of esterification with reagents adsorbing on Brønsted sites ($B^+$). Reprinted from Z. Zeng, L. Cui, W. Xue, J. Chen, Y. Che, Recent Developments on the Mechanism and Kinetics of Esterification Reaction Promoted by Various Catalysts, *Chemical Kinetics*, Vivek Patel [88]. Copyright (2012), with permission from IntechOpen.

The reaction rate on the catalyst surface ($-r_s$) can be estimated from Equation 5 for the dual-site mechanism.

$$-r_s = \frac{kC_AC_B}{(1 + K_1C_A + K_2C_B)^2} \qquad 5$$

where $K_1$ and $K_2$ are the adsorption equilibrium constants for each reagent on the catalyst surface.

*2.3.1 Reaction Model*

The esterification of octanoic acid with methanol (Equation 6) was chosen as a model reaction for testing the activity of the catalysts in this research. Also known as caprylic acid, octanoic acid naturally occurs in coconut oil (8.0 wt%) and palm kernel oil (0.3 wt%) [95], both of which are used for biodiesel production. Moreover, methyl octanoate (the product of octanoic acid esterification) is an important ester for the food industry and agrochemical manufacturing [96]. Being a medium chain length free fatty acid, octanoic acid is a good model compound for esterification over petcoke-derived catalysts, since various other applications can be extrapolated by this research.

$$C_7H_{15}COOH + CH_3OH \rightleftharpoons C_7H_{15}COOCH_3 + H_2O \qquad 6$$

Water is another product of this reaction. The kinetics of octanoic acid esterification with methanol or ethanol was studied over several catalysts, including doped (sulfated, tungstated, titania) zirconia, niobic acid, sulfuric acid, SAC-13 (Nafion/silica nanocomposite), sulfated tin oxide, sulfated carbon, sulfated aluminum phosphate, acidic ionic liquid, heteropolyacid-based ionic liquid, and acid-activated clays [23], [37], [38], [48], [51], [76], [97]–[103]. Based on those studies, varied reaction conditions were tested, and the materials showed conversions in the range of 10 - 100%. The most active catalysts at mild conditions (60 - 65 °C and 3 - 4 h), however, were sulfuric acid and niobic acid, followed by ionic liquid and sulfonated carbon.

*2.3.2 Activation Energy*

The activation energy ($E_a$) is defined as "*the minimum energy required for a chemical reaction to take place. During this process, the energy of the system increases to a maximum, then decreases to the energy of the products. It is the energy barrier that has to be overcome for the reaction to*

*proceed*" (Rennie & Law, 2016) [104]. The Arrhenius equation relates the activation energy to the rate constant, which depends on temperature as given by Equation 7,

$$k = Ae^{-E_a/RT} \quad (7)$$

where $k$ is the rate constant of the forward reaction ($min^{-1}$); $A$ is the pre-exponential (or frequency) factor ($min^{-1}$), related to the frequency of successfully oriented collisions between molecules; $E_a$ is the activation energy (J/mol), normally called "apparent activation energy" in catalytic reactions; $R$ is the universal gas constant (8.314 J/mol·K); and $T$ is the temperature of reaction (K). The pre-exponential factor is also related to the number or concentration of active centers for reaction [105]. Effective catalysts decrease the activation energy of reaction, hence increasing the reaction speed. In the absence of other transfer resistances, high values (> 25 kJ/mol) of activation energy may imply that the reaction is controlled kinetically and not diffusively [106]. Despite that, experimental tests of catalyst loading and calculated parameters, including the Thiele modulus and effectiveness factor, are other factors to be evaluated regarding kinetic control and transfer limitations.

### *2.3.3 Heat and Mass Transfer Limitations*

Heterogeneous catalysts are subject to heat and mass transfer effects to and from the solid-fluid interface. Those limitations stem from the nature of the catalyst, as solid catalysts are normally prepared on porous supports, and a three-phase reaction occurs (solid-liquid-liquid) [39]. While external transfer resistances occur from the bulk of the reactant system to the outer particle surface of the catalyst, the internal transfer takes place from the outside of the particle to the active sites inside the pores [107].

Mass transfer limitations generally decrease the observed reaction rate. Heat transfer limitations also affect the reaction rate. For endothermic reactions, heat transfer limitations are responsible for decreasing the equilibrium conversion since not enough heat is supplied to the catalyst surface. In exothermic reactions, the released heat is not removed effectively, increasing the reaction rate and shifting the equilibrium conversion. The heat and mass limitations may be additive or counteract one another [107].

Therefore, it is important to avoid those effects in kinetic studies. Only when external and internal transfers are fast enough can the intrinsic reaction rate be measured [90]. As demonstrated by Figure 2-3, the effects of transfer limitations also impact the activation energy of the reaction.

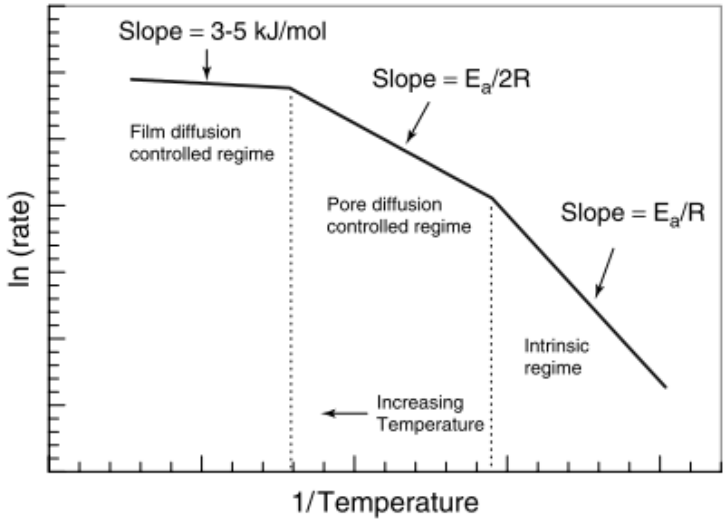


Figure 2-3. Effects of transfer limitations on catalytic activity. Reprinted from M. Boudart, G. W. Huber, J. A. Dumesic, Principles of Heterogeneous Catalysis, *Handbook of Heterogeneous Catalysis*, vol 1, ch 1.1 [13]. Copyright (2008), with permission from John Wiley and Sons.

For diffusion-limited reactions, the activation energy may be as low as 3 - 5 kJ/mol for the film diffusion-controlled regime and 10 - 15 kJ/mol for the pore diffusion-controlled regime. In the absence of other limiting factors, the reaction rate should be governed by an intrinsic regime – a truly chemical step – when the activation energy exceeds 25 kJ/mol [108].

## 2.4 Thermodynamics

The thermodynamics of a reaction is related to the spontaneity of reaction as well as selectivity of products, based on reaction conditions and equilibrium constants. While a catalyst can change the kinetics of the reaction, a catalyst does not change its thermodynamics. Therefore, in any kinetic study, it is also important to pay attention to the thermodynamic limitation and its predictions for the reaction of interest.

The equilibrium constant is related to the chemical potential of the reactants and products in terms of a property defined as 'fugacity' [109]. When the fugacities of components in a mixture do not show a significant dependence with pressure, however, and when the system can be considered an ideal solution, the expression for the equilibrium constant can be simplified in terms of composition [109], as given by Equation 8,

$$K_e = \frac{C_C C_D}{C_A C_B} \qquad 8$$

where $K_e$ is the equilibrium constant for a reaction at a given temperature; and $C_A$, $C_B$, $C_C$ and $C_D$ are the concentrations (mol/mL) of carboxylic acid, alcohol, ester, and water, respectively.

As a reversible reaction, the rate to reach equilibrium may be affected by the presence of products, which shifts the reaction progress towards the reverse reaction. Therefore, the use of excess alcohol during the reaction progress favors the forward reaction increasing the equilibrium conversion [10], [31]. Moreover, the use of molecular sieves or silica gel to remove (by adsorption) the water formed also promotes the forward reaction [110].

The equilibrium constant is also related to the Gibbs free energy of reaction ($\Delta G_r^o$) under the standard state condition – which considers pure components at 1.0 M concentration – and can be

calculated by Equation 9. The Gibbs free energy determines the extent of reaction, is a function of temperature and does not depend on pressure or reagents concentration [111].

$$K_e = \exp\left(\frac{-\Delta G_r^o}{RT}\right) \quad 9$$

where $\Delta G_r^o$ is the reaction Gibbs free energy (J/mol); $R$ is the universal gas constant (J/mol·K); and $T$ is the temperature of reaction (K). The Gibbs free energy of reaction can also be calculated through Equation 10. Knowing the Gibbs free energy of formation of all the species involved in the reaction, those values are scaled by the stoichiometric coefficients [109]. The values for the Gibbs free energies of formation are generally available at the standard condition of 25 ºC.

$$\Delta G_r^o = \sum v_i \left(\Delta G_f^o\right)_i \quad 10$$

where $\Delta G_f^o$ is the Gibbs free energy of formation (J/mol); and $v_i$ is the generalized stoichiometric coefficient.

The enthalpy of reaction is related to the amount of energy absorbed or released during chemical reactions due to the rearrangement of bonds within the molecules [109]. It is an important parameter that accounts for the influence of temperature on the reaction progress.

Similar to the Gibbs free energy of reaction, the standard enthalpy of reaction can be determined using enthalpies of formation, Equation 11,

$$\Delta H_r^o = \sum v_i \left(\Delta H_f^o\right)_i \quad 11$$

where $\Delta H_r^o$ is the standard enthalpy of reaction (J/mol); and $\Delta H_f^o$ is the standard enthalpy of formation (J/mol). The values of enthalpies of formation are generally available at the standard condition of 25 ºC.

### 2.5 Knowledge Gaps

Considering the available literature, acid-modified petcoke-derived catalysts have the potential for the catalysis of esterification reactions. Therefore, the main knowledge gap identified was the application of this new solid acid material for esterification.

Xiao & Hill (2020) have already found good conversion results for an esterification reaction catalyzed by functionalized petcoke-derived materials [21]. This thesis focuses on confirming their hypothesis. For that, in Chapter Four, the method setup – reactor and quantification analysis – was established by evaluating several parameters and conditions, and the limitations of the kinetic study were determined.

In Chapter Five, a kinetic study evaluated the performance of different functionalized petcoke samples for a model esterification reaction in comparison to a standard catalyst. The analysis was based on investigating the required parameters in terms of activity, selectivity, and stability.

# Chapter Three: EXPERIMENTAL METHODS

This chapter describes the experimental setup and conditions for the catalytic tests; the techniques used for the analysis of reaction progress and measurement of catalyst acidity; the methods for evaluation of activity and stability of catalysts; and the determination of kinetic parameters, such as rate constant, initial reaction rate, and activation energy. The catalysts consisted of a set of functionalized petcoke-derived materials and standard available catalysts for comparison. Additionally, sources of experimental error are discussed.

## 3.1 Materials

Solid acid catalysts derived from petcoke were prepared by other members of the Laboratory for Environmental Catalytic Applications (LECA) group – Qing Huang, Ye Xiao, and Robert Pryde – by using delayed petcoke from an oil sands company (Suncor Energy Inc., Alberta, Canada). Most samples were treated with concentrated sulfuric acid or nitric acid to develop sulfonic group acidity on the petcoke surface without previous chemical activation [21], [112]; meanwhile, one sample was functionalized with 12-tungstophosphoric acid. Those materials were then used for the catalysis of esterification reactions. The standard catalysts used for comparison were sulfuric acid ($H_2SO_4$, 98%, EM Science) and Amberlyst-15 ion exchange resin (Styrene-DVB, Alfa Aesar).

The experimental tests reported in Chapters 4 and 5 were based on the model reaction between octanoic acid ($C_8H_{16}O_2$, 98+%, Alfa Aesar) and methanol ($CH_4O$, $\geq$ 99.8%, Sigma-Aldrich), using dodecane ($C_{12}H_{26}$, $\geq$ 99%, Sigma-Aldrich) as the internal standard for analysis. Methyl octanoate ($C_9H_{18}O_2$, > 99.0%, TCI America) is the reaction product. A calibration curve for the gas chromatograph (GC) was developed to quantify the amount of ester produced.

More details on the materials and experimental procedures are given in Sections 4.2 and 5.2.

## 3.2 Activity Measurement

Petcoke-derived catalysts were compared to commercially (homo- and heterogeneous) available catalysts. A batch reactor was employed for the tests due to its simplicity for liquid reactants with solid catalysts [107].

### *3.2.1 Reactor Setup*

The reactor consisted of a two-neck round bottom flask with a capacity of 100 mL placed in a water bath. The water bath consisted of a 2 L beaker with a diameter of 13 cm and a height of 19 cm. A stirring hotplate (Corning® PC-420D) and an egg-shaped stir bar of 25.4 x 12.7 mm were used to agitate and heat the reaction mixture. A schematic of the reactor setup is presented in Figure 3-1.

The flask center top joint was connected to a reflux condenser (Graham type, with 24/40 joint, 500 mm jacket length, borosilicate glass coil); meanwhile, the other top joint was connected to an adapter, serving as a sampling port. The adapter had a thread at the top to accept a cap with a hole and a PTFE-faced septum, enabling the insertion of a needle to withdraw samples.

Octanoic acid, dodecane (internal standard), and catalyst were placed into the flask after weighing on the analytical balance AB304-S model (Mettler Toledo, Columbus, OH, USA). Methanol was placed lastly through the sampling port to start the reaction. A typical reaction used 5 mL of octanoic acid, 1 mL of dodecane, ~ 0.1 - 0.2 g of catalyst (2 - 4.5 wt%), and 25 mL of methanol. The septum was replaced for each reaction, and the needle was 7” length (180 mm) and gauge 18 (nominal O.D. 1.2 mm). Samples of less than 0.5 mL were withdrawn periodically (typically every 15 min) from the reaction media. The overall amount of liquid removed decreased the reaction volume by less than 15% of the initial volume. After sampling, the mixture was filtrated using

membrane filters EZFlow® (Foxx Life Sciences) of 0.45 or 0.22 µm of pore sizes. Depending on the particle size of the catalyst, a prefiltration was required (0.45 µm pore size), followed by filtration for fine particle removal using 0.22 µm. The samples were placed in 2 mL vials until the analysis could be completed.

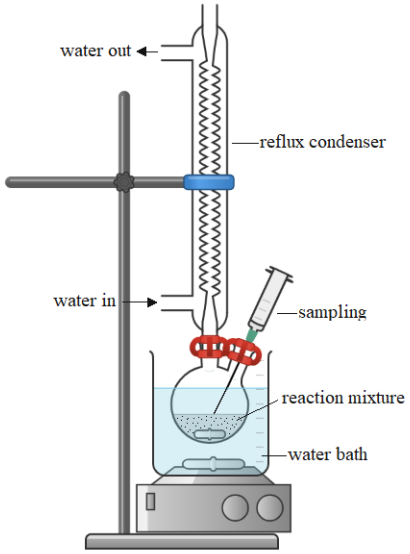


Figure 3-1. Schematic of the reactor setup.

*3.2.2 Reaction Progress Quantification*

The reaction progress was analyzed by GC with a flame ionization detector (GC–FID). Gas chromatography is a technique for the identification and quantification of organic compounds in a mixture. The gas chromatography principle is based on the vaporization of a mixture and the time separation of its components as they absorb on and elute from a column [113].

A gas chromatograph contains five primary components: carrier gas, inlet, column, detector, and computer chemstation, as illustrated in Figure 3-2. The carrier gas from a pressurized cylinder – typically helium, hydrogen, nitrogen, or argon – carries the sample through the column. Liquid samples are normally injecting into the inlet, a heated injection port, by using microliter syringes.

A sample must be volatile without thermal breakdown at temperatures below 400 °C to go through the column by the carrier gas flow (mobile phase). The column, which can be a capillary or packed type, is coated by a stationary phase – liquid or porous solid support. The separation into individual components of the sample mixture happens based on the ability of components to partition between the mobile and stationary phase. In other words, analytes are separated by various physical or chemical mechanisms, but mostly according to solubility and boiling point. An oven controls the column temperature [113].

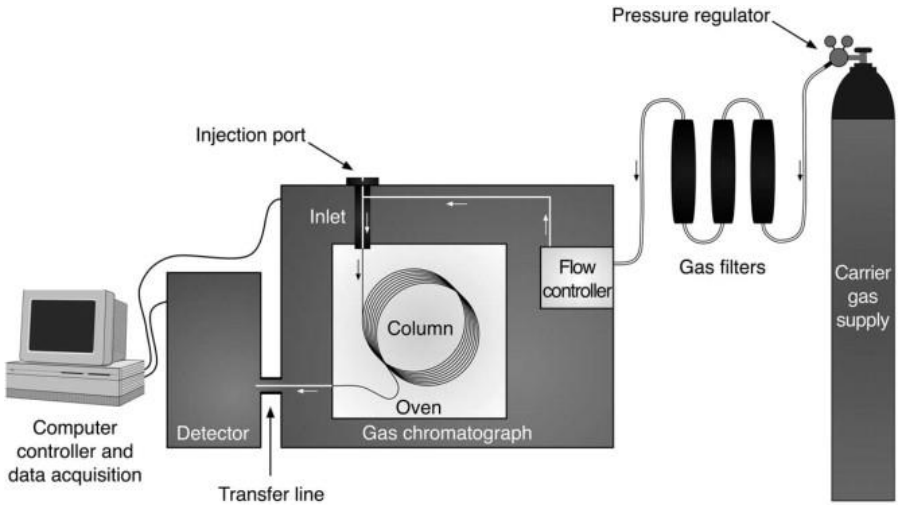


Figure 3-2. The main components of a gas chromatograph. Reprinted from *Fire Debris Analysis*, 1. ed, E. Stauffer, J. A. Dolan, R. Newman, ch. 8 - Gas Chromatography and Gas Chromatography-Mass Spectrometry. [114]. Copyright (2008), with permission from Elsevier.

After the sample separation, the compounds elute from the column into a detector that responds to the physical or chemical properties of each component and converts this response into an electrical signal in the detector. A computer chemstation – or integrator – processes those signals from the GC, giving the information as a chromatogram. Finally, the computer system measures the amount of each component based on their peak sizes and identifies those components based on their retention times [113].

Calibration curves with internal standards were previously made for analysis of reaction samples. The analysis consisted of injection of 0.1 µl of each solution (sample without catalyst) into the GC 6890N (Agilent Technologies, Santa Clara, CA, USA) equipped with a capillary column. The temperature program (oven) varied accordingly to the internal standard (toluene, dibenzothiophene, or dodecane) and capillary column employed (HP-5 or DB FATWAX UI), as well as the carrier gas (nitrogen or helium – purity of both equal to 99.999%) and inlet split ratio (25:1 or 50:1). Note, several internal standards were tried initially (as described in Section 4.3.4) before using dodecane exclusively. The compounds identified by the FID included the reagents octanoic acid and methanol, the internal standard, and the product methyl octanoate – normally referred to as 'ester' in this study. Water is not analyzed by this kind of detector, as it does not burn. The amount of remaining octanoic acid in solution, however, was not well determined due to incompatibility or uncertainty of those columns for the analysis of this specific compound.

Calibration curves for octanoic acid and methyl octanoate (ester) were made for the determination of their quantities by GC analysis. 10 mL samples of known composition were prepared in volumetric flasks in the range of concentration expected for the reaction. The system compounds were weighed with a known fixed amount of internal standard, proportional to the reaction system. During experiments, the response factor (ratio 'analyte'/'internal standard') was then converted into analyte (acid or ester) mass using the corresponding calibration curve, Equation 12,

$$m_i = R_f \times \frac{m_{st}}{CC} \qquad 12$$

where $R_f$ is the response factor given by $A_i/A_{st}$, where $A_i$ and $A_{st}$ are the peak areas of analyte and internal standard, respectively; $m_i$ and $m_{st}$ are their corresponding masses in solution (g); and $CC$ is the value of the calibration curve.

*3.2.3 Ester Yield*

The reaction progress was analyzed in terms of octanoic acid conversion (limiting reagent) and/or ester yield, as these quantities are related and given in percentage. The ester yield expresses the amount of the product obtained according to the amount of reactant converted and its selectivity for the reaction. In other words, the ester yield ($Y$) is given by Equation 13:

$$Y = x \times S \qquad 13$$

where $x$ is the conversion of octanoic acid; and $S$ is the selectivity for esterification. Considering a selectivity of 100%, the ester yield can also be calculated by comparing the mass of ester in solution with the theoretical maximum mass that could be formed if all octanoic acid presented in the reaction mixture converts to ester, Equation 14.

$$Y = \frac{m_E}{m_{E,max}} \times 100\% \qquad 14$$

where $m_E$ is the mass of ester in solution measured by GC analysis (g); and $m_{E,max}$ is the theoretical maximum mass of ester in solution (g), assuming total conversion of octanoic acid.

*3.2.4 Test of Conditions*

In general, esterification studies reported in the literature use a variety of conditions to evaluate the performance of a catalyst: stirring speed, catalyst loading, alcohol-to-acid (molar) ratio, temperature, and time of reaction. Tests of conditions are important to evaluate if the experiments are in the kinetic region or are transfer limited. In this regard, a calculation of transfer limitation proposed by the literature is presented in Appendix A.

The influence of those parameters on the reaction rate, except time, was evaluated mainly using Amberlyst-15, because of its large concentration of acid sites compared to the petcoke-derived catalysts. Thus, it is more likely to present issues regarding transfer limitations. The influence of time was not investigated, because the kinetic study was focused only on the beginning of the reaction (details in Section 3.4). For the catalyst loading and temperature, a petcoke sample was tested as well, as the behavior might be different from the Amberlyst-15 at those conditions. Appropriate conditions were selected for the subsequent experiments as described in Section 4.3.5.

*3.2.5 Acidity Measurement by Titration*

The catalysts selected for tests were previously characterized by the ion-exchange titration method to determine acidic site concentration on the catalyst surface [18,19]. The strong acid concentration (exchanged $H^+$) of petcoke-derived catalysts was measured by titration of a diluted sample of 0.1 g of solid to 5 mL of 0.1 M sodium chloride solution (NaCl, ≥ 99.0%, EMD Chemicals). For Amberlyst-15, 10 mL of 2.0 M sodium chloride solution was used for the ion exchange procedure (detailed explanation in Appendix B). After shaking in an oscillator VWR Symphony 5000I Shaker (Henry Troemner LLC, Thorofare, NJ, USA) at 25 °C and 250 rpm for 24 h, the solids were removed by filtration and the liquid was titrated with 0.005 M sodium hydroxide solution (NaOH, ≥ 97%, Sigma-Aldrich), using phenolphthalein as indicator. The strong acidity was quantified according to Equation 15:

$$[H^+] = \frac{V_{NaOH} \times C_{NaOH}}{m_{c,eq}} \qquad 15$$

where $[H^+]$ is the strong acidity of the catalyst (mmol/g), mostly related to the sulfonic group ($-SO_3H$) concentration in this study; $V_{NaOH}$ is the volume of sodium hydroxide solution (titer)

(mL); $C_{NaOH}$ is the molarity of titer (mmol/mL); and $m_{c,eq}$ is the equivalent mass of catalyst for titration (g).

The total acidity was determined by a similar procedure of titration. A sample of 0.1 g was added to 5 mL of 0.1 M NaOH solution, shaken at 25 °C and 250 rpm for 24 h, removed the solids by filtration, and titrated with 0.01 M hydrochloric acid (HCl, 37%, Sigma-Aldrich). Triplicate analyses were performed to determine the uncertainty of the titration method.

*3.2.6 Acidity Measurement by XPS*

Titration is not always capable of distinguishing between strong and weak acid sites for carbon-based materials. A technique based on elemental analysis, however, is more reliable for determining the acid density [115]. Thus, the surface elemental composition of some samples of petcoke functionalized with nitric acid was analyzed by the X-ray photoelectron spectroscopy (XPS) technique, carried out by a third-party laboratory at the University of Alberta in Edmonton (Nanofabrication and Characterization Facility – nanoFAB). The surface chemistry composition was calculated using CasaXPS (Version 2.3.22PR1.0, Casa Software Ltd, Teignmouth, UK). From the spectra, the S2p peak area assigned to oxidized S (C-$SO_x$, x = 2, 3, 4, and -$SO_3H$) was deconvoluted into 2-3 peaks of sulfur species [112]. The peak at 168 eV was attributed to -$SO_3H$ species [72], quantified and reported as strong acidity based on the content of sulfonic groups.

*3.2.7 Turnover Frequency Calculation*

The Turnover Frequency (TOF) provides a more direct comparison of catalysts than specific reaction rates, thus being a useful parameter to quantify the catalytic activity [116]. TOF value is

expressed by the number of molecules reacting per active site per unit of time at the conditions of the experiment [11]. TOF is given by Equation 16,

$$TOF = \frac{k \times C_{A0} \times V}{m_c \times [H^+]} \quad 16$$

where $k$ is the pseudo-first-order rate constant ($min^{-1}$); $C_{A0}$ is the initial concentration of octanoic acid (mmol/mL); $V$ is the volume of the reaction solution (mL); $m_c$ is the mass of catalyst added (g) into the reactor; and $[H^+]$ is the number of active sites assumed as the strong acidity of the catalyst (mmol/g).

Another way of calculating the turnover frequency is in terms of a specific product yield per unit of time and catalytic site [53], [116]. In this case, Equation 17 is applied.

$$TOF = \frac{N_E}{m_c \times [H^+] \times t} \quad 17$$

where $N_E$ is the amount of ester produced (mmol); $t$ is the time in a batch reactor (min). Equation 17 is useful to report the catalyst performance when the reaction rate is difficult to measure (not uniform within the catalyst pellets or the catalytic reactor) [13].

In any equation, all sites are assumed to be active for reaction. Thus the method used in counting sites must be reliable and provide all information about the nature of active sites [116]. The application of the TOF concept is only valid when the number of catalytic sites can be precisely defined [13][116].

In this study, the strong acidity of petcoke-derived catalysts was assumed as the concentration of the sulfonic groups, given by titration or XPS analysis. That is a reasonable assumption because

only the acid site density based on S content has sufficient acidity to promote the esterification reaction [20], [74]–[76]. The exception was the petcoke sample functionalized with 12-tungstophosphoric acid (TPA). In this case, the strong acidity corresponded to the TPA functional group concentration. Also, when $H_2SO_4$ was used as the catalyst, two protons ($H^+$) per molecule of sulfuric acid were considered to determine the number of strong acid sites.

### 3.3 Stability Test

An advantage of using a heterogeneous catalyst is the reusability, since solids are easy to recover from the reaction system. It is required for the material to be mechanical and chemically stable in terms of resistance to abrasion and crushing and chemical inertness towards the reaction solution [13].

The petcoke-derived catalysts are powders. Thus, they were not tested mechanically. Meanwhile, the chemical stability was tested with a leaching experiment to verify the stability of functional groups on the catalyst surface. The test consisted of placing 0.1 g of catalyst in 25 mL methanol at 60 °C (typical reaction temperature) for 90 min. After this time, the solid was recovered by filtration. The recovered methanol was placed into the reactor with 5 mL of octanoic acid (and 1 mL of internal standard) at 60 °C for 90 min, without any addition of catalyst. Samples of < 0.3 mL were periodically withdrawn from the reactor (every 15 min), and the sample composition was analyzed by GC-FID.

## 3.4 Kinetic Parameters Determination

### *3.4.1 Rate Constant*

Only the model of pseudo-homogenous reaction was taken into consideration, while the investigation of the reaction mechanism on the catalyst surface is beyond the scope of this study. The reactions were tested at conditions to assure the surface rate was the limiting step of the reaction, avoiding some transfer limitations observed at specific conditions (Section 4.3.5).

The first-order reaction is a valid assumption, as long as the alcohol concentration can be considered unchanged throughout the process. Moreover, the forward rate constant ($k_1$) is much larger than the backward rate constant ($k_2$), especially at the beginning of the reaction [117]. Therefore, the initial reaction rate ($-r_A$) depends only on the carboxylic acid concentration, and Equation 3 can be applied instead of Equation 2.

The pseudo-homogeneous first-order model represented by Equation 3 can be converted to Equation 20 by integrating the reagent concentration over time as follows,

$$-r_A = -\frac{dC_A}{dt} = kC_A \qquad 18$$

$$\int_{C_{A0}}^{C_A} \frac{dC_A}{C_A} = -\int_0^t k\, dt \qquad 19$$

$$C_A = C_{A0}e^{-kt} \qquad 20$$

where $C_A$ and $C_{A0}$ are the concentrations (mmol/mL) of octanoic acid at a time $t$ (min) and time zero, respectively; $k$ is the pseudo-first-order rate constant ($min^{-1}$). The initial rate constant can be determined by Equation 20, plotting the octanoic acid concentration *versus* the reaction time. The fitted exponential curve gives the initial rate constant ($k$) as the negative exponent of base $e$. The

data were fit by the software OriginPro® with a non-linear least squares approach. The Levenberg Marquardt algorithm was used to fit the two-parameter exponential function.

*3.4.2 Reaction Rate*

As a reversible reaction, the assumption of the first-order model is only valid at the beginning of the reaction, in the range of 0 - 15% of the equilibrium conversion [76], [118], [119]. As the product concentration increases, the reaction rate decreases until equilibrium. The reaction rate can be determined from the mass balance of the batch reactor. In the mass balance, the generation equals the accumulation, and the reaction solution is considered perfectly mixed, Equation 21.

$$-r_A V = -\frac{dN_A}{dt} \quad (21)$$

where $-r_A$ is the initial reaction rate (mol/mL·min); $V$ is the reaction volume (mL); $N_A$ is the number of moles (mol) of octanoic acid at a time *t* (min). The number of moles of octanoic acid in solution at a specific time is related to its conversion by Equation 22. After substitution, Equation 23 is obtained.

$$N_A = N_{A0}(1 - x) \quad (22)$$

$$-r_A = \frac{N_{A0}}{V}\frac{dx}{dt} \quad (23)$$

where $N_{A0}$ is the initial number of moles of octanoic acid (mol); and $x$ is the (octanoic) acid conversion. Therefore, the plot of acid conversion ($x$ < 10%) *versus* reaction time will be linear and can be used to determine the initial reaction rate.

*3.4.3 Activation Energy*

The activation energy was determined by using a petcoke-derived catalyst to evaluate the effectiveness of this material in catalyzing the esterification. In addition, the activation energy using Amberlyst-15, a commercial catalyst, was also determined for comparison. The Arrhenius equation (7), in the linearized form (Equation 24), shows the temperature effect on the catalytic activity according to Figure 2-3.

$$ln\ k = ln\ A - \frac{E_a}{RT} \qquad 24$$

where $k$ is the pseudo-first-order rate constant ($min^{-1}$); $A$ is the pre-exponential factor ($min^{-1}$); $E_a$ is the activation energy (J/mol); $R$ is the universal gas constant (8.314 J/mol·K); and $T$ is the temperature of reaction (K).

The catalysts were tested in the range of 40 - 80 °C. For each temperature, data were fitted by Equation 20 to obtain the pseudo-first-order rate constants below 10% conversion. The software OriginPro® was used for fitting the data to obtain the values of the activation energy and the pre-exponential factor. Both fits – linear and exponential – were tested and discussed in Section 5.3.3. A linear least squares approach was used for Equation 24, while a non-linear approach was used for Equation 7, using the Levenberg Marquardt algorithm to fit the two-parameter exponential function.

**3.5 Sources of Error**

Errors are classified into two main categories: systematic and random errors. Systematic errors result from a problem present throughout the whole experiment or analysis, e.g., wrong equipment calibration. Systematic errors are consistent errors that deviate the correct value in one direction

(high or low measurements), affecting accuracy [101], and can be corrected. On the other hand, random errors have no pattern. Random errors are fluctuations of measurement always present due to the equipment precision. Random errors deviate in both directions influencing the precision of a measurement [120], and can be diminished by repeated measurements.

Regarding the quantification of compounds present in the reaction media, the GC method is subject to some sources of errors. Sample losses are caused by systematic errors, such as incomplete sample manipulation and variations in the analytical procedure [121]. Sample losses always might occur during manipulation and transfer steps, which may affect the measured concentration. Thereby, careful sample preparation is necessary to minimize this kind of error. The incompatibility of the capillary columns concerning the octanoic acid is another source of error.

Also related to the product quantification, there are some errors associated with the sample collection. The time of withdrawing a sample from the reactor may vary by 0 - 30 s. This procedure was done manually, which may also introduce some error (up to ± 3.6%).

Random errors can be inconsistencies when analyzing a sample due to the precision of the GC method and injections. This error was minimized by using an internal standard during the reaction. Hence, the error is similar for the analyte and the internal standard, keeping the ratio of signals nearly constant. Autosamplers, however, can reduce the injection errors by 1 - 2% of relative standard deviation [121]. Without autosamplers, the injections are normally large sources of errors due to the possible evaporation of compounds from the needle of the microsyringe during insertion into the hot inlet. The injected samples had a volume of 0.1 µl, while the microsyringe used had an uncertainty of 0.01 µl.

The sample standard deviation ($s$) for triplicate analyses carried out by GC is given by Equation 25 [122].

$$s = \sqrt{\frac{\sum_{i=1}^{n}(X_i - \bar{X})^2}{n-1}} \qquad 25$$

where $X_i$ is the sample value; $\bar{X}$ is the mean value; and $n$ is the number of analyses. As the proportion of compounds in the mixture is kept the same with more or less volume inside the syringe, the results of GC analysis – given in terms of a ratio of integrated areas, $R_f$ – were not affected by the injection uncertainty. More details about errors of GC analysis are discussed in Section 4.3.4.

The analytical procedure of reaction preparation includes some errors, which might be both systematic and random errors. Therefore, during the weighing of compounds on the analytical balance and manipulation of related elements, i.e., chemicals and laboratory tools, attention was taken to avoid systematic errors and reduce random ones. The analytical balance used in the experiments was an AB304-S model (Mettler Toledo, Columbus, OH, USA), with a maximum capacity of 320 g and uncertainty of 0.0001 g. The catalyst samples were normally an amount of 0.1 g, with a weighing uncertainty around 0.1%. For the other compounds, this error was smaller, as larger amounts were weighed – around 4.5 g of octanoic acid and 0.7 g of internal standard.

The water bath temperature was controlled by a stirring hotplate coupled to a thermocouple, with an uncertainty of 1 °C. The common experimental temperature was 60 °C, and so the uncertainty is approximately 1.7%. Fluctuations in the temperature setpoint, however, were rarely observed during the experiments, being assessed by an external thermometer – Cole Parmer Digi-sense Type K Thermocouple.

The titration method also has some errors. For the uncertainty of titration, the standard deviation of triplicate analysis was considered. The NaOH solution was standardized with potassium hydrogen phthalate (KHP, ≥ 99.95%, Sigma-Aldrich), a primary standard for acid-base titration. The burette used for titration was 10 mL of capacity, with an uncertainty of 0.05 mL. Even using a low concentration of NaOH solution, some petcoke samples only consumed 0.50 mL of volume, given errors as high as 10%. Other errors associated with this technique are the error in the volume of the 5 mL pipette used for adding the solution of NaCl to 0.1 g of catalyst before shaking for ion exchange; and the error in the volume of the 1 mL micropipette used for obtaining a sample for titration; while the evaporation of solution was considered minimal (well-sealed vial).

# Chapter Four: METHOD SETUP AND LIMITATIONS OF KINETIC STUDY OF ESTERIFICATION REACTION

## 4.1 Introduction

Before starting the kinetic study for analysis of the performance of petcoke-derived catalysts in comparison to standard materials, it is important to have a robust method. This method should have a minimal experimental error on the reaction setup, data collection and analysis, and measure the intrinsic reaction rate to assess the catalytic activity appropriately. Therefore, the assessment of method limitations presented here is intended to provide a solid basis for the determination of kinetic parameters and required properties of catalysts in the next chapter.

The following section details the materials and techniques used for the assessment of the method for catalytic tests. Section 4.3 presents some preliminary experiments, the evaluation of reactor setup and quantification analysis in terms of uncertainty, tests of conditions to avoid mass and heat transfer limitations, and analysis of equilibrium conversion. Section 4.4 summarizes the relevant discussion and conclusions of this chapter.

## 4.2 Materials & Methods

Preliminary experiments were carried out with a simplified reactor setup, which was later substituted by another more robust and reliable setup.

Chemicals used in this study were: octanoic acid ($C_8H_{16}O_2$, 98+%) and Amberlyst-15 (H) ion exchange resin (Styrene-DVB) from Alfa Aesar; methanol ($CH_4O$, ≥ 99.8%), toluene ($C_7H_8$, ≥ 99,9%), dodecane ($C_{12}H_{26}$, ≥ 99%), naphthalene ($C_{10}H_8$, 99+%), and dibenzothiophene ($C_{12}H_8S$, 98%) from Sigma-Aldrich; sulfuric acid ($H_2SO_4$, 98%) and anthracene ($C_{14}H_{10}$, 96+%) from EM Science; and methyl octanoate ($C_9H_{18}O_2$, > 99.0%) from TCI America.

Compositional analysis was performed using a gas chromatograph with a flame ionization detector (GC–FID) (6890N, Agilent Technologies, Santa Clara, CA, USA), equipped with capillary columns HP-5 (5% phenyl-methylpolysiloxane, 30 m × 320 µm × 0.25 µm; Agilent Technologies, Santa Clara, CA, USA) and DB-FATWAX UI (polyethylene glycol-type, 30 m × 0.25 mm × 0.25 µm; Agilent Technologies, Santa Clara, CA, USA). Using the HP-5 column, the temperature program consisted of 50 °C held for 2 min, a ramp of 30 °C/min up to 220 °C, for analysis with toluene; or 50 °C held for 0.25 min, a ramp of 40 °C/min up to 220 °C, held for 5.5 min at the final temperature, for analysis with dibenzothiophene (DBT). Nitrogen was used as the carrier gas; injection using split mode (ratio 25:1). The temperatures of the inlet and detector were set at 260 °C and 270 °C, respectively. Using the DB-FATWAX UI column, the temperature program of the GC consisted of 0.5 min at 50 °C, a ramp of 40 °C/min to 200 °C, and 2 min at the final temperature. Helium was used as the carrier gas, and the injection used the split mode (ratio 50:1). The temperatures of the inlet and detector were set at 250 and 300 °C, respectively. The detector mode used was constant makeup flow.

The catalysts used in the preliminary set of experiments were provided by members of the LECA group from the University of Calgary. The first set of catalysts included PC-S (sulfonated petcoke [21]) produced by Ye Xiao, and $H_2SO_4$, a standard liquid catalyst. The catalysts included in the second set of experiments were: P-S-24, P-N/S-24, P-N-24, produced by Qing Huang [112]. In these catalyst names, P refers to the petcoke starting material, S refers to treatment with sulfuric acid, and N refers to treatment with nitric acid. The P-N/S-24 sample was treated with a mixture of both acids, and all catalysts were treated with the acid(s) at 120 °C for 24 h. The properties are given in Table 4-1.

The new reactor setup and reaction conditions were tested using Amberlyst-15, a commercial sulfonated cation-exchangeable material. P-S-3 and P-N-3, petcoke-derived catalysts produced by Qing Huang using treatment with sulfuric acid and nitric acid at 120 °C for 3 h, were also included in the test of temperatures and catalyst loadings, respectively.

Table 4-1. Properties of catalysts used for the preliminary reactor tests.

| **Catalyst** | **Strong acidity (mmol/g)** [1] | **Total acidity (mmol/g)** [2] | **Physical properties** | **Reference** |
|---|---|---|---|---|
| **PC-S** | 1.25 | 2.82 | Particle size: 45 - 90 μm | [21] Ye Xiao |
| **$H_2SO_4$** | 20.4 | 20.4 | -- | Calculated |
| **P-S-24** | 0.25 | 1.49 | Pore size: 0.4 - 0.8 nm<br>Surface area:<br>4.6 $m^2/g$ [3] - 174 $m^2/g$ [4] | [112] Qing H. |
| **P-N/S-24** | 0.73 | 5.46 | Pore size: 0.4 - 0.6 nm<br>Surface area:<br>2.3 $m^2/g$ [3] - 125 $m^2/g$ [4] | [112] Qing H. |
| **P-N-24** | 0.70 | 5.25 | Pore size: 0.4-0.6 nm<br>Surface area:<br>4.1 $m^2/g$ [3] - 151 $m^2/g$ [4] | [112] Qing H. |
| **Amberlyst-15** | 4.70 | 4.70 | Particle size: > 500 μm | Experimental/ manufacturer |
| **P-S-3** | 0.25 | 1.05 | Particle size: < 63 μm | Qing H. |
| **P-N-3** | 0.35 | 4.67 | Particle size: < 50 μm<br>Surface area:<br>3.2 $m^2/g$ [3] - 217 $m^2/g$ [4] | Qing H. |

[1] [-$SO_3H$] determined by titration with NaCl; [2] determined by titration with NaOH; [3] by $N_2$ adsorption; [4] by $CO_2$ adsorption.

## 4.3 Results & Discussion

### *4.3.1 Simplified Reactor Setup*

The methodology used by Xiao & Hill (2020) [21] was employed as the initial setup for this study. The reaction took place in an Erlenmeyer flask, with a capacity of 125 mL, housed in a water bath,

which was a beaker of 1 L. A stirring hotplate (Corning® PC-240D) and Graham condenser (with 24/40 joint, 500 mm jacket length, borosilicate glass coil) were used for heating and reflux. A distillation adapter with a sampling port was used for catalyst insertion and sample withdrawal using a tube and syringe. The reagents were added into the flask: 5 mL of octanoic acid, 50 mL of methanol, and 5 mL of toluene – the latter was used as the internal standard for the subsequent analyses. The octanoic acid was weighed before the mixture with the other compounds on the analytical balance AB304-S model (Mettler Toledo, Columbus, OH, USA). In a typical experiment, the reaction mixture was heated up to 60 °C and stirred at a speed of 500 rpm. The catalyst was placed into the reaction media only after the temperature stabilized (approximately 15 min after reaching 60 °C); then, the reaction time was started.

Samples of approximately 1 mL of the suspension were withdrawn periodically by a tube connected to a plastic syringe through the sampling port (the sampling decreased the volume by less than 15% of the initial reaction volume). The samples were filtrated using membrane filters of 0.45 and 0.22 µm (pore size), EZFlow® (Foxx Life Sciences), to remove the solid catalyst and prevent further reaction. After filtration, samples were placed inside vials of 20 mL while waiting for GC analysis for composition determination.

### *4.3.2 Preliminary Experiments*

The experimental conditions used for the two preliminary tests with the simplified reactor setup are summarized in Table 4-2. These preliminary tests were carried out as a first evaluation of the effectiveness of functionalized petcoke for catalyzing esterification reactions.

Table 4-2. Experimental conditions used for the preliminary tests with the simplified reactor setup.

| | 1st set of experiments | 2nd set of experiments |
|---|---|---|
| **Catalysts** | $H_2SO_4$, PC-S | P-S-24, P-N-24, P-N/S-24 |
| **Temperature** | 60 °C | 60 °C |
| **Stirring speed** | 500 rpm | 500 rpm |
| **Catalyst loading** | 2 wt% ($H_2SO_4$), 4.5 wt% (PC-S) | 10 wt% |
| **Time** | 2 h ($H_2SO_4$), 3 h (PC-S) | 4 h |
| **Methanol-to-acid ratio** | 40:1 | 20:1 |

The first preliminary set of reactions tested $H_2SO_4$ and PC-S over 2 - 3 h of reaction. The results were obtained in terms of acid conversion and ester yield (by GC analysis with capillary column HP-5), as shown in Figure 4-1.

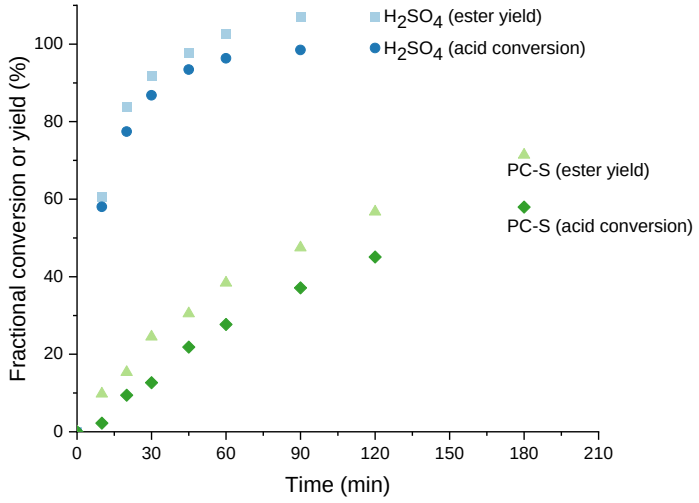


Figure 4-1. Results using the simplified reactor with catalysts PC-S and $H_2SO_4$. The reaction conditions were 60 °C, 500 rpm, methanol-to-acid ratio equal to 40:1, and catalyst loading of 4.5 wt% (octanoic acid) for PC-S and 2 wt% for $H_2SO_4$.

Almost complete conversion was achieved after only 1 h of reaction catalyzed by $H_2SO_4$, while with catalyst PC-S, 60% conversion was achieved after 3 h of reaction.

The selectivity of reaction was assumed to be 100% towards the ester product, as no other peaks were observed by GC analysis besides the reagents, internal standard, and ester. If other products resulted from the reaction, however, they might have remained adsorbed on the catalyst surface or as traces in solution, not being detected by GC-FID as the water product. Most studies in the literature [29], [31], [79], [88] only report ester and water as products of this reaction over a wide range of catalysts.

The carbon balance, however, did not equate in those reactions, highlighting some experimental issues. To compare at the same baseline, the results were given in percentage and not in mass of compounds. As can be seen, the amount of ester produced was higher than the corresponding amount of acid converted. Furthermore, the ester was overestimated (> 100%) at the end of the reaction with $H_2SO_4$. This overestimation might be related to sample losses (especially methanol and toluene evaporation), which will be explained later in Section 4.3.4. This error affects more high concentration values in GC analysis, which is the case of ester when reaching the equilibrium level. The GC analysis error was estimated as high as 8.9% (standard deviation) for these reactions.

The TOF values were found through both Equations 16 and 17, based on the reaction rate constant or the product amount, for this first set of experiments. In order to obtain the rate constant necessary for Equation 16, the reaction data were fitted into a pseudo-homogeneous first-order model, dependent only on acid concentration, according to Equation 20 (Figure 4-2). The model fit the data obtained with both catalysts, although there were minimal data (i.e., only three points) for the reaction with $H_2SO_4$ as it is a much more active catalyst.

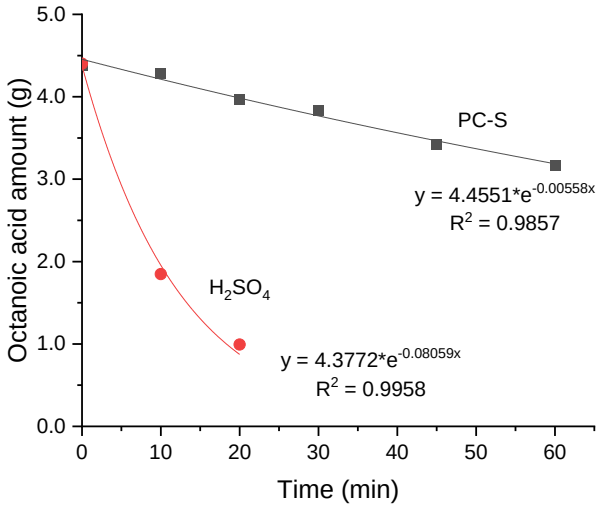


Figure 4-2. Pseudo-homogeneous first-order model fit to the esterification data shown in Figure 4-1 for catalysts PC-S and $H_2SO_4$.

Applying the corresponding rate constants ($k$) to Equation 16, the TOF values found were 92 $h^{-1}$ and 40 $h^{-1}$ for the $H_2SO_4$ and PC-S, respectively. Using the same methodology [21], however, the previously reported values were 87 $h^{-1}$ and 48 $h^{-1}$, for $H_2SO_4$ and PC-S, respectively, which indicates reproducibility issues with the simplified setup.

Using Equation 17, in which the TOF is based on the product produced rather than the reactant consumed (Equation 16), over the same time periods used above (i.e., 20 min for $H_2SO_4$ and 60 min for PC-S), the TOF values were 47 $h^{-1}$ and 45 $h^{-1}$, respectively. The values for the PC-S catalyst using either Equation 16 or 17 are within experimental error. The different values with $H_2SO_4$ may be because the reaction rate had a non-linear behavior, being not well represented by the pseudo-first-order model. Different methodologies for calculating the TOF are likely responsible for the variety of values reported in the literature. In addition, data is not always obtained below 10% of the equilibrium conversion, above which the presence of products (~ 80%

ester yield, in this case) affects the net reaction rate, invalidating the assumption of the pseudo-first-order model.

Another set of materials was tested, specifically, petcoke samples functionalized with sulfuric acid, nitric acid, or a mixture of both. In this case, the conditions differed slightly from before: catalyst loading of 10 wt% (octanoic acid), methanol-to-acid ratio equal to 20:1, and 4 h reaction. The purpose of increasing the amount of catalyst was to accelerate the conversion by providing a comparable number of acid sites in the reactor – these catalysts had fewer acid sites per catalyst mass. The ester yields and acid conversions are shown in Figure 4-3.

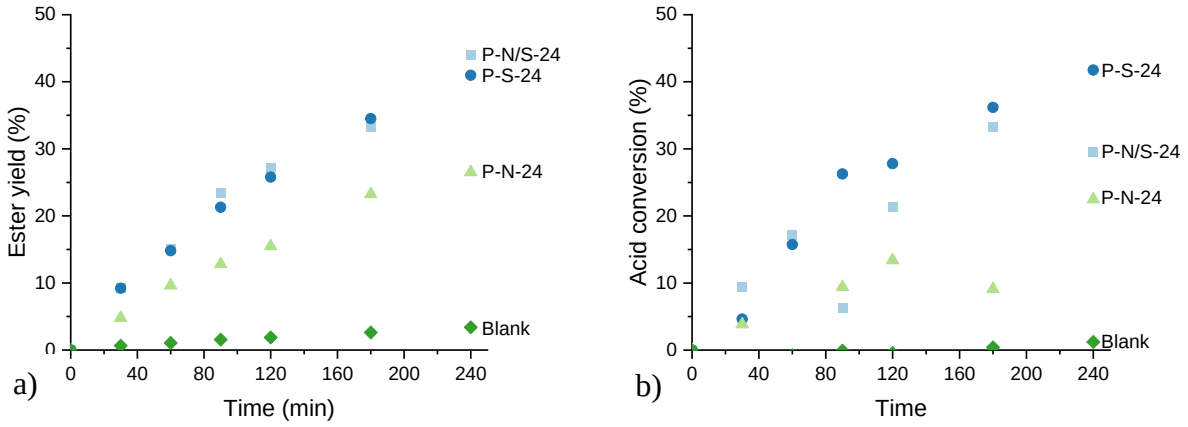


Figure 4-3. Results using the simplified reactor with catalysts P-S-24, P-N/S-24 and P-N-24; a) ester yield, b) acid conversion. The reaction conditions were 60 °C, 500 rpm, methanol-to-acid ratio equal to 20:1, and catalyst loading of 10 wt% (octanoic acid).

The ester yield was lower than with the previous catalysts ($H_2SO_4$ and PC-S) even after increasing the catalyst loading and running the reactions for 4 h. The ester yield decreased in the order of P-N/S-24 (44%) = P-S-24 > P-N-24 (27%). Functionalization with nitric acid was effective in oxidizing the inherent sulfur in the petcoke and developing sulfonic groups [112], as P-N-24 was approximately 68% as active as the sulfonated sample P-S-24.

The results of acid conversion (Figure 4-3b) were inconsistent with the values expected by the ester yield, which was surprising considering the relatively good agreement (Figure 4-1) for the first set of materials tested. With the second set of materials, the reaction rate was lower and the GC column may have been saturated by octanoic acid. The reproducibility of the GC analysis was much worse for the acid conversion (error increased from 5% to up to 23%).

Thus, only Equation 17 was applied for the TOF calculation. The time used in the equation varied from catalyst to catalyst since data at a maximum of 10% ester yield (initial TOF) were used. The strong acidity values (from Table 4-1) were used for this calculation. The results are shown in Table 4-3. For comparison, the TOF values were also calculated for the total reaction time (4 h).

Table 4-3. TOF values for petcoke-catalyzed reactions (preliminary set of experiments).

| **Experiment** | **Initial TOF ($h^{-1}$)** | **TOF of 4h ($h^{-1}$)** |
|---|---|---|
| P-N/S-24 | 17 | 10 |
| P-S-24 | 50 | 28 |
| P-N-24 | 9 | 6 |

The initial TOF values pointed out that P-S-24 is the most active catalyst of this group and not P-N/S-24, as observed in Figure 4-3. The TOF values of 4 h are only illustrative of the decrease of reaction progress with time due to the large presence of product species. Hence, TOF determination through Equation 17 only makes sense for the beginning of a reversible reaction, as esterification reactions show an approximately linear behavior with time at conversions lower than 15% [123].

Besides that analysis, another parameter that requires special attention in the TOF calculation is the strong acidity of the functionalized petcoke. For this set of materials, the value corresponded

to the sulfonic group concentration and was determined using the ion-exchange titration method. Those values, however, might be overestimated due to the presence of other acidic groups on the samples treated with nitric acid only, which contributed to the exchanged $H^+$ [112]. Therefore, those initial TOF values are still not reliable.

After analysis of the preliminary results, other sources of error were identified related to the reaction system and data collection. Sample loss – due to evaporation during the reaction (not well-sealed system), handling, filtration, and/or waiting time for analysis – was one of the main causes of uncertainties. As a study involving liquid-vapor equilibrium, the mixture composition is very sensitive to any source of disturbance. In addition, the GC analysis was less reproducible, which will be discussed later in this chapter (Section 4.3.4). Therefore, a new reactor setup was proposed, with improvements to solve those issues and obtain more reliable results.

### *4.3.3 New Reactor Setup*

In the second setup, the major modifications were the reactor and sampling method. The new reactor consisted of a two-neck round bottom flask with a capacity of 100 mL. This setup was used for many conditions, including the different alcohol-to-acid ratios, adjusted accordingly to keep the reaction volume constant. The total reaction volume filled less than half of the reactor capacity, providing enough space for the vapor phase.

The flask center top joint was connected to a Graham condenser, the same as the previous setup; meanwhile, the other top joint was connected to an adapter, which was the new sampling port. Plastic clamps of size 24 were used to hold the glassware joints together. The adapter, 24/40 joint, had a thread at the top to accept a cap with a hole and PTFE (polytetrafluoroethylene) faced septum, enabling the needle insertion. The PTFE/silicon was chosen based on its compatibility

with the reaction mixture, and resealing capability so that multiple samples could be withdrawn by a syringe needle during an experiment. The septum was replaced after each experiment.

In a typical reaction, 5 mL of octanoic acid, 0.1 - 0.2 g of catalyst, and 1 mL of the internal standard were weighed on the analytical balance AB304-S model (Mettler Toledo, Columbus, OH, USA) and placed inside the flask before heating up. When the system reached the desired temperature, 25 mL of methanol was inserted through the sampling port, starting the reaction.

The sampling was done by inserting a needle through the septum connected to a plastic syringe of 10 mL. The needle was 7" in length (180 mm) and of Gauge 18 (nominal O.D. 1.2 mm). The 18 gauge is suitable for sampling with all catalysts employed, petcoke-derived and Amberlyst-15. In the latter case, although the beads are large, no needle clogging was observed. During experiments, samples < 0.5 mL were collected periodically from the reaction media, which decreased the volume by less than 15% of the initial reaction volume. The sampling was done 7 - 8 times in each experiment, keeping the needle connected to the septum to avoid multiple punctures and loss of reaction compounds; meanwhile, the syringe was disconnected from the needle and immediately replaced by another syringe to keep the sampling port closed. The system was well sealed by applying silicone lubricant on the glass joints (Dow Corning® high vacuum grease), which also reduced the loss of compounds. Evaporation from the system was believed to be minimal since the reflux condenser was operated at room temperature. Thus, the methanol loss from the system at this temperature was significantly reduced.

The heating method did not change – use of the stirring hotplate Corning® PC-240D and a 2 L beaker as a water bath. For agitation, an egg-shaped stir bar of 19 x 9.5 mm was used inside the flask. Figure 4-4 illustrates the final assembly of the new reactor setup.

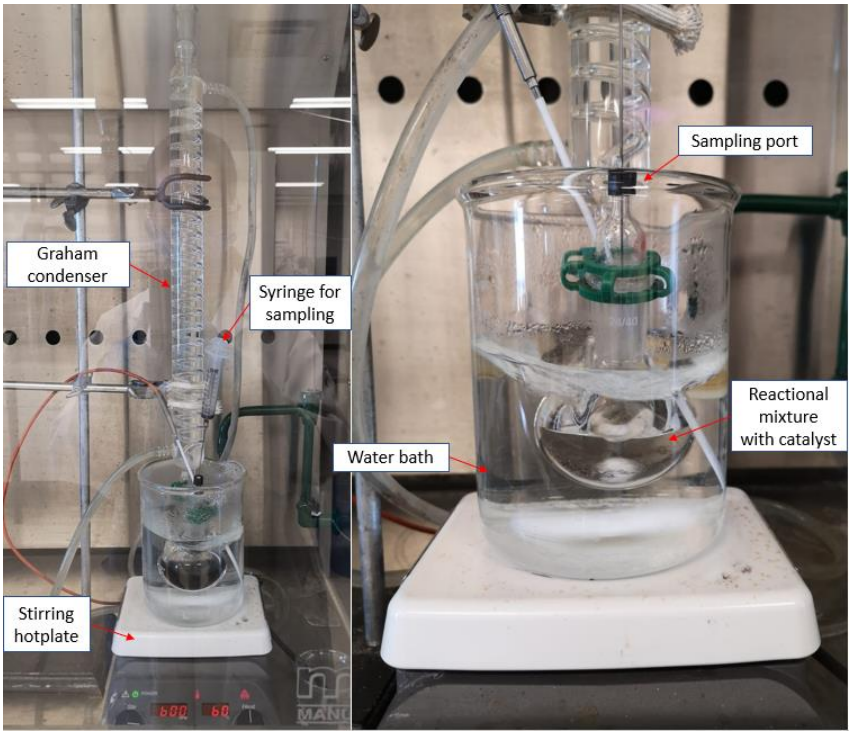


Figure 4-4. Assembly of new reactor setup used for testing catalysts in the esterification of octanoic acid.

The samples were filtrated using the same membrane filters, EZFlow® (Foxx Life Sciences), with pore sizes of 0.45 or 0.22 µm. Depending on the catalyst particle size, however, a prefiltration was done using a 0.45 µm pore size filter, followed by filtration for fine particles removal using a 0.22 µm pore size filter. In other cases, only one filtration was required. After filtration, the solution was placed into small vials of 2 mL to reduce the available headspace over the sample and avoid significant methanol in the vapor phase. Vials were covered with parafilm M (PM-996, Bemis). Samples for analysis were collected by puncturing the covering film (without opening the vials) with the GC microsyringe. The samples were injected into the gas chromatograph (GC) immediately.

*4.3.4 Internal Standard and GC Analysis*

The capillary column used for GC analysis was an HP-5, a multi-purpose column for non or slightly polar components. Although the column is not designed for a mixture involving an organic acid, alcohol, and ester, the separation was possible, and some preliminary results were collected by using it.

The fronting peaks of octanoic acid demonstrated its incompatibility for analysis with the HP-5 column. Fronting peaks are caused by either an incompatible stationary phase or column overloading (more material onto the column that it can handle) [124]. To solve the first issue, it would be necessary to choose a column with a stationary phase more compatible with the material to be injected. If the second cause is the problem, it could be solved by choosing a column with a thicker stationary phase or reducing the column loading by injecting less material onto the column. The latter option would not be possible in this case since injections of 0.1 µL were already being used. As verified later, another more adequate column was chosen for this analysis.

An internal standard was employed during – and not after – the reaction to account for sample losses due to handling and transfer. The choice of an adequate internal standard improves the precision and accuracy of results obtained by the GC method. The ratio 'analyte'/'internal standard' is kept almost constant from reactor sampling to analysis. The internal standard should be properly chosen based on [125]:

- chemical similarity to the analyte in terms of functional groups, boiling points, and activity; besides, it should never be naturally found in the sample;
- resolution from other peaks, as it should not co-elute with other peaks (overlapping), which precludes the quantification of areas;

- inertness to the reaction and stability, as it must be constant throughout the reaction.

Toluene was initially used as the internal standard. The peak areas were not constant, however, suggesting some evaporation from the system and /or sample. The vapor pressure of toluene at 60 °C is 0.18 atm [126], which corresponds to the evaporation of 5 - 7% at the reaction temperature. Considering boiling point and inertness, dodecane was a potential candidate for this purpose. Compared to toluene, its vapor pressure at 60 °C is 80 times lower (0.0022 atm) [126]. The chromatogram of GC analysis with the HP-5 column, however, showed co-elution of dodecane with octanoic acid, preventing its use as an internal standard. Naphthalene also co-eluted with octanoic acid, even testing several oven temperature programs. Anthracene has a higher boiling point of 340 °C, and was expected to elute from the capillary column after all the other compounds. The low solubility of anthracene in methanol, however, excluded its use.

The final internal standard tested was dibenzothiophene (DBT). DBT showed well-resolved peak areas, has a high boiling point (332.5 °C) eluting separately at the end of the analysis, and was inert to the reaction system when tested in a reaction catalyzed by $H_2SO_4$. The stability of DBT was tested at 60 °C. Using dodecane as an internal standard for the DBT quantification, the ratios 'DBT'/'dodecane' were analyzed over a 3 h test, with one sample collected per hour. The standard deviation of GC analysis was as high as 15.1% for the same sample and 3.2% between samples.

Moreover, samples of known concentrations were prepared at approximate conversions, $x$, of 0, 50, and 90%. The purpose was the verification of the accuracy and precision of the GC analysis (with the HP-5 column) when using DBT as an internal standard. The results are given in Table 4-4.

Table 4-4. Test of GC analysis using known samples and DBT as internal standard.

| | Acid | | Ester | |
|---|---|---|---|---|
| $x$ (%) | $\bar{x}$ (%) | Error (%) | $\bar{x}$ (%) | Error (%) |
| 00 | 2.23 | 2.3 | 0.15 | -- |
| 50 | 49.3 | 0.4 | 46.4 | 7.5 |
| 90 | 89.9 | 2.9 | 83.3 | 9.4 |

The conversion values were calculated through the masses given by the DBT calibration curve. The mean conversion ($\bar{x}$) is the mean value obtained for sample analysis in triplicate. The error was calculated as the difference between the weighed amount using an analytical balance and the mean value obtained by GC. In other words, it is related to the random error of measurement by GC. No ester was inserted in sample 0%; this way, no error was calculated for this analysis.

Despite the results obtained in Table 4-4, the analyses were more complicated when working with a reaction system, as the samples were not completely stable while waiting for analysis. The instability was due to the leaching of sulfonic species from the catalyst surface, which possibly promoted the reaction inside the sample vials (more details in Section 5.3.2). In reactions catalyzed by $H_2SO_4$, the catalyst could not be separated from the reaction mixture as well.

The reproducibility of the new setup was tested in a standard reaction using Amberlyst-15 (catalyst loading of 4.5 wt%) and the following conditions: 60 °C, 600 rpm, 4 h, and methanol-to-acid ratio equal to 40:1. The reaction was run three times, and the mass of the catalyst varied by no more than 6.2%. This difference was due to the bead shape of Amberlyst-15, which complicates its weighing. The results are shown in Figure 4-5.

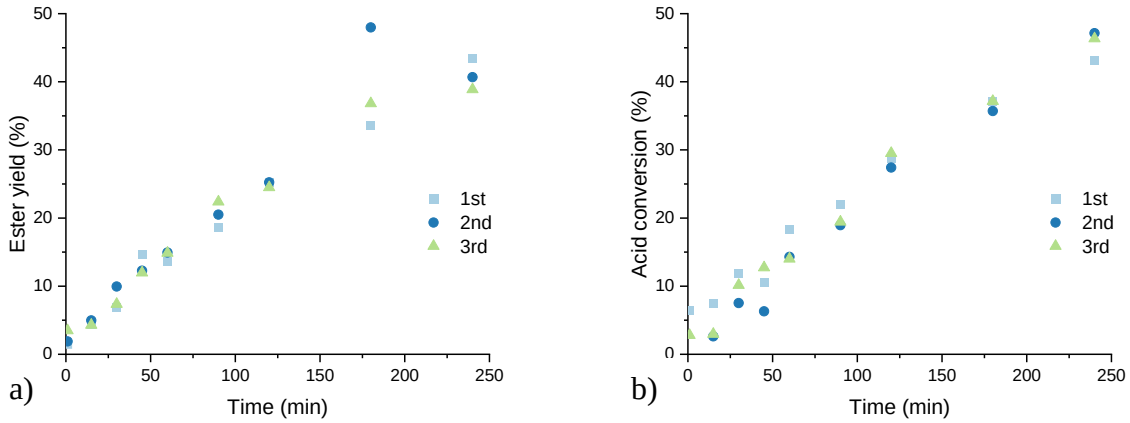


Figure 4-5. Results of reproducibility tests of the new reactor setup using Amberlyst-15; a) ester yield, b) acid conversion. The reaction conditions were 60 °C, 600 rpm, 4 h, methanol-to-acid ratio equal to 40:1, and catalyst loading of 4.5 wt% (octanoic acid).

The figures above demonstrated that the reproducibility is generally better for the ester quantification at low conversions and for the acid quantification at higher conversions (longer reaction times). This result was expected since the ester amount is minimal initially, and variations in concentration due to sample losses affect the ester less. The opposite was expected as conversion reaches the equilibrium level, and errors due to sample loss affect the ester values (high concentration) more.

The standard deviation results for measuring the acid amount were as large as 170% at the beginning of the reaction, with conversion values between [-1.9 – 6.4%] at 1 min of reaction progress. The negative value means that more acid amount was measured by GC analysis than the initial mass weighed on the analytical balance and inserted into the flask. At approximately 50% conversion, the standard deviation for the acid amount was approximately 5%. Ester results were not so spread at the beginning of the reaction as the acid, but the standard deviation was as large as 20% at some points. These variations resulted in the ester yield not continuously increasing with

time. For example, during the first reaction, the ester yield was 14.7% at 45 min and 13.6% at 60 min.

During the reaction progress, no known concentration is available for comparison with the GC analysis. Therefore, analyses in triplicate were used to estimate the standard error associated with the uncertainty of equipment. Doing a triplicate analysis for the same sample at around 20% conversion, a standard deviation of 14% was found for the ester amount. This error was expected to be lower, especially at the beginning of the reaction, which is the most important data range for this kinetic study.

All the errors found in this set of experiments pointed out the incompatibility of the HP-5 column for the analysis of this reaction system. Therefore, as the last step in the new setup setting, a more suitable capillary column was adopted for this analysis.

DB-FATWAX Ultra Inert (UI) is a specific capillary column for analyzing esters and organic acids, showing well-resolved peaks, and no co-elution of compounds. It is the best column for complex samples, including alcohols, organic acids, and others. The manufacturer Agilent reported tests for a mixture of alcohol, hydrocarbon, acid, ester, etc., in which they did not have co-elution even using a short analysis time [127]. They obtained a standard deviation of absolute peak areas within 2% for 15 repetitive injections in that report.

A DB-FATWAX UI column was purchased and installed in the GC-FID equipment. Besides the new column assembly, a complete cleaning was done on the equipment, including the split/splitless inlet and the flame ionization detector. As regular maintenance to avoid contamination (responsible for ghost peaks and other issues during analysis), some inlet parts were replaced. Those parts included ultra inert split liner, ultra inert gold seal with washer, split vent trap, o-ring,

and bleed temperature-optimized (BTO) septa. Fixed parts of the inlet in addition to the collector and jet (parts of the detector) were cleaned using the procedure described in the manual. An oxygen trap was also installed in the carrier gas line to protect the column against oxidation at GC operating temperature.

Preliminary tests showed no co-elution of compounds, enabling the use of dodecane – the most suitable compound for the reaction mixture – as the internal standard. The new column, however, required a longer time to elute all the reaction compounds. To keep the analysis at a feasible sampling time (i.e., every 15 min for composition quantification), the carrier gas was changed from $N_2$ to He at an initial flow rate of 1.6 mL/min. The total analysis time was 14 min, considering the temperature program of 50 °C (held for 0.5 min), a ramp of 40 °C /min until 200 °C (held for 2 min), plus the time to cool down the equipment for subsequent analysis.

Although all the measures were taken with the new column, the peak associated with octanoic acid still showed small tailing, probably due to the column incompatibility with that specific compound or contamination in the system. The second hypothesis was disregarded because many actions mentioned above were taken to minimize contamination. On the other hand, the column is completely compatible with the ester (methyl octanoate), showing sharp well-resolved, and symmetric peaks (Figure A-1 in Appendix A). The injection volume of 0.1 µL with a split ratio of 50:1 was in agreement with both the column capacity and the split liner volume, avoiding any issues related to the volume expansion inside the liner and overloading the column causing front peaks.

Reaction tests were performed using two different reagent ratios, Figure 4-6, to confirm that the new column would provide better reproducibility, independent of the ratio of the reagents chosen.

In this case, the new DB-FATWAX UI (green lines) and old HP-5 (blue lines) columns were tested at 60 °C, 600 rpm, 4 h, catalyst loading of 4.5 wt%, and methanol-to-acid ratio equal to 40:1 or 20:1.

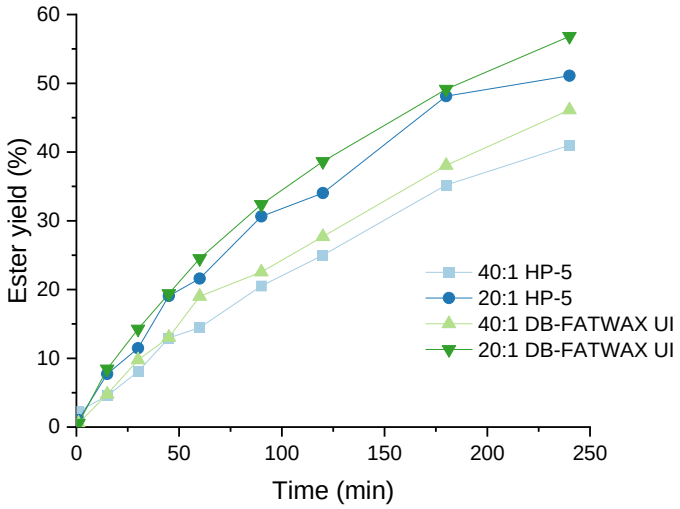


Figure 4-6. Results of ester yield analyzed by GC columns HP-5 and DB-FATWAX UI; reactions with Amberlyst-15 at same conditions (60 °C, 600 rpm, 4 h, catalyst loading of 4.5 wt%), and methanol-to-acid ratio equal to 40:1 or 20:1.

A more consistent trend in the ester yield with time was observed after the new column installation. Triplicate analysis of the same sample at ~40% conversion – range expected to show an increase in the uncertainty of ester quantification –, showed a standard deviation between 0.6 - 1.3% in the ester quantification for ratios 40:1 and 20:1. Therefore, the analysis of reaction progress for the kinetic study was preferred in terms of the ester yield since it has a low concentration at the beginning of the reaction, resulting in less error in its determination using the calibration curve.

As previously mentioned, the tailing peaks of the acid are problematic, so the trends were still not good with the new column. The higher uncertainty in the acid quantification is related to the high concentration at the beginning of the reaction and would happen even if the column was totally

compatible. Therefore, the acid amounts were not used in the kinetic study after this point. The acid results for the same reactions of Figure 4-6 are displayed in Figure A-2, in Appendix A.

*4.3.5 Test of Conditions*

The effect of external mass transfer resistances is normally evaluated in the literature by performing experiments at different stirring speeds [14], [89], [128], [129]. Based on theory, in the presence of external mass transfer resistance, the specific reaction rate constant ($k_r$) is much greater than the mass transfer coefficient ($k_c$): $k_r \gg k_c$. Therefore, the reaction rate will be proportional to the mass transfer coefficient and consequently to the superficial velocity when external mass transfer is the limiting step, Equation 26.

$$-r''_A \propto k_c C_A \propto U^{\frac{1}{2}} \qquad 26$$

where $-r''_A$ is the rate of reaction per area of catalyst surface; $C_A$ is the bulk reactant concentration; and $U$ is the superficial velocity of the fluid. The mass transfer coefficient increases with the square root of the superficial velocity of the fluid flowing past the particle, according to Equation 27,

$$k_c = 0.6 \frac{D_{AB}^{2/3}}{\nu^{1/6}} \frac{U^{1/2}}{d_p^{1/2}} \qquad 27$$

where $k_c$ is the mass transfer coefficient; $D_{AB}$ is the diffusivity of the limiting reactant in the solvent; $\nu$ is the kinematic viscosity; $d_p$ is the diameter of the catalyst particle. For example, if velocity is doubled, the rate of reaction should increase by a factor of 41%: $(U_2/U_1)^{0.5} = 2^{0.5} = 1.41$.

The stirring speeds were tested in the range between 200 - 800 rpm using the Amberlyst-15 catalyst. The other conditions were 60 °C, catalyst loading of 2 wt%, methanol-to-acid ratio of 20:1, and 90 min reaction. The resulting yields are presented in Figure 4-7.

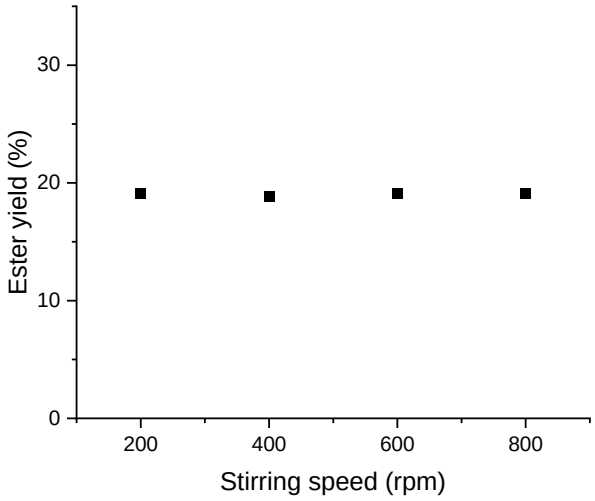


Figure 4-7. Influence of stirring speed on the ester yield; results after 90 min of reaction at 60 °C, catalyst loading of Amberlyst-15 equal to 2 wt%, and methanol-to-acid ratio of 20:1.

The ester yield was essentially the same for all conditions. Moreover, the initial reaction rate was almost constant at 2.2 x $10^{-6}$ mol/mL·min, suggesting that external mass transfer limitations are not present. The stirring speed of 600 rpm was selected for further experiments.

The catalyst loading was investigated in the range of 1 - 4.5 wt% (relative to the mass of octanoic acid). Results are presented in Table 4-5. The increase of the catalyst loading is expected to cause a proportional increase in the volumetric reaction rate and product yield in the absence of mass transfer resistance [11]. The reaction rate is only the limiting step when the catalyst is fully utilized for the reaction. From the results of Table 4-5, it is possible to conclude that there are some transfer limitations with the mass of 0.2 g (4.5 wt%) of Amberlyst-15. Not all active sites were accessible by the reactants; otherwise, the increment on the volumetric reaction rate and ester yield would

not be 1.6 x from mass 0.1 to 0.2 g, but around the double, as the mass was doubled. Therefore, 2 wt% was selected as the adequate catalyst loading for the third set of experiments in the kinetic study (Section 5.3.1).

Table 4-5. Results of ester yield and initial reaction rate using different catalyst loadings for the reaction: 60 °C, 90 min, 600 rpm, and methanol-to-acid ratio equal to 20:1.

| **Amberlyst-15 (g)** | **Initial rate (mol/mL·min x $10^6$)** | **Ester yield (%)** |
|---|---|---|
| 0.0552 | 1.38 | 11.2 |
| 0.1017 | 2.51 | 20.3 |
| 0.2015 | 4.64 | 32.4 |

For petcoke-derived catalysts, however, the mass transfer limitations should not be expected with a loading of 4.5 wt%, as the concentration of active sites is reduced compared to the acidity of Amberlyst-15. Increasing the mass of P-N-3, for example, from 0.1 to 0.2 g, the ester yield increased from 3.6 to 7.0 %, with a proportional increase in the initial reaction rate. Therefore, a catalyst loading of 4.5 wt% was selected for the fourth set of catalysts of the kinetic study (Section 5.3.4).

External mass transfer limitations were unsuccessfully assessed by a calculation method from the literature, as described in Appendix A. That evaluation was not possible, probably due to the uncertainties in the estimation of some parameters and other assumptions. The same uncertainties affected the internal mass transfer calculation, unfortunately.

The methanol-to-acid ratio was evaluated keeping constant the other conditions, i.e., 600 rpm, 60 °C, catalyst loading of 2 wt% (relative to the mass of octanoic acid), and 4 h reaction. The methanol-to-acid ratio was adjusted accordingly for the experiments, keeping the total mixture

volume of 31 mL constant. In this case, a longer reaction time was employed to observe the effect of excess methanol in the reaction progress. The results are presented in Figure 4-8.

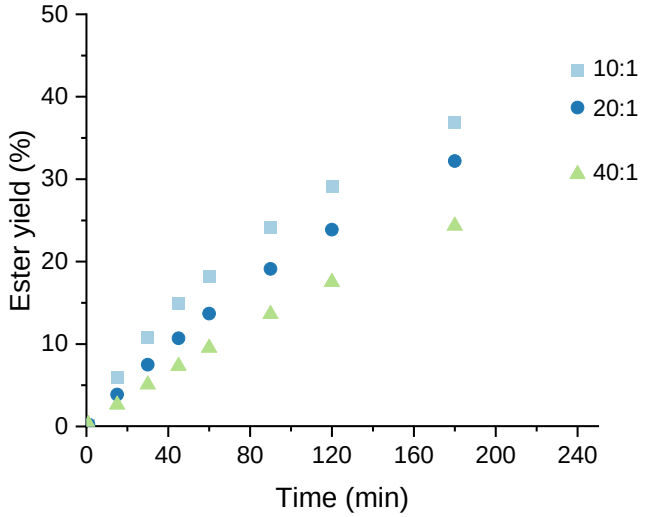


Figure 4-8. Influence of methanol-to-acid ratio on the ester yield; results after 4 h of reaction at 600 rpm, 60 °C, and catalyst loading of Amberlyst-15 equal to 2 wt%.

Besides the highest ester yield, the methanol-to-acid ratio 10:1 also showed the best performance in terms of the initial reaction rate, equal to 5.6 x $10^{-6}$ mol/mL·min in comparison to 2.2 x $10^{-6}$ mol/mL·min and 0.9 x $10^{-6}$ mol/mL·min for methanol-to-acid ratios 20:1 and 40:1, respectively. Nevertheless, to keep the same proportion of acid sites for reaction relative to the mass of octanoic acid, the amount of catalyst in solution was larger for the condition of 10:1. Approximately 0.18 g was the necessary mass of catalyst (2 wt%) in this condition, suggesting some transfer limitations. This issue was tested and confirmed by the results in Table 4-6.

Table 4-6. Test of transfer limitation for the condition of methanol-to-acid ratio equal to 10:1, 60 °C, 90 min, 600 rpm, and catalyst loading of Amberlyst-15 equal to 2 wt%.

| **Amberlyst-15 (g)** | **Initial rate (mol/mL·min x $10^6$)** | **Ester yield (%)** |
|---|---|---|
| 0.1797 | 5.62 | 43.2 |
| 0.0900 | 3.41 | 30.6 |

Similar to the conclusion obtained by the results in Table 4-5, not all active sites were accessed in reaction with a methanol-to-acid ratio of 10:1 using 0.18 g of catalyst (2 wt%). Otherwise, using less mass of Amberlyst-15, the initial reaction rate and ester yield would be proportional. The methanol-to-acid ratio of 5:1 was not tested for that same reason. During the experiment preparation, it was verified that the amount of catalyst necessary to keep the proportion of 2 wt% (relative to the mass of octanoic acid in solution) would result in 0.28 g, implying the same problem of transfer limitation.

The methanol-to-acid ratio equal to 20:1 was selected as the most appropriate condition for the subsequent tests, avoiding transfer limitations and favoring a high conversion of the limiting reagent. Excess methanol up to the optimum level tends to improve the diffusion and miscibility between reagents [130]. Even though the excess methanol would theoretically increase the ester yield, the opposite was observed for the methanol-to-acid ratio of 40:1. Due to an excessive amount of methanol that increases the dispersibility of the catalyst, less interaction resulted among octanoic acid, solvent, and catalyst, consequently decreasing the production of ester [131]. Moreover, as methanol has not been recovered in this study, it would also increase the production cost.

The temperature effect was evaluated keeping constant the other conditions, i.e., 60 °C, 600 rpm, methanol-to-acid ratio of 20:1, catalyst loading of 2 wt%, 90 min reaction. Amberlyst-15 and P-S-3 were chosen for this analysis, as they showed similar performances with time. Further determination of the corresponding activation energies was assessed in Section 5.3.3. The results are presented in Figure 4-9.

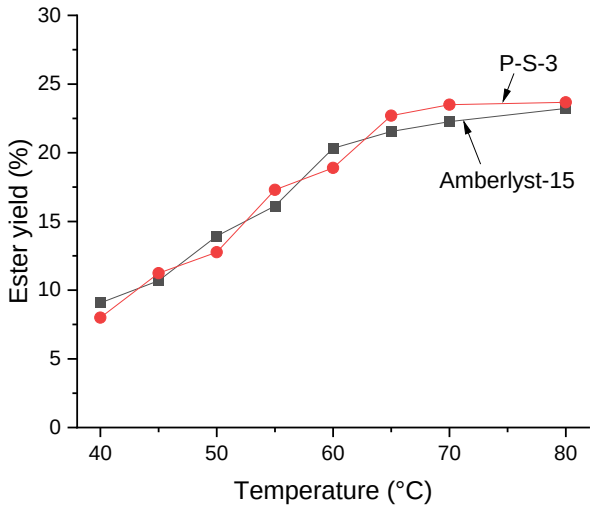


Figure 4-9. Influence of temperature on the ester yield using catalysts Amberlyst-15 and P-S-3; results after 90 min of reaction at 60 °C, 600 rpm, methanol-to-acid ratio of 20:1, and catalyst loading of 2 wt%.

As expected, the reaction conversion increased for both catalysts with temperature. As the temperature increases, the fraction of collisions with sufficient energy to overcome the activation energy and form products also increases [90]. Over the methanol boiling point (64.7 °C), however, the observed increase in the ester yield was not significant. Using Amberlyst-15, even the reaction at 60 °C had a similar rate as those at higher temperatures. As confirmed later in Section 5.3.3, at temperatures above the methanol boiling point, transfer limitations existed. Niu *et al.* [65] also reported poor mass transfer during the esterification of oleic acid with ethanol over the alcohol boiling point. This observation confirms the selection of 60 °C as an adequate temperature to investigate the kinetics of this reaction and determine the catalyst activities.

The effect of temperature on the equilibrium conversion was not experimentally confirmed in this study due to the method limitations. In the next Section 4.3.6, small differences were predicted in the equilibrium conversion in the range of 25 - 200 °C. Considering all the uncertainties associated with the method, it would not be possible to confirm the influence of temperature in the range 25

- 80 °C. Higher temperatures would require a different setup for temperature control than a water bath.

*4.3.6 Equilibrium Conversion*

For reversible reactions, the equilibrium conversion is an important parameter to determine the reaction extent. The thermodynamic parameters, Gibbs free energy of reaction ($\Delta G_r^o$), enthalpy of reaction ($\Delta H_r^o$), and equilibrium constant ($K_e$), given by Equations 9-11, were calculated to evaluate the effect of temperature on the chemical equilibrium. For their estimation, data from the literature for the Gibbs free energy and enthalpy of formations of the octanoic acid and methyl octanoate compounds showed some discrepancy between sources. Therefore, a simulation of required data was made using Aspen Plus®. The enthalpies and Gibbs free energies of formation were calculated in the thermal range of 25 - 200 °C, so no approximation using equations of heat capacity for each component was necessary. The thermodynamic method chosen was UNIQUAC with Hayden-O'Connell equation of state as vapor phase model. The UNIQUAC model is predictive for strongly nonideal liquid solutions (combination of polar and non-polar compounds) and liquid-liquid equilibria [132]. The reaction was considered isothermal, at a pressure of 1 atm, and with a stoichiometric feed of reagents (1.0 M concentration of each compound). The calculated parameters are illustrated in Figure 4-10, and the data are available in Table A-6 in Appendix A.

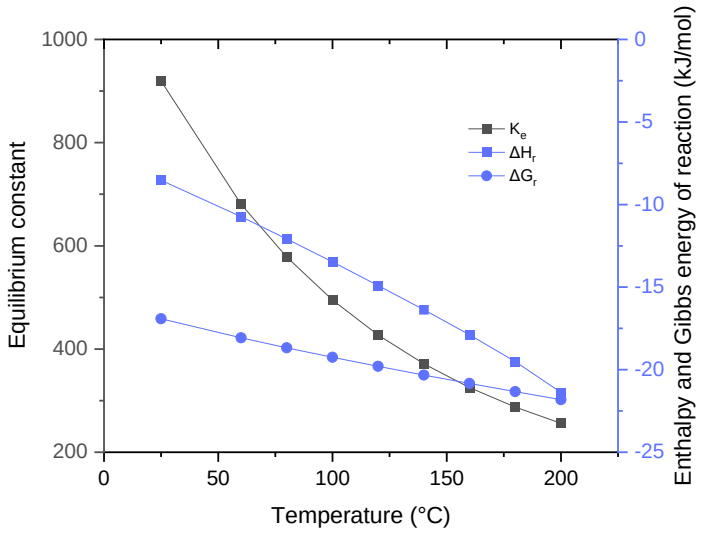


Figure 4-10. Influence of temperature on thermodynamic parameters of the octanoic acid esterification with methanol.

The enthalpy of reaction decreases with temperature, which means the reaction between octanoic acid and methanol is exothermic, and the increase of temperature reduces the product formation. The enthalpy of reaction at 25 ºC is -8.5 kJ/mol. The standard Gibbs free energy of reaction was determined as -16.9 kJ/mol (25 ºC), being a spontaneous reaction throughout the analyzed thermal range.

The equilibrium constant at 25 ºC is much greater than one, so the forward reaction is favored, meaning the concentration of products is larger than the reagents at equilibrium, according to Equation 8. Although the equilibrium constant decreases significantly with temperature, the equilibrium conversion at a typical reaction temperature of 60 ºC did not differ so much from 25 ºC, as confirmed by the values in Table 4-7. The equilibrium conversion values were calculated using the methanol-to-acid ratio ($\theta$) equal to 1 in Equation 4.

Table 4-7. Expected equilibrium conversion for stoichiometric esterification of octanoic acid with methanol as calculated by the Gibbs free energy of reaction with simulated values from Aspen Plus®.

| **Temperature (°C)** | **Equilibrium constant, $K_e$** | **Equilibrium conversion, $x_e$** |
|---|---|---|
| 25 | 919 | 0.968 |
| 60 | 681 | 0.963 |
| 80 | 578 | 0.960 |
| 100 | 495 | 0.957 |
| 120 | 427 | 0.954 |
| 140 | 371 | 0.951 |
| 160 | 325 | 0.947 |
| 180 | 287 | 0.944 |
| 200 | 256 | 0.941 |

The results above confirmed what is expected for exothermic reactions: the higher the temperature, the lower the equilibrium conversion. Operating at reduced temperatures, however, leads to diminished reaction rates [109]. In this case, even though the thermodynamics favors the product, only in the presence of a catalyst the reaction is kinetically feasible [109].

Another aspect to be pointed out in reversible reactions is that the time required to essentially reach equilibrium may be prohibitive (e.g., it may take several hours up to days, depending on the catalyst activity). Also, to achieve high equilibrium conversion, excess alcohol is provided most of the time to favor the forward reaction. The effect of excess alcohol can be evaluated through Equation 4 by substituting the methanol-to-acid ratio ($\theta$) accordingly. In this case, $x_e$ tends to 1 for all temperatures.

Therefore, experimental tests to confirm the values of equilibrium conversion (Table 4-7) were not carried out due to the method limitations: GC analysis with a standard deviation of ± 1% would

not differentiate those values. Moreover, the tendency of the reaction mixture in the equilibrium to segregate between phases using large alcohol-to-acid ratios [133] would lead to another experimental error.

### 4.4 Concluding Remarks

Several issues arose from the old setup, related to the reaction system and data collection, being the cause of low precision of the analyses. After modifications to a new reactor setup, precautions to avoid sample loss, choice of more appropriate internal standard (dodecane), and GC analysis with a more compatible column (DB-FATWAX UI), the relative error of GC analysis was minimized to approximately ± 1%. At the same time, the reproducibility of experiments was satisfactory.

The preliminary experiments confirmed the potential application of petcoke for catalyzing esterification reactions. Functionalized petcoke with sulfuric acid, nitric acid, or a mixture of both resulted in significant conversions of the model reaction. The sample treated with nitric acid only, P-N-24, was approximately 68% as active as the sulfonated sample P-S-24 in terms of ester yield.

The assumption of the pseudo-first-order model is only valid at the beginning of the reaction, at conversions below 10%, when the esterification (reversible reaction) has a linear behavior. Therefore, the calculation of turnover frequency must follow this condition, while the equation based on the initial rate constant seems to be more reliable.

Tests using different temperatures and catalyst loadings showed the conditions at which diffusion is limiting the overall rate of reaction. Those limitations would be successfully avoided for the

kinetic study using the conditions: 60 °C, 600 rpm, methanol-to-acid ratio 20:1, catalyst loading of 2 wt% (or up to 4.5 wt% for petcoke).

# Chapter Five: KINETIC STUDY OF ESTERIFICATION REACTION CATALYZED BY ACID-MODIFIED PETROLEUM COKE

## 5.1 Introduction

The purpose of this chapter is the evaluation of the kinetic performance of different petcoke-derived catalysts over a model reaction: esterification of octanoic acid with methanol at 60 °C, and the analysis of the influence of acidic, structural, and physical features on the catalytic performance. The materials were tested in terms of activity for reaction, chemical stability in solution, and activation energy. A comparison with a standard catalyst was always provided.

The following section details the materials and methods used during the catalytic and stability tests. Section 5.3 consists of the kinetic study and includes the following topics: the catalytic activity in terms of reaction rate and turnover frequency, the catalyst deactivation by leaching of active sites, the determination of activation energies and error analysis, and the relationship of performance with acidity. Section 5.4 summarizes the relevant discussion and conclusions of this chapter.

## 5.2 Materials & Methods

All experiments were carried out with the "new" reactor setup after improvements discussed in Chapter 4. Reaction results are presented hereafter only in terms of ester yield (described in Section 4.3.4) for the esterification of octanoic acid with methanol, using GC analysis with the capillary column DB FATWAX UI.

The chemicals used in the kinetic study were described in Chapter 3. A third set of catalysts (first and second sets described in Chapter 4) was used for activity and stability tests. The materials P-N-3 and P-S-3 were produced by Qing Huang. They were treated with nitric acid (N) or sulfuric

acid (S) for 3 h at 120 °C. PC-TPA was prepared by Robert Pryde: wet-ball-milled petcoke (using isopropanol as solvent) doped with wet impregnation of 12-tungstophosphoric acid. Amberlyst-15 (H) ion exchange resin (Styrene-DVB, Alfa Aesar) was used for comparison. This commercial catalyst is a polystyrene-based ion exchange (styrene-DVB 20%) resin with attached sulfonic groups on its polymer matrix [110]. P-S-3 and Amberlyst-15 were also used for the determination of activation energies.

The fourth set of catalysts was entirely provided by Qing Huang and used for activity tests and analysis of the relationship between performance and acidities. This set consisted of petcoke samples treated only with nitric acid: P-N-3/120, P-N-3/80, P-N-24/120, B-N-3/120, plus BP and PC. The numbers 3 or 24 refer to the treatment time in hours, while the last numbers 80 or 120 refer to the treatment temperature in °C. The samples B-N-3/120 and BP correspond to petcoke ball-milled ("B" in name) for 4 h (using isopropanol as solvent) before the functionalization, and ball-milled petcoke without further treatment. The sample PC corresponds to petcoke sieved without further treatment.

All the catalysts employed in this kinetic study and their available properties are described in Table 5-1. Except for the standard catalysts $H_2SO_4$ and Amberlyst-15, all properties listed below were measured and provided by the person who provided the catalyst. For $H_2SO_4$, the acidity was calculated directly by the number of protons and molar weight, while for Amberlyst-15, it was measured by the ion-exchange titration method (details are presented in Table B-1, Appendix B).

Table 5-1. Properties of catalysts used for the kinetic study of esterification reaction.

| Catalyst | Strong acidity (mmol/g) [1] | Total acidity (mmol/g) [2] | Physical properties | Reference |
|---|---|---|---|---|
| **Amberlyst-15** | 4.70 | 4.70 | Particle size: > 500 μm | Experimental/ manufacturer |
| **P-S-3** | 0.25 | 1.05 | Particle size: < 63 μm | Qing H. |
| **P-N-3/120 (or P-N-3)** | 0.35 | 4.67 | Particle size: < 50 μm<br>Surface area:<br>3.2 $m^2/g$ [3] - 217 $m^2/g$ [4] | Qing H. |
| **PC-TPA** | 1.69 | 7.82 | -- | Robert P. |
| **$H_2SO_4$** | 20.4 | 20.4 | -- | Calculated |
| **P-N-3/80** | 0.20 | 2.90 | Surface area: 231 $m^2/g$ [4] | Qing H. |
| **B-N-3/120** | 0.33 | 5.18 | Surface area: 200 $m^2/g$ [4] | Qing H. |
| **P-N-24/120** | 0.70 | 5.25 | Pore size: 0.4 - 0.6 nm<br>Surface area:<br>4.1 $m^2/g$ [3] - 151 $m^2/g$ [4] | [112]<br>Qing H. |
| **PC** | 0.0 | 0.34 | Pore size: 0.4 - 0.7 nm<br>Surface area:<br>1.5 $m^2/g$ [3] - 84 $m^2/g$ [4] | [112]<br>Qing H. |
| **BP** | 0.0 | 0.55 | Surface area: 172 $m^2/g$ [4] | Qing H. |

[1] [-$SO_3H$] determined by ion exchange with NaCl and titration with NaOH; [2] determined by ion exchange with NaOH and titration with HCl; [3] by $N_2$ adsorption; [4] by $CO_2$ adsorption.

## 5.3 Results & Discussion

The esterification of octanoic acid with methanol is slowly autocatalyzed by the acid (without an external catalyst), resulting in 1.6% of ester yield after 90 min (or 3.4% after 4 h) of reaction, at conditions of 60 °C, 600 rpm, and methanol-to-acid ratio 20:1.

### *5.3.1 Activity of Catalysts*

The third set of catalysts was tested using the conditions established in Chapter 4: 60 °C, 600 rpm, methanol-to-acid ratio 20:1, and catalyst loading of 2 wt%. The focus is the beginning of each

reaction ($x$ < 10%), thus, the reactions were carried out for only 90 min. The results are given in Figure 5-1.

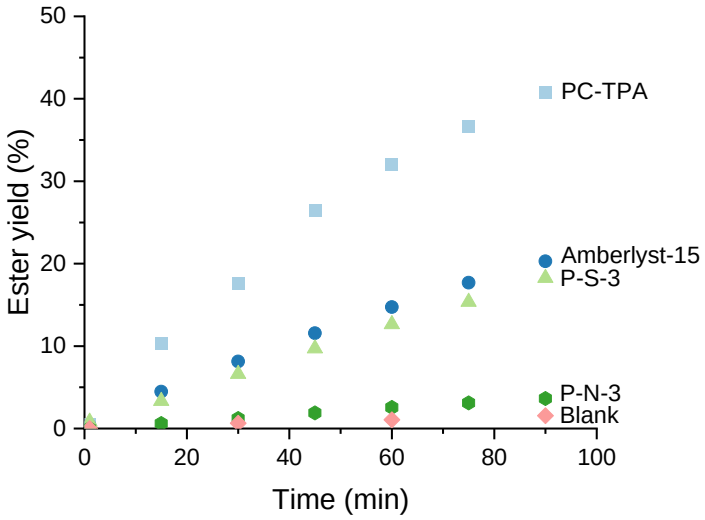


Figure 5-1. Results of ester yield using the third set of catalysts: PC-TPA, Amberlyst-15, P-S-3, and P-N-3 at reaction conditions: 60 °C, 600 rpm, methanol-to-acid ratio equal to 20:1, catalyst loading of 2 wt%, and 90 min.

The fractional yield decreased in the order of PC-TPA (40.7%) > Amberlyst-15 > P-S-3 > P-N-3 (3.6%). The absolute error of ester yield was in the range of ± 0.1 - 1.5% for this set of experiments.

The product amounts were converted through mass balance (molar basis) to the consumed acid, and then the pseudo-homogeneous first-order model was fit to the data of the beginning of reaction ($x$ < 10%) to obtain the initial rate constant, according to Equation 20. Initial TOF values were calculated from Equation 16, using the strong acidity estimated by titration as the active sites for reaction. Table 5-2 summarizes the activity results of those materials, including the initial reaction rate obtained by Equation 23.

Table 5-2. Results of activity of the third set of catalysts.

| Catalyst | Strong acidity [1] (mmol/g) | Total acidity [1] (mmol/g) | Initial TOF [2] ($h^{-1}$) | Initial rate (mol/mL·min) | Ester yield after 90 min (%) |
|---|---|---|---|---|---|
| P-N-3 | 0.35 | 4.67 | 22 | $0.37 \times 10^{-6}$ | 3.6 |
| P-S-3 | 0.25 | 1.05 | 159 | $2.0 \times 10^{-6}$ | 18.3 |
| PC-TPA | 1.69 | 7.82 | 87 | $5.8 \times 10^{-6}$ | 40.7 |
| Amberlyst-15 | 4.70 | 4.70 | 11 | $2.5 \times 10^{-6}$ | 20.3 |
| Blank | -- | -- | -- | $0.14 \times 10^{-6}$ | 1.6 |

[1] Determined by ion-exchange titration method; [2] calculated with the strong acidity estimated by titration.

Even though the best catalyst in terms of yield and initial reaction rate was PC-TPA, normalizing the activity by the active sites, P-S-3 showed the best performance in terms of the turnover frequency. Interestingly, this catalyst has the lowest number of acid sites for reaction.

As water is one product of the reaction, studies suggested that the process of adsorption and desorption of the carboxylic acid on the active sites of the catalyst is constrained on more hydrophilic surfaces [53], [77], [78]. In other words, the reaction rate decreases over more hydrophilic surfaces, which results from a high content of total acidity (Figure 5-2). Thus, the low content of acid sites on P-S-3 (total acidity of 1.05 mmol/g) is likely responsible for keeping this catalyst surface more hydrophobic than the other materials. Therefore, the high activity of P-S-3 could be explained by an appropriate balance of hydrophilicity/hydrophobicity of the catalyst surface. Another possible explanation for such behavior is based on the strength of Brønsted acid sites in this carbon material. Some sulfonic groups may be linked by strong hydrogen bonds, resulting in a stronger acidity due to mutual electron-withdrawal [62], [64].

Sulfonic groups are much stronger and more active for reaction than other oxygen-containing groups. Sulfonic groups, however, suffer easy deactivation by poisoning with water produced by esterification and other strongly bonded intermediates/byproducts of reaction [38]. Deactivation by water is among the major causes of decreasing the catalytic activity of solid acids with more hydrophilic surfaces [78]. When the presence of products reaches a threshold, the water forms a layer over the hydrophilic species [79]. The mechanism of protonation of the reagent on the catalyst surface becomes more difficult, resulting in a slow reaction rate [78]. The hydration of active sites might explain the low activity of Amberlyst-15 in comparison to P-S-3 and PC-TPA in terms of initial TOF and conversion, despite the large number of acid sites on Amberlyst-15. Ion exchange resins may also suffer dissociation of sulfonic acid groups in the solution in the presence of water [13]. Thus, the acidic sites of Amberlyst-15 are likely easier to deactivate by water [38] than the other catalysts. Other studies also reported low conversions of this catalyst for esterification reactions [7], [68], [73], [115], [134], [135].

Catalyst P-N-3 did not show a good performance either. Many reasons can be suggested: low strong acidity, an excessive amount of weak acid sites (carboxylic and phenolic groups) competing for adsorption of molecules, and reduced accessibility of reactants to the active sites. As explained earlier, titration overestimates the $-SO_3H$ concentration during the ion exchange procedure for samples functionalized with nitric acid [112]. Indeed, the strong acidity of P-N-3 quantified by XPS was 0.12 mmol/g, significantly smaller than the value reported in Table 5-1 as 0.35 mmol/g by titration.

Catalyst PC-TPA showed the best performance in terms of ester yield. The strength of PC-TPA for catalyzing esterification is related to a different functionalization treatment for this sample, being a more complex material than the other petcoke samples with $-SO_3H$, -COOH, and -OH

functional groups. The functionalization with 12-tungstophosphoric acid is expected to incorporate Brønsted acid sites on the surface of supported TPA catalysts [17], [136], although some Lewis acidity may also be generated, contributing to the activity in catalysis of esterification reactions [93], [137]. Therefore, the TOF value of 87 $h^{-1}$ might not be correct, as it was calculated considering only the strong acidity ($B^+$) estimated by titration as the active sites for reaction. Further analysis of this catalyst is beyond the scope of this study, but more characterization is suggested about the strength distribution and nature of active sites to understand their influence on catalytic activity.

The hydration of acid sites, explained above, might be responsible for the low activity of P-N-3 and Amberlyst-15 because of their high concentration of acid sites, as shown schematically in Figure 5-2. The functional groups on each catalyst surface include strong sites in red and weak sites in black, in the approximate proportion estimated by titration (Table 5-2).

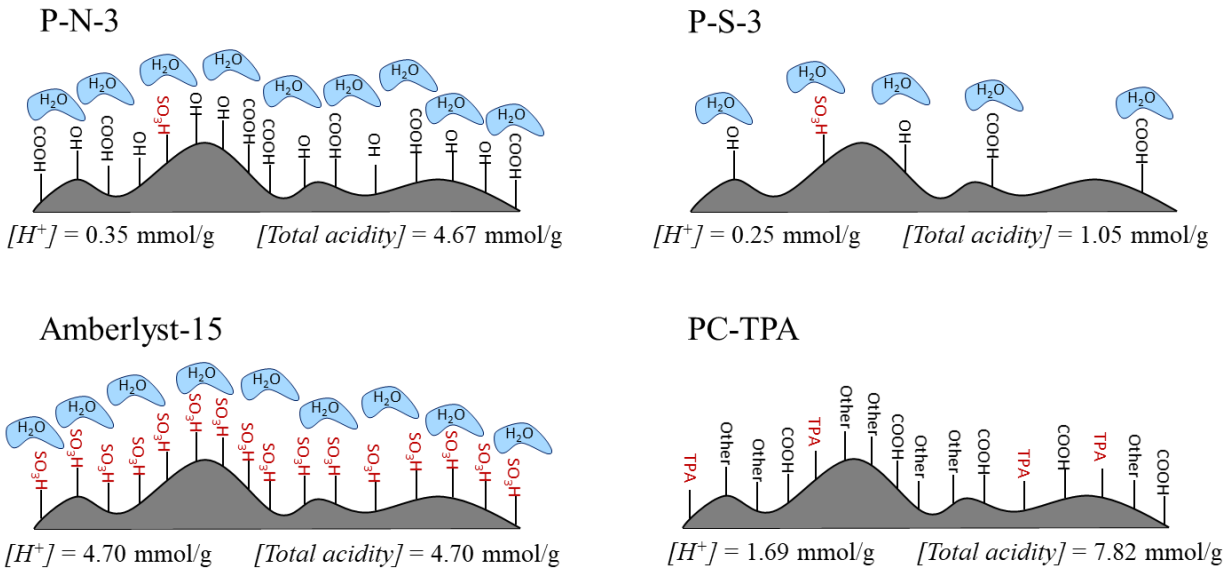


Figure 5-2. Hydration of acid sites for various catalysts used for the esterification nof octanoic acid with methanol.

The presence of carboxylic and hydroxyl groups, as well as sulfonic species should increase the hydrophilicity of the surface. As the concentration of water in the reaction medium increases, more of the hydrophilic sites will be covered, stearically hindering access to the active sites and reducing the reaction rate. The low number of acid groups on sample P-S-3 results in a lower coverage by water molecules. Understanding the nature of the surface of sample PC-TPA requires more information regarding the composition of functional groups and their affinities with water.

For this set of materials, no direct relationship was observed between the properties of the catalyst (e.g., strong acidity) and its performance during the reaction. This knowledge would be helpful as feedback for the fabrication process in order to improve the catalyst activity.

Many studies reported data for this esterification model reaction, but mostly in terms of final conversion and not using turnover frequency values, as presented in Table 5-3. Beyond the different conditions applied, the acid conversion varies according to the catalyst performance for reaction. Catalyst activity, in turn, is conditional on its structural, physical, and acidic features, which depend on the preparation method [102]. Hence, it is complex to compare the results of this study with the literature deeply.

Table 5-3. Esterification of octanoic acid with methanol over different acid catalysts.

| **Catalyst** | **Catalyst loading (wt%)** | **Molar ratio, $\theta$** | **Temp. (°C)** | **Time (h)** | **Max. conversion (%)** | **Reference** |
|---|---|---|---|---|---|---|
| Nafion/silica | 5.6 | 2:1 | 60 | 11 - 24 | 40 - 58 | [23] |
| Ionic liquid | 6 | 5:1 | 60 | 3 | 87 | [97] |
| Amberlyst-15 | 5 | 3:1 | 60 | 4 | 44 | [38] |
| $H_2SO_4$ | 5 | 3:1 | 60 | 4 | ~100 | [38] |
| Sulfonated carbon | 5 | 3:1 | 60 | 4 | 72 | [38] |
| Sulfonated carbon | ~6 | 2:1 | 60 | 1 | 19 | [76] |
| Sulfated zirconia | 0.5 | 10:1 | 60 | 7 | 98 | [102] |
| Niobic acid | 15 | 14:1 | 65 | 3 | 98 | [51] |
| Titania zirconia,<br>Tungstated zirconia,<br>Sulfated zirconia | ~16 | 2:1[2] | 75 | 4 | 10<br>20<br>60 | [48] |
| Tungstated zirconia-alumina | 4 g[1] | 4.5:1 | 175 - 200 | 20 | 94 - 100 | [100] |
| Titania zirconia,<br>Alumina zirconia | 4 g[1] | 4.5:1 | 175 - 200 | 20 | 100 | [101] |
| Sulfated zirconia | 4 g[1] | 4.5:1 | 80 - 120<br>150 - 200 | 20<br>20 | < 20<br>99 - 100 | [103] |
| Sulfated tin oxide | 4 g[1] | 4.5:1 | 60<br>80 - 120 | 20<br>20 | 44<br>95 - 100 | [103] |
| Heteropolyacid-based ionic liquids | 6 | 5:1 | 90 | 3 | 63 - 91 | [37] |
| Commercial acid clay (K-10),<br>Acid-activated clay (smectite) | ~35 | 3:1 | 100 | 4 | 85<br>99 | [98] |
| Sulfated aluminum phosphate | 1.5 | 6:1[2] | 75 | 4 | 76 - 92 | [99] |

[1] The authors did not report the catalyst loading in wt% or the mass of reagents for calculation; [2] esterification with ethanol.

Compared to the previous table, some petcoke-derived catalysts (P-S-3 and PC-TPA) showed higher activities than typical solid acid catalysts, as Nafion/silica, Amberlyst-15, and modified

zirconias. The better performance of P-S-3 and PC-TPA can be inferred in terms of mild conditions applied to reaction, lower catalyst loading, lower temperature, or shorter reaction time. Reaction with PC-TPA, for example, at 60 °C, 600 rpm, methanol-to-acid ratio 20:1, and catalyst loading of 4.5 wt% resulted in 86% ester yield after 4 h.

From Table 5-3, only one study [38] compared the catalysts in terms of turnover frequencies. Sulfonated carbon with a performance of 72% conversion after 4 h of reaction revealed an initial TOF value equal to 0.79 $min^{-1}$ (47 $h^{-1}$) for a strong acidity of 0.45 mmol/g (measured by EDX – Energy-dispersive X-ray spectroscopy). Even though the reaction progressed faster (~40% conversion after 90 min) with a larger catalyst loading, the catalyst had a lower activity per acid site than P-S-3. The authors also explained the high result of conversion due to an adequate balance of strong and weak acid sites, which helped prevent the catalyst from deactivation [38]. For Amberlyst-15 and $H_2SO_4$, the results were 3.6 and 29 $h^{-1}$, respectively, much lower than the values obtained in this thesis.

### *5.3.2 Stability of Catalysts*

The previous set of catalysts was also tested regarding the chemical stability in solution, placing the materials in methanol for 90 min at the reaction temperature of 60 °C. The same catalyst loading of 2 wt% (0.1 g) was used for comparison to the reference reactions (Table 5-2). After filtration for solids removal, the methanol was reacted with octanoic acid at conditions of methanol-to-acid ratio equal to 20:1, 60 °C, 600 rpm, and 90 min. Results are presented in Table 5-4.

Table 5-4. Results of the leaching experiment using the third set of catalysts.

| Catalyst | Ester yield (%) [1] | Initial rate (mol/mL·min) [1] | Ester yield of leaching test (%) [2] | Initial rate of leaching test (mol/mL·min) [2] |
|---|---|---|---|---|
| P-N-3 | 3.6 | $0.37 \times 10^{-6}$ | 0.5 | $0.05 \times 10^{-6}$ |
| Amberlyst-15 | 20.3 | $2.5 \times 10^{-6}$ | 5.9 | $0.6 \times 10^{-6}$ |
| PC-TPA | 40.7 | $5.8 \times 10^{-6}$ | 31.8 | $4.8 \times 10^{-6}$ |
| P-S-3 | 18.3 | $2.0 \times 10^{-6}$ | 19.0 | $2.5 \times 10^{-6}$ |
| Blank | 1.6 | $0.14 \times 10^{-6}$ | -- | -- |

[1] Reaction with catalyst; [2] reaction with only leached sites to methanol.

All materials showed leaching of soluble species to methanol. The petcoke-derived catalysts P-S-3 and PC-TPA suffered noticeable leaching of active sites, exhibiting significant contribution of homogeneous catalysis by the leached functional groups. Even though Amberlyst-15 is reported as a stable material, some species were leached, contributing 2.7x for the acid conversion compared with the blank reaction.

The slightly high ester yield of P-S-3 in the leaching experiment could be due to experimental error, resulting in P-S-3 ester yield equal to 19.0 ± 0.8%. The initial reaction rate of leached species to methanol, however, was 25% higher than the reaction with the catalyst in solution. This observation might suggest the active sites of P-S-3 had more access to reactants when in solution, and perhaps the pore size is constraining the reaction on active sites inside the pores.

Despite the explanations related to the acidities of materials in Section 5.3.1, the location of acid sites also plays an important role in the catalyst activity. Tamborini *et al.* [66] showed by studying particle size of porous-carbon catalysts that mesopores (2-50 nm) increase the contact of reactants with internal and external sulfonic groups, leading to high catalytic activity. Samples of petcoke treated with sulfuric acid or nitric acid and characterized by $CO_2$ adsorption showed a similar pore

size distribution in the range 0.4 - 0.8 nm (micropores) (Table 4-1). The acid sites located inside the pores might not be accessible for large reactants, negatively affecting the activity [138].

P-N-3 may not have suffered leaching of actives sites to methanol, but this sample was not active for the reaction as well. The low leaching of -$SO_3H$ might be related to the large concentration of carboxylic groups as weak acid sites. Hara [62] suggested that -COOH groups contribute largely to the stability of -$SO_3H$ groups bonded to amorphous carbon. While carboxylic groups compete for adsorption of molecules and favor the surface hydration, decreasing the material activity [64], the presence of these groups might be beneficial for chemical stability [68]. As the total acidity of P-N-3 (4.67 mmol/g) is proportionally huge compared with its strong acidity (0.35 mmol/g by titration or 0.12 mmol/g by XPS), the presence of the weak acid group -COOH might explain the reduced ester yield of methanol after leaching test. The solvent, however, significantly affects the behavior of active sites towards leaching [139]. The hydrophilic nature of acid sites increases the solubility in methanol (polar media) of active sites not strongly bonded to the surface.

Therefore, a better explanation for this sample stability is related to the strength of moieties bondings. P-N-3 was functionalized with nitric acid, and thus, the sulfonic groups are possibly more strongly attached to the catalyst surface due to modification of the inherent sulfur.

Even though PC-TPA possesses a higher proportion of weak acid sites than P-S-3, the active sites might not be “completely” leached from the petcoke surface, since the conversion of the leaching experiment was lower than the reaction with the catalyst in solution. This result may infer that those functional groups are also more strongly attached to the surface, providing some stability in comparison to the sulfonic groups.

The ester yield of P-N-3 equal to 0.5 ± 0.1% is different from the blank reaction (1.6 ± 0.2%). Unless other experimental issues resulted in that lower conversion compared to the autocatalyzed reaction, one speculation is that the reaction might have been constrained by the leaching of other functional groups from the P-N-3 surface, since the treatment with nitric acid also incorporates some nitrogen hetero doping [87]. A piece of evidence for the leaching of some soluble species from this sample is that the methanol – after removal of solids – was recovered in yellow color; meanwhile, it was colorless for the other materials.

Several studies reported the deactivation of carbon-derived catalyst – and other sulfonated solid acids – by leaching of sulfonic groups to methanol [38], [76], [77], [139], [140]. The polarity of methanol is responsible for attracting the hydrophilic sulfonic groups causing the leaching of active sites [76]. This effect leads to homogeneous catalysis consequently. In comparison to homogeneous catalysis, however, the initial reaction rates obtained were lowered. A reaction using a minimal amount (one drop) of $H_2SO_4$, for example, had 0.57 mmol of active sites in solution, resulting in an initial reaction rate in the order of magnitude of $1.0 \times 10^{-4}$ mol/mL·min. Considering that all active sites were leached to methanol from P-S-3 – a petcoke sample functionalized with $H_2SO_4$ –, the homogeneous catalysis with 0.025 mmol resulted in an initial reaction rate 40x slower ($2.5 \times 10^{-6}$ mol/mL·min). Therefore, the strength of those leached active sites is reduced compared to the liquid catalyst.

The poor stability of the catalysts demonstrated by the solubility in polar media can be attributed to the weak interaction (loosely bonded attachment) of the functional groups with the surface of the carbon structure [77]. Studies reported the material stability was improved against leaching using high temperatures during the catalyst sulfonation [141], while the same effect was observed

for the calcination temperature [134]. Moreover, the incorporation of surfactants, as reported by Souza *et al.* [142], on the catalyst surface help increase the hydrophobicity and consequently decrease the solubility in polar media. Mo *et al.* suggested the use of a structure-directing agent for improving stability. The sulfonation of an integrated carbon-polymeric matrix precursor resulted in a more stable catalyst [143].

The strong acidities of spent catalysts were not measured due to the difficulty of recovering the materials. The mass of material recovered was less than 50% from each experiment. Besides the weight reduction due to leaching in methanol, some material remained attached to the filter membrane and vial walls, decreasing the mass of material available for analysis.

### *5.3.3 Activation Energy Determination*

Using the Arrhenius equation, the activation energy values and the pre-exponential factor were determined for the esterification of octanoic acid with methanol catalyzed by Amberlyst-15 and P-S-3. The experiments were carried out in the range of 40 - 80 °C at the established conditions in Chapter 4: catalyst loading of 2 wt%, methanol-to-acid ratio 20:1, 600 rpm, and 90 min. Reaction results are given in Figure 5-3.

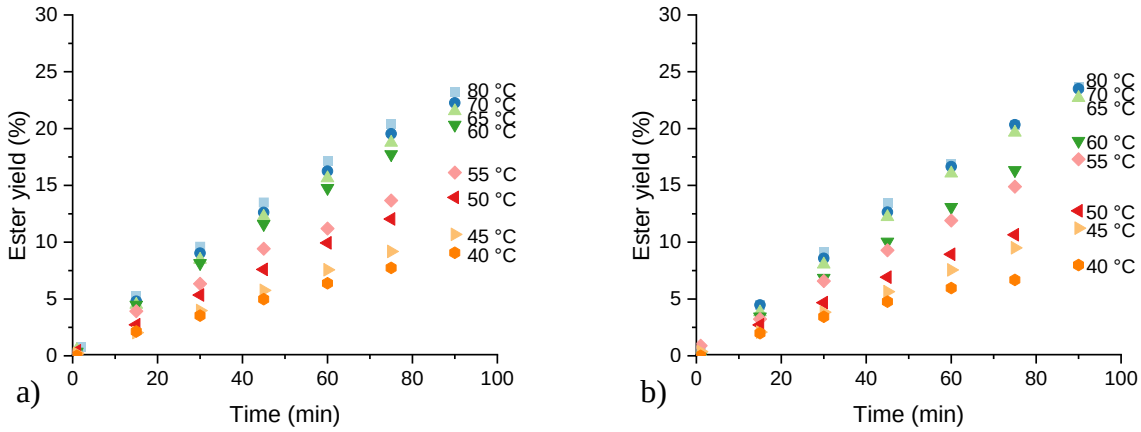


Figure 5-3. Results of ester yield for the model reaction catalyzed by a) Amberlyst-15, and b) P-S-3. Reaction conditions: catalyst loading of 2 wt%, methanol-to-acid ratio equal to 20:1, 600 rpm, 90 min, and temperature range of 40 - 80 °C.

For each temperature, Equation 20 was fit to the data to obtain the pseudo-first-order rate constants below 10% conversion (initial rate constants). The values are presented in Table 5-5.

Table 5-5. Initial rate constants for the esterification of octanoic acid and methanol catalyzed by Amberlyst-15 and P-S-3 in the range of 40 - 80 °C.

| **Temperature (°C)** | **Initial rate constant, *k* ($min^{-1}$)** | |
|---|---|---|
| | **Amberlyst-15** | **P-S-3** |
| 40 | $0.92 \times 10^{-4}$ | $0.83 \times 10^{-3}$ |
| 45 | $1.26 \times 10^{-3}$ | $1.29 \times 10^{-3}$ |
| 50 | $1.70 \times 10^{-3}$ | $1.39 \times 10^{-3}$ |
| 55 | $2.16 \times 10^{-3}$ | $2.07 \times 10^{-3}$ |
| 60 | $2.81 \times 10^{-3}$ | $2.15 \times 10^{-3}$ |
| 65 | $2.77 \times 10^{-3}$ | $2.80 \times 10^{-3}$ |
| 70 | $3.15 \times 10^{-3}$ | $2.89 \times 10^{-3}$ |
| 80 | $3.32 \times 10^{-3}$ | $3.04 \times 10^{-3}$ |

Plotting the data from Table 5-5 according to Figure 2-3 using the linearized form of Arrhenius equation, makes it easier to observe the effects of temperature on the catalytic activity, Figure 5-4.

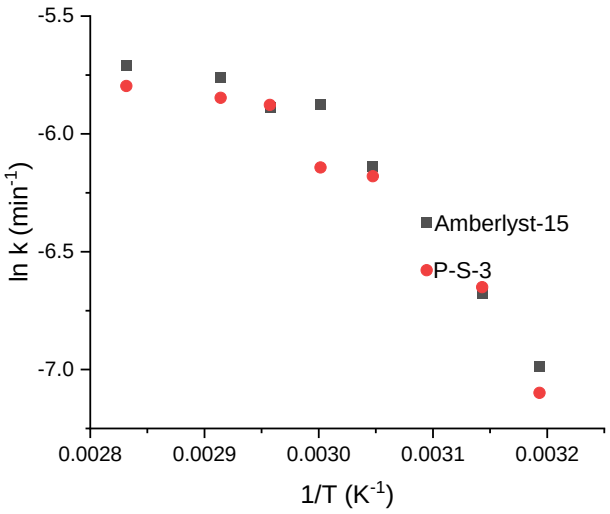


Figure 5-4. Arrhenius plot of esterification of octanoic acid and methanol catalyzed by Amberlyst-15 and P-S-3 in the range of 40 - 80 °C.

The behavior illustrated above by the first three points for each catalyst identifies some concerns with the reaction rate at temperatures over the boiling point of methanol (64.7 °C). In fact, the apparent activation energy in the range of 65 - 80 °C was determined as low as 11 and 5.3 kJ/mol for Amberlyst-15 and P-S-3, respectively. Those values of apparent activation energy (< 20 kJ/mol) indicate that the reaction is not kinetically but diffusively controlled in that range of temperature [117]. This limitation is related to the formation of another phase. Therefore, the apparent activation energy was determined in the range of 40 - 60 °C for both catalysts, where methanol and octanoic acid form one liquid phase at normal pressure, Figure 5-5.

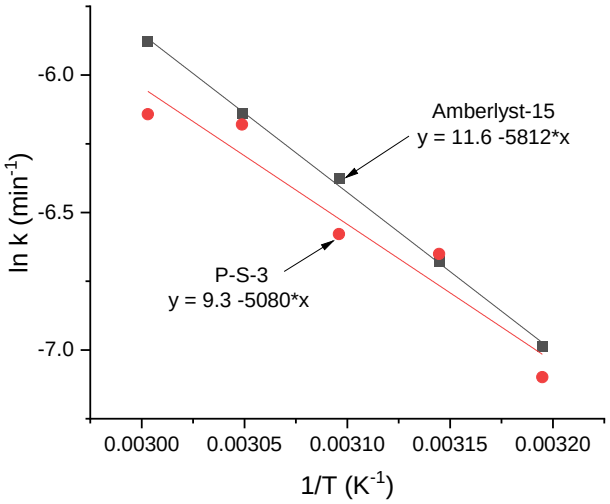


Figure 5-5. Determination of apparent activation energy for the esterification of octanoic acid and methanol catalyzed by Amberlyst-15 and P-S-3 in the range of 40 - 60 °C.

The values of the activation energy ($E_a$) and pre-exponential factor ($A$) for the esterification of octanoic acid with methanol over Amberlyst-15 and P-S-3 are presented in Table 5-6.

Table 5-6. Activation energies and pre-exponential factors for the esterification of octanoic acid with methanol over different acid catalysts.

| **Catalyst** | **Temperature (°C)** | **$E_a$ (kJ/mol)** | **$A$ (min$^{-1}$)** | **Reference** |
|---|---|---|---|---|
| Amberlyst-15 | 40 - 60 | 48.3 ± 1.5 | 108 x $10^3$ ± 2 | This study |
| P-S-3 | 40 - 60 | 42.2 ± 6.7 | 11 x $10^3$ ± 12 | This study |
| Halogen-free ionic liquid | 50 - 90 | 33.7 | 2.86 x $10^3$ | [97] |
| Tungstated zirconia | 75 - 120 | 60.7 | -- | [48] |

Without considering the uncertainty values, the activation energy for the reaction catalyzed by Amberlyst-15 is larger than by P-S-3, meaning the reaction rate of the former is more sensitive to temperature. A few degrees of temperature considerably affect the rate constant ($k$), and consequently, the reaction rate [90]. Generally, a lower activation energy corresponds to a more effective catalyst. As discussed and analyzed below in the error analysis, however, those activation

energies are within experimental error. Therefore, it is not possible to infer that P-S-3 is a more effective catalyst than Amberlyst-15.

The higher pre-exponential factor for Amberlyst-15 means a higher frequency of collision between molecules of reagents. A phenomenon named “compensation” might be the case here. Compensation commonly occurs in heterogeneous catalysis and results in an observed linear correlation of activation energy with *ln A* [105]. Thus, it is not possible for one catalyst of a series to have the lowest activation energy and highest pre-exponential factor simultaneously [105]. Because of uncertainties due to experimental error and restricted data collection – only two catalysts and a small range of $E_a$ –, no further analysis was done in this regard.

The only reported activation energy for this reaction was 33.7 kJ/mol using a homogeneous catalyst – ionic liquid $[HSO_3\text{-pmim}]^+(½Zn^{2+})SO_4^{2-}$ [97]. A priori, the reported catalyst seems more effective for the esterification of octanoic acid with methanol. The conditions applied, however, were different, especially the range of temperature 50 - 90 °C, even at ambient pressure. The authors used a similar setup for reaction and did not mention any precautions regarding transfer limitations over the methanol boiling point. They also used microporous molecular sieves to remove the water produced during the reaction and excess methanol. Thus, the esterification could be considered an irreversible reaction, dependent only on the acid concentration, and the rate constants were determined at higher acid conversions (70 - 90%).

The reported activation energy using tungstated zirconia is for the simultaneous transesterification reaction of tricaprylin with ethanol and subsequent esterification of caprylic acid (octanoic acid). Thus, it is more complicated to compare with this study.

*Error Analysis*

An error analysis of the activation energies of Amberlyst-15 and P-S-3 was carried out to verify if those values are indeed distinct or the difference is due to the propagation of experimental errors.

After all the improvements made for the new reactor setup and ester quantification by GC analysis, the standard deviation of GC response given by triplicate injections of the same sample was measured as ± 1.1% for this set of experiments, according to Equation 25.

A calibration curve was necessary to determine the mass of ester in solution, according to Equation 12. Calibration curves associate known masses measured by analytical balance of a compound with measured values of response factor given by GC. The resulting calibration value comes from the slope of a plot $m_x/m_{is}$ *versus* $A_x/A_{is}$ and the error associated with that was taken as the standard error of the slope. The error of the calibration curve of ester was determined in the range of ± 0.2 - 4.0%. New calibration curves were obtained periodically in case there was any change in the column response. Over six months, the calibration curves changed by 2.6%.

The error of mass of ester in solution was an association of calculation steps, involving multiplication of response factor with the mass of internal standard and division by the calibration curve. Therefore, Equation 28 applies for the error, where $z = ab$ or $a/b$.

$$\Delta z = z\sqrt{\left(\frac{\Delta a}{a}\right)^2 + \left(\frac{\Delta b}{b}\right)^2} \qquad 28$$

The relative error of ester quantification resulted in ± 1.2 - 4.1%. The mass of ester was then transformed into the number of moles to result in the mass of converted acid eventually. The acid in solution was calculated by subtracting the converted acid from the initial mass of acid weighed

on the balance. Thus, the error associated with the amount of acid in each sample withdrawn from the reactor was calculated according to Equation 29.

$$\Delta z = \sqrt{\left(\frac{\Delta a}{a}\right)^2 + \left(\frac{\Delta b}{b}\right)^2} \qquad 29$$

For each temperature, values below 10% conversion were used for fitting the rate constant according to Equation 20. In the plot time *versus* mass of octanoic acid, maximum and minimum slopes of the curve were taken by summing or subtracting those errors of acid amount accordingly. Figure 5-6 illustrates the procedure for determining the rate constant of the model reaction using Amberlyst-15 at 60 °C with the error associated with that value. The points correspond to 1, 15, and 30 min.

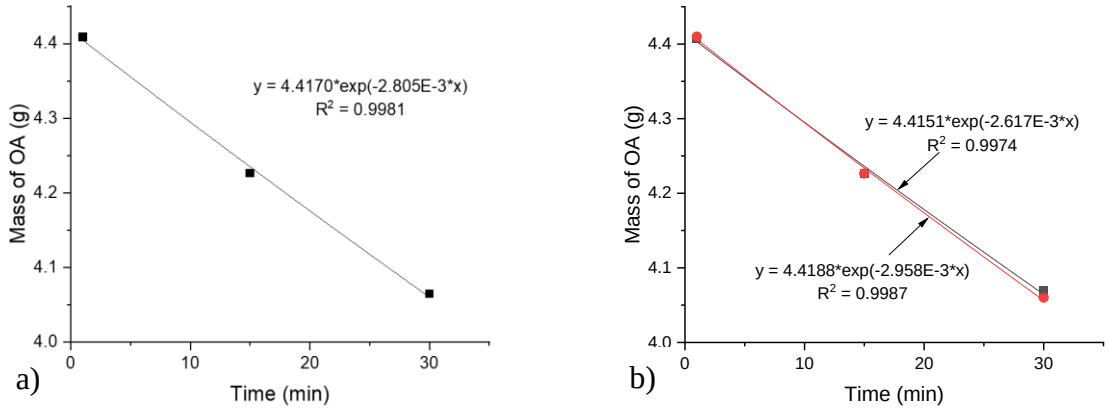


Figure 5-6. Fitted curves for determination of the rate constant (a) and associated error (b) for the esterification of octanoic acid with methanol catalyzed by Amberlyst-15 at 60 °C.

The mean rate constant was estimated as 2.805 x $10^{-3}$ $min^{-1}$. From maximum and minimum slopes, the rate constant values were estimated as 2.958 x $10^{-3}$ $min^{-1}$ and 2.617 x $10^{-3}$ $min^{-1}$. Therefore, $\Delta k$ was considered as 0.171 x $10^{-3}$ $min^{-1}$. Those fits were made for every temperature using both catalysts, and the error of each rate constant was computed in the linear and exponential fits for

determining the activation energy, as Figure 5-7. The error associated with the values of ln $k$ is given by Equation 30, where $z = \ln A$.

$$\Delta z = \frac{\Delta a}{a} \qquad 30$$

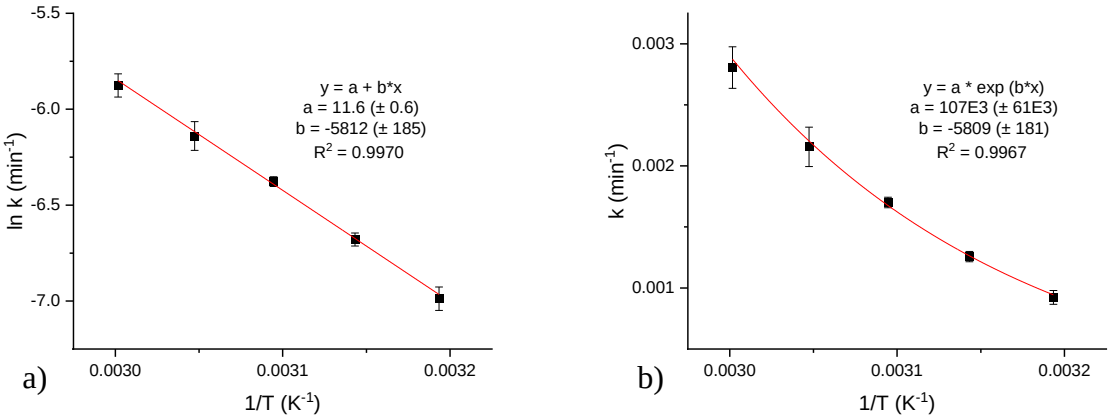


Figure 5-7. Fitted curves for determination of the activation energy of the esterification of octanoic acid with methanol catalyzed by Amberlyst-15 in the range of 40 - 60 °C; a) linear plot, and b) exponential plot of Arrhenius equation.

The activation energy was determined from the slope of the linear curve, according to Equation 24, or from the negative exponent of the exponential curve, as given in Equation 7. From Figure 5-7, the activation energy for the reaction in the range of 40 - 60 °C catalyzed by Amberlyst-15 resulted in similar values from both plots, being estimated as 48.3 kJ/mol at a level of confidence of 95%. The final error of activation energy was taken as the standard error of slope of those fits corresponding to ± 1.5 kJ/mol. Similarly, the final error of the pre-exponential factor was taken as the standard error of intercept. For Amberlyst-15, $A$ = 108 x $10^3$ ± 2 $min^{-1}$.

The same methodology was applied for calculating the error associated with the activation energy of reaction catalyzed by P-S-3, Figure 5-8. Due to the significant error associated with the rate constants, however, the exponential fit did not converge for those values. Therefore, the activation energy and pre-exponential values were determined only from the linear plot of the Arrhenius

equation. For the range of 40 - 60 °C, the activation energy was estimated as 42.2 ± 6.7 kJ/mol at a level of confidence of 95%, while the pre-exponential factor was equal to 11 x $10^3$ ± 12 $min^{-1}$.

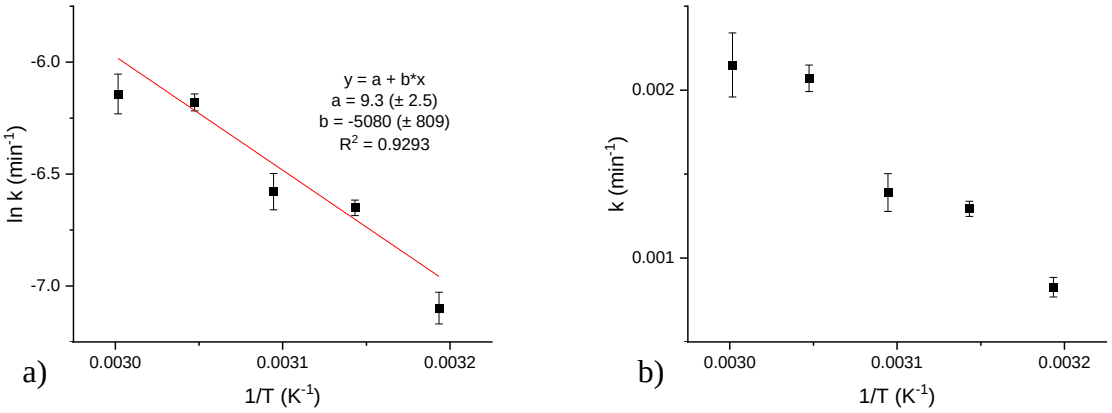


Figure 5-8. Fitted curves for determination of the activation energy of the esterification of octanoic acid with methanol catalyzed by P-S-3 in the range of 40 - 60 °C; a) linear plot, and b) exponential plot of Arrhenius equation.

The analysis of residual plots for the fitted curves showed no trends (Figure B-1 and Figure B-2, Appendix B). Random scatter on either side of the fitted line means no biases on the fit. The coefficient of determination ($R^2$) is a measure of correlation between the variables. For both Amberlyst-15 and P-S-3, there are high levels of correlation with values of 99% and 93%, respectively. The lower value for sample P-S-3 reflects the higher level of uncertainty in the data for this sample.

The error of activation energy of P-S-3 might be a little overestimated by the methodology applied, as the error associated with the GC calibration curve for P-S-3 was higher than Amberlyst-15, affecting the final result significantly. On the other hand, the analysis was limited to errors on the *x*-axis. The temperature, which does influence the reaction rate, was considered fixed by the water bath due to small fluctuations in the setpoint.

*5.3.4 Relationship between Performance and Acidity*

The fourth set of catalysts consisted of petcoke samples only functionalized with nitric acid. The conditions used were 60 °C, 600 rpm, methanol-to-acid ratio 20:1, catalyst loading of 4.5 wt%, and 4 h reaction. In this case, the amount of catalyst was increased as these catalysts had fewer acid sites per catalyst mass. Moreover, a longer time was used to better observe the differences in conversion, as some materials have low activity ($x$ < 10% after 90 min). Results are given in Figure 5-9. For this set, the initial turnover frequencies were calculated with the strong acidity determined by XPS, as presented in Table 5-7.

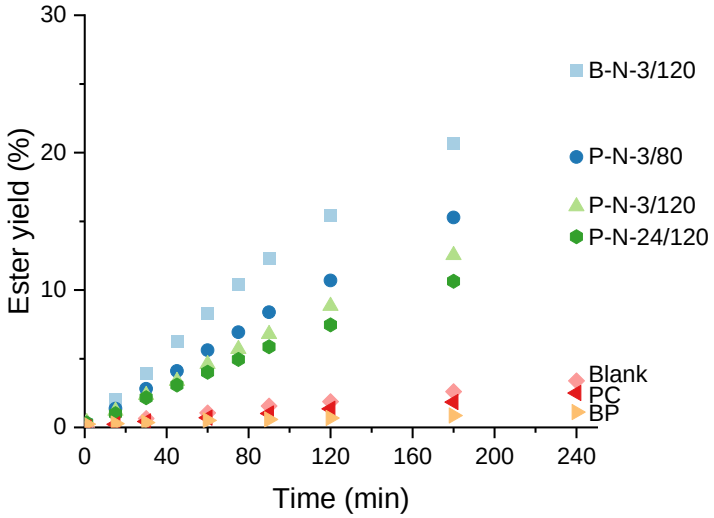


Figure 5-9. Results of ester yield using the fourth set of catalysts: P-N-3/80, P-N-3/120, P-N-24/120, B-N-3/120, PC, and BP at reaction conditions: 60 °C, 600 rpm, methanol-to-acid ratio equal to 20:1, catalyst loading of 4.5 wt%, and 4 h.

The fractional yield decreased in the order of B-N-3/120 > P-N-3/80 > P-N-3/120 > P-N-24/120; meanwhile, the TOF values almost followed the same trend. Petcoke samples without functionalization (PC and BP) resulted in a lower ester yield than the blank reaction. The absolute error of ester yield was in the range of ± 0.2 - 0.5% for this set of experiments.

Table 5-7. Results of activity of the fourth set of catalysts.

| Experiment | Strong acidity [1] (mmol/g) | Strong acidity [2] (mmol/g) | Total acidity [1] (mmol/g) | Initial TOF [3] ($h^{-1}$) | Initial rate (mol/mL·min) | Ester yield after 4 h (%) |
|---|---|---|---|---|---|---|
| B-N-3/120 | 0.33 | 0.20 | 5.18 | 67 | $1.4 \times 10^{-6}$ | 26.0 |
| P-N-3/80 | 0.20 | 0.13 | 2.90 | 68 | $0.91 \times 10^{-6}$ | 19.7 |
| P-N-3/120 | 0.35 | 0.12 | 4.67 | 60 | $0.72 \times 10^{-6}$ | 16.1 |
| P-N-24/120 | 0.70 | 0.16 | 5.25 | 37 | $0.61 \times 10^{-6}$ | 13.9 |
| PC | -- | -- | 0.34 | -- | $0.10 \times 10^{-6}$ | 2.5 |
| BP | -- | -- | 0.55 | -- | $0.04 \times 10^{-6}$ | 1.1 |
| Blank | -- | -- | -- | -- | $0.14 \times 10^{-6}$ | 3.4 |

[1] Determined by ion-exchange titration method; [2] determined by elemental analysis with XPS; [3] calculated with the strong acidity determined by XPS.

The strong and total acidities determined by titration did not correlate to the catalyst activity (TOF and ester yield). As discussed before, the ion-exchange titration method is not accurate in determining the effective number of acidic sites on the surface of petcoke samples functionalized with nitric acid. Those values are overestimated due to the presence of weak acidic groups developed on the material surface. The dissociation of the carboxylic group (-COOH) is enhanced by the aromatic nitro structures generated from the treatment of petcoke with nitric acid, contributing to the ion exchange during the titration of strong acidity [112]. The presence of the carboxylic group on the surface of carbon-derived catalysts was also reported by Okamura *et al.* and Mo *et al.* as a contributor to the exchanged $H^+$ during titration [72], [76]. Also, no direct relationship was observed between the surface area of the catalyst and its activity (initial rate, TOF, or ester yield) during the reaction.

On the other hand, except for the P-N-24/120 sample, the strong acidity determined by XPS showed a proportional relationship with the initial reaction rate and ester yield. The strong acidity

positively affects reaction conversion, as the sulfonic group is the active site for catalyzing this reaction. X-ray photoelectron spectroscopy (XPS) is a technique for surface characterization: elemental composition, electronic structure, and chemical bonding states of the elements within a material [144]. Because XPS is a surface-sensitive technique, the acidity inside the pores may not be counted, and consequently, the determination of strong acidity by XPS may not be truly accurate. Nevertheless, the elemental sulfur analysis for estimation of sulfonic group concentration is more realistic and accepted in the literature than the ion-exchange titration method [61], [72], [76], [145].

The larger value of strong acidity of B-N-3/120 might be responsible for a high turnover frequency and the best performance in terms of ester yield. In agreement with the results of the third set of catalysts, P-N-3/80 resulted in the best performance in terms of TOF, having the lowest total acidity among the catalysts tested in this set (2.9 mmol/g). The low content of weak acid sites supports the better activity of P-N-3/80 in comparison to P-N-3/120. Both materials have almost the same strong acidity; thus, the more hydrophobic surface of P-N-3/80 would explain its higher activity. Nevertheless, the large concentration of weak acid groups presented in this whole set of catalysts, compared to P-S-3 (total acidity of 1.05 mmol/g), resulted in less active materials.

The turnover frequency is a normalization of activity by the number of active sites (strong acidity and mass of catalyst); thus, the results of Table 5-7 suggested that the active sites of P-N-24/120 are less active than the other materials. Despite the total acidity being believed to reduce the activity, other parameters might affect the reaction rate negatively. The acidity strength of P-N-24/120, developed in a long time, would be responsible for its opposite performance from B-N-3/120, although the similar total acidities. Therefore, a strength distribution of the actives sites (sulfonic group) might better explain the behavior of those samples and correlate their

acidities with the catalytic activities. For zeolites, for example, a linear correlation was found between the activity and concentration of Brønsted sites [55], [146]. These materials can have an excellent crystallinity, with identical and noninteracting catalytic sites, which results in accurate activity values regarding the true active sites [116].

The use of materials PC and BP resulted in lower ester yields than the blank reaction (Figure 5-9). These results can be explained by the produced ester molecules adsorbing on those materials. The presence of weak acid groups confirmed by the total acidity values is probably responsible for this behavior. Those weak acid groups improve the hydrophilicity of the material surface [75]. Besides bonding with the water produced from the reaction (hydration) [64], those oxygen-containing groups might bond to the hydrogen bonding acceptors in esters as well [147], [148]. Therefore, the ball-milled petcoke (sample BP) showed an even lower ester yield due to the higher amount of weak acid groups on the surface, i.e., total acidity equal to 0.55 mmol/g.

### 5.4 Summary

Petcoke-derived catalysts functionalized with sulfuric acid (P-S-3) or 12-tungstophosphoric acid (PC-TPA) showed better performance at similar reaction conditions (60 °C, methanol-to-acid ratio of 20:1, and 600 rpm) than petcoke functionalized with nitric acid, P-N samples. Even increasing the reaction time (4 h) and doubling the catalyst loading (~0.2 g) for the latter, the highest ester yields achieved were only 26% for B-N-3/120 and 20% for P-N-3/80. Meanwhile, PC-TPA and P-S-3 resulted, respectively, in 41% and 18% of ester yield in a shorter time (90 min) with half catalyst loading (~0.1 g).

The catalyst P-S-3 had a similar performance to Amberlyst-15 at the same reaction conditions, and according to the error analysis, the activation energies of both these catalysts were within experimental error. By decreasing the standard deviation of GC analysis, the relative experimental error was reduced to less than ± 5%, which decreased the absolute error of ester yield to the range of ± 0.1 - 1.5%, depending on the conversion results. For example, PC-TPA ester yield was equal to 40.7 ± 1.5%, while for P-N-3 was 3.6 ± 0.1%.

Besides the difficulties in measuring intrinsic kinetic data (described in Section 4.3.5), the determination of true active sites for petcoke-derived catalysts also impacts the reliability of activity results in terms of turnover frequency. Also, the catalytic activity in terms of ester yield was not completely correlated to the strong acidity of materials. Other properties may also affect the interaction of active sites and reactants, including the concentration of weak acid sites and the strength of Brønsted acid sites.

The leaching test illustrated that most active species leached from the surface of the P-S-3 catalyst to the methanol solution, and so this catalyst could not be reused. PC-TPA had a similar behavior during the leaching experiment, with slightly superior stability. The carbon structure and chemical environment seem to affect the catalyst stability. Thus, a strong attachment to the petcoke surface is required for the stability of active sites.

# Chapter Six: CONCLUSIONS AND RECOMMENDATIONS

## 6.1 Conclusions

This thesis aimed to evaluate the performance of petcoke-derived catalysts for an esterification reaction. The potential application of petcoke for the fabrication of solid acid catalysts was demonstrated by the good catalytic performance of some samples. A petcoke sample functionalized with 12-tungstophosphoric acid resulted in double ester yield (41%) and reaction rate (5.8 x $10^{-6}$ mol/mL·min) than Amberlyst-15 at the same reaction conditions (20%, 2.5 x $10^{-6}$ mol/mL·min). On the other hand, a sulfonated sample, P-S-3, showed a greater performance in terms of turnover frequency (> 14x) than the commercial catalyst. The determined activation energies in the range 40 - 60 °C were 42.1 ± 6.8 kJ/mol for P-S-3 and 48.3 ± 1.5 kJ/mol for Amberlyst-15.

Despite the different treatments for functionalizing the petcoke, chemical stability was not achieved for the active sites on the petcoke surface. All materials, including the commercial catalyst, suffered from leaching of active phases to methanol, which prevents their reuse, as supposed for solid catalysts. This concern, however, has become often widely reported for many new heterogeneous catalysts, especially the lixiviation of sulfonic groups from solid acid catalysts during esterification reactions, which requires more research on catalyst design.

Many challenges were addressed throughout this study. First, the reactor setup was improved to minimize the errors during the reaction and sampling, while the method was enhanced to analyze the reaction progress. The relative uncertainty of the GC analysis was significantly reduced to ± 1.0%, which reduced the absolute error associated with the ester yield quantification to the range of ± 0.1 - 1.5%, depending on the conversion. Secondly, the conditions for ensuring that the

intrinsic reaction rate (kinetically controlled rather than diffusion controlled) was measured were established.

Thirdly, a proper method for the determination of active sites was chosen. Titration is not a reliable method for determining the concentration of functional groups on the petcoke surface. This technique overestimates the acidity of sulfonic groups due to the presence of other acidic groups. On the other hand, the XPS technique was more reliable for determining the sulfonic group concentration, since the analysis is based on the sulfur elemental content. This technique may undercount the sulfonic group concentration inside the pores, although they might not contribute significantly to the reaction due to the small pore size (< 0.8 nm) of some samples.

While TOF provides a comprehensive approach to compare catalysts based on the available intrinsic rate, turnover frequency values cannot be inferred as true site activities. Therefore, it should be acknowledged that even though all acid sites count for the TOF calculation, many of them might not be active and accessible for reaction. The inaccuracy in the active site determination is probably the main reason why so few studies report esterification results in terms of turnover frequency. Moreover, the leaching of active sites leads to homogeneous catalysis, further making it difficult to calculate the turnover frequency values.

The determination of turnover frequencies highlighted that not only the strong acidity influences the activity. Strength (weak, intermediate, or strong), nature (Brønsted or Lewis acid sites), and location of active phases on the catalyst surface also play an important role in the catalytic performance. Therefore, the concentration of active sites influences the activity significantly, but other parameters, such as the strength of active sites, may also affect the catalytic performance of petcoke-derived catalysts.

A balance in the surface hydrophobicity/hydrophilicity should be achieved to improve the heterogeneous catalytic activity and stability. The surface hydrophobicity decreases the water adsorption and consequently enhances the selective adsorption of oily hydrophobic molecules, increasing the catalytic activity. Nonetheless, hydrophobicity does not prevent deactivation by leaching of actives sites that are now less stable on the surface. Meanwhile, hydrophilicity might help stabilize the sulfonic groups on the catalyst surface. Additionally, the hydrophilic nature of acid sites increases the solubility in methanol of active sites not strongly bonded to the surface. Therefore, a strong attachment of the active sites on the petcoke surface is required for more stable materials in polar media.

Catalytic properties – selectivity, activity, and stability – must be considered together as they express the usefulness of a catalyst for an industrial application. Overall, this study was effective in providing information on those characteristics. The selectivity of the esterification of octanoic acid with methanol was 100% towards the formation of the methyl octanoate product, as no byproducts were observed by GC analysis.

### 6.2 Recommendations

Besides the concentration of functional groups, more characterization of petcoke-derived catalysts is suggested regarding the strength distribution and nature of active sites (Brønsted / Lewis), which would lead to a better understanding of the influence of acidity on the activity. In this regard, the technique pyridine-DRIFTS (Diffuse Reflectance Infrared Fourier Transform Spectroscopy) could be useful for bringing more information. Improvement on the pore size distribution is also recommended, as the reaction may suffer transfer limitations due to the poor access of reactant

molecules to the active sites inside the microporous. An interconnected mesoporous system minimizes diffusional effects of medium/long-chain reactant molecules [53].

More studies are necessary on the rational design of catalysts to reduce the deactivation mechanisms. The adequate structural properties to avoid leaching of active sites may be achieved by catalyst synthesis methods at high temperatures [141], although it possibly results in lower catalytic activity [77], [134]. In this case, the trade-offs should be negotiated. Modifications on the catalyst by the addition of promoters may also improve the stability [139]. Based on the leaching results of PC-TPA, investigation of other functional groups with a different interaction and possibly a stronger attachment to the petcoke surface is also recommended. Methanol recovered in yellow color during the leaching experiment with P-N-3 also suggested that different species might be leaching from the petcoke surface. Therefore, the analysis of solution by UV-Vis (ultraviolet-visible) spectroscopy would provide information on which functional groups are leaching to methanol. Besides the leaching of active phases, water adsorption also decreases the activity of catalytic protons throughout the reaction. The development of catalysts with more hydrophobic surfaces, e.g., by the incorporation of surfactants [142], would prevent the deactivation of catalytic sites by excluding polar molecules [53].

In addition to the effect on activity, water favors the reverse hydrolysis reaction inhibiting the esterification of carboxylic acid [149]. Oliveira *et al.* reported water removal as a more efficient way to achieve high ester yields than excess alcohol [150]. Therefore, investigation of catalytic performance is also recommended with water removal. Several studies reported the use of molecular sieves for this purpose [97], [110], [150], [151]. Lucena *et al*. describe an effective apparatus for water adsorption, which embraces a column connected on top of the reactor, consisting of a riser section (for water and methanol evaporation) and a downer section filled with

the zeolite 3A (for condensate return and water adsorption) [152], [153]. Zeolite Type 3A (3 angstroms) is a selective adsorbent for water removal, considering the critical diameter of the water molecule, excluding the methanol adsorption [154].

REFERENCES


[1] J. A. Caruso, K. Zhang, N. J. Schroeck, B. McCoy, and S. P. McElmurry, “Petroleum coke in the urban environment: A review of potential health effects,” *Int. J. Environ. Res. Public Health*, vol. 12, no. 6, pp. 6218–6231, 2015, doi: 10.3390/ijerph120606218.

[2] “Petroleum Coke,” *United Nations Statistics Division*, 2020. http://data.un.org/Data.aspx?d=EDATA&f=cmID%3APK (accessed Apr. 16, 2020).

[3] J. M. Hill, A. Karimi, and M. Malekshahian, “Characterization, gasification, activation, and potential uses for the millions of tonnes of petroleum coke produced in Canada each year,” *Can. J. Chem. Eng.*, vol. 92, no. 9, pp. 1618–1626, 2014, doi: 10.1002/cjce.22020.

[4] Y. Zhang *et al.*, “Airborne Petcoke Dust is a Major Source of Polycyclic Aromatic Hydrocarbons in the Athabasca Oil Sands Region,” *Environ. Sci. Technol.*, vol. 50, pp. 1711–1720, 2016, doi: 10.1021/acs.est.5b05092.

[5] J. M. Hill, “Sustainable and/or waste sources for catalysts: Porous carbon development and gasification,” *Catal. Today*, vol. 285, pp. 204–210, 2017, doi: 10.1016/j.cattod.2016.12.033.

[6] A. Karimi, O. Thinon, J. Fournier, and J. M. Hill, “Activated carbon prepared from Canadian oil sands coke by CO2 activation: I. Trends in pore development and the effect of pre-oxidation,” *Can. J. Chem. Eng.*, vol. 91, no. 9, pp. 1491–1499, 2013, doi: 10.1002/cjce.21774.

[7] K. Nakajima and M. Hara, “Amorphous Carbon with SO3H Groups as a Solid Brønsted Acid Catalyst,” *Am. Chem. Soc.*, vol. 2, pp. 1296–1304, 2012, doi: 10.1021/cs300103k.

[8] F. C. Ballotin *et al.*, “New Magnetic Fe Oxide-Carbon Based Acid Catalyst Prepared from Bio-Oil for Esterification Reactions,” *J. Braz. Chem. Soc.*, vol. 31, no. 8, pp. 1714–1724, 2020, doi: 10.21577/0103-5053.20200057.

[9] T. Iwasaki, Y. Maegawa, T. Ohshima, and K. Mashima, “Esterification,” in *Kirk-Othmer Encyclopedia of Chemical Technology*, John Wiley & Sons, Inc., 2012, p. 33.

[10] G. D. Yadav and P. H. Mehta, “Heterogeneous Catalysis in Esterification Reactions: Preparation of Phenethyl Acetate and Cyclohexyl Acetate by Using a Variety of Solid Acidic Catalysts,” *Ind. Eng. Chem. Res.*, vol. 3, no. 9, pp. 2198–2208, 1994, doi: 10.1021/ie00033a025.

[11] V. K. S. Pappu, V. Kanyi, A. Santhanakrishnan, C. T. Lira, and D. J. Miller, “Butyric acid esterification kinetics over Amberlyst solid acid catalysts: The effect of alcohol carbon chain length,” *Bioresour. Technol.*, vol. 130, pp. 793–797, 2013, doi: 10.1016/j.biortech.2012.12.087.

[12] T. Joseph, S. Sahoo, and S. B. Halligudi, “Brönsted acidic ionic liquids: A green, efficient and reusable catalyst system and reaction medium for Fischer esterification,” *J. Mol. Catal. A Chem.*, vol. 234, no. 1–2, pp. 107–110, 2005, doi: 10.1016/j.molcata.2005.03.005.

[13] G. Ertl, H. Knözinger, F. Schüth, and J. Weitkamp, *Handbook of Heterogeneous Catalysis*. Weinheim, Germany: Wiley-VCH, 2008.

[14] Z. Jiang, J. Xu, Z. Zeng, W. Xue, and S. Li, “Kinetics of the Esterification between Lactic Acid and Isoamyl Alcohol in the Presence of Silica Gel-Supported Sodium Hydrogen Sulphate,” *Can. J. Chem. Eng.*, vol. 96, pp. 1972–1978, 2018, doi: 10.1002/cjce.23127.

[15] C. S. M. Pereira, S. P. Pinho, V. M. T. M. Silva, and A. E. Rodrigues, “Thermodynamic Equilibrium and Reaction Kinetics for the Esterification of Lactic Acid with Ethanol

Catalyzed by Acid Ion-Exchange Resin," *Ind. Eng. Chem. Res.*, vol. 47, pp. 1453–1463, 2008, doi: 10.1021/ie071220p.
[16] J. A. Melero, J. Iglesias, and G. Morales, "Heterogeneous acid catalysts for biodiesel production: Current status and future challenges," *Green Chem.*, vol. 11, no. 9, pp. 1285–1308, 2009, doi: 10.1039/b902086a.
[17] B. S. Rana, D. Cho, K. Cho, and J. Kim, "Total Acid Number (TAN) reduction of high acidic crude oil by catalytic esterification of naphthenic acids in fixed-bed continuous flow reactor," *Fuel*, vol. 231, pp. 271–280, 2018, doi: 10.1016/j.fuel.2018.05.074.
[18] S. H. Shuit and S. H. Tan, "Biodiesel Production via Esterification of Palm Fatty Acid Distillate Using Sulphonated Multi-walled Carbon Nanotubes as a Solid Acid Catalyst: Process Study, Catalyst Reusability and Kinetic Study," *Bioenergy Res.*, vol. 8, no. 2, pp. 605–617, 2015, doi: 10.1007/s12155-014-9545-2.
[19] S. Liu, H. Wang, P. Neumann, C. S. Kim, and K. J. Smith, "Esterification over Acid-Treated Mesoporous Carbon Derived from Petroleum Coke," *ACS Omega*, vol. 4, no. 3, pp. 6050–6058, 2019, doi: 10.1021/acsomega.8b03472.
[20] M. Wu *et al.*, "SO3H-modified petroleum coke derived porous carbon as an efficient solid acid catalyst for esterification of oleic acid," *J. Porous Mater.*, vol. 23, no. 1, pp. 263–271, 2016, doi: 10.1007/s10934-015-0078-7.
[21] Y. Xiao and J. M. Hill, "Solid acid catalysts produced by sulfonation of petroleum coke: Dominant role of aromatic hydrogen," *Chemosphere*, vol. 248, p. 125981, 2020, doi: 10.1016/j.chemosphere.2020.125981.
[22] K. S. Bankole and G. A. Aurand, "Kinetic and Thermodynamic Parameters for Uncatalyzed Esterification of Carboxylic Acid," *Res. J. Appl. Sci. Eng. Technol.*, vol. 7, no. 22, pp. 4671–4684, 2014, doi: 10.19026/rjaset.7.850.
[23] Y. Liu, E. Lotero, and J. G. J. Goodwin, "Effect of carbon chain length on esterification of carboxylic acids with methanol using acid catalysis," *J. Catal.*, vol. 243, pp. 221–228, 2006, doi: 10.1016/j.jcat.2006.07.013.
[24] A. Sharma, A. K. Dalai, and S. P. Chaurasia, "Thermodynamic study of hydrolysis and esterification reactions with immobilized lipases," *Eur. Int. J. Sci. Technol.*, vol. 4, no. 2, pp. 128–136, 2015, doi: 2304-9693.
[25] E. Altuntepe, T. Greinert, F. Hartmann, A. Reinhardt, G. Sadowski, and C. Held, "Thermodynamics of enzyme-catalyzed esterifications: I. Succinic acid esterification with ethanol," *Appl. Microbiol. Biotechnol.*, vol. 101, no. 15, pp. 5973–5984, 2017, doi: 10.1007/s00253-017-8287-4.
[26] W. Huang, Y.-M. Xia, H. Gao, Y.-J. Fang, Y. Wang, and Y. Fang, "Enzymatic esterification between n-alcohol homologs and n-caprylic acid in non-aqueous medium under microwave irradiation," *J. Mol. Catal.*, vol. 35, no. 4–6, pp. 113–116, 2005, doi: 10.1016/j.molcatb.2005.06.004.
[27] J. Lilja *et al.*, "Kinetics of esterification of propanoic acid with methanol over a fibrous polymer-supported sulphonic acid catalyst," *Appl. Catal. A Gen.*, vol. 228, no. 1–2, pp. 253–267, 2002, doi: 10.1016/S0926-860X(01)00981-4.
[28] S. Torres, M. D. Baigorí, S. L. Swathy, A. Pandey, and G. R. Castro, "Enzymatic synthesis of banana flavour (isoamyl acetate) by Bacillus licheniformis S-86 esterase," *Food Res. Int.*, vol. 42, no. 4, pp. 454–460, 2009, doi: 10.1016/j.foodres.2008.12.005.
[29] J. Otera and J. Nishikido, *Esterification: Methods, Reactions, and Applications*. Weinheim, Germany: John Wiley & Sons, Incorporated, 2010.

[30] Y. Feng *et al.*, "Biodiesel production using cation-exchange resin as heterogeneous catalyst," *Bioresour. Technol.*, vol. 101, no. 5, pp. 1518–1521, 2010, doi: 10.1016/j.biortech.2009.07.084.
[31] M. W. Formo, "Ester Reactions of Fatty Materials," *J. Am. Oil Chem. Soc.*, vol. 31, pp. 548–559, 1954.
[32] F. Leyva, A. Orjuela, D. J. Miller, I. Gil, J. Vargas, and G. Rodríguez, "Kinetics of propionic acid and isoamyl alcohol liquid esterification with amberlyst 70 as catalyst," *Ind. Eng. Chem. Res.*, vol. 52, no. 51, pp. 18153–18161, 2013, doi: 10.1021/ie402349t.
[33] T. A. Peters, N. E. Benes, A. Holmen, and J. T. F. Keurentjes, "Comparison of commercial solid acid catalysts for the esterification of acetic acid with butanol," *Appl. Catal. A Gen.*, vol. 297, no. 2, pp. 182–188, 2006, doi: 10.1016/j.apcata.2005.09.006.
[34] M. Trejda, A. Nurwita, and D. Kryszak, "Synthesis of solid acid catalysts for esterification with the assistance of elevated pressure," *Microporous Mesoporous Mater.*, vol. 278, pp. 115–120, 2019, doi: 10.1016/j.micromeso.2018.11.009.
[35] Y. Zhou *et al.*, "Solid Acid Catalyst Based on Single-Layer α-Zirconium Phosphate Nanosheets for Biodiesel Production via Esterification," *Catalysts*, vol. 8, no. 1, p. 17, 2018, doi: 10.3390/catal8010017.
[36] A. P. da L. Corrêa, R. R. C. Bastos, G. N. da Rocha Filho, J. R. Zamian, and L. R. V. da Conceição, "Preparation of sulfonated carbon-based catalysts from murumuru kernel shell and their performance in the esterification reaction," *RSC Adv.*, vol. 10, no. 34, pp. 20245–20256, 2020, doi: 10.1039/d0ra03217d.
[37] X. Han *et al.*, "Novel Keggin-type H4PVMo11O40-based ionic liquid catalysts for n-caprylic acid esterification," *J. Taiwan Inst. Chem. Eng.*, vol. 58, pp. 203–209, 2016, doi: 10.1016/j.jtice.2015.07.005.
[38] K. Ngaosuwan, J. G. Goodwin, and P. Prasertdham, "A green sulfonated carbon-based catalyst derived from coffee residue for esterification," *Renew. Energy*, vol. 86, pp. 262–269, 2016, doi: 10.1016/j.renene.2015.08.010.
[39] J.-S. Lee and S. Saka, "Biodiesel production by heterogeneous catalysts and supercritical technologies," *Bioresource Technology*, vol. 101, no. 19. pp. 7191–7200, 2010, doi: 10.1016/j.biortech.2010.04.071.
[40] J. H. Clark, "Solid Acids for Green Chemistry," *Acc. Chem. Res.*, vol. 35, no. 9, pp. 791–797, 2002, doi: 10.1021/ar010072a.
[41] S. H. Ali, A. Tarakmah, S. Q. Merchant, and T. Al-Sahhaf, "Synthesis of esters: Development of the rate expression for the Dowex 50 Wx8-400 catalyzed esterification of propionic acid with 1-propanol," *Chem. Eng. Sci.*, vol. 62, no. 12, pp. 3197–3217, 2007, doi: 10.1016/j.ces.2007.03.017.
[42] A. Engin, H. Haluk, and K. Gurkan, "Production of lactic acid esters catalyzed by heteropoly acid supported over ion-exchange resins," *Green Chem.*, vol. 5, no. 4, pp. 460–466, 2003, doi: 10.1039/b303327a.
[43] V. S. Chandane, A. P. Rathod, K. L. Wasewar, and S. S. Sonawane, "Esterification of propionic acid with isopropyl alcohol over ion exchange resins: Optimization and kinetics," *Korean J. Chem. Eng.*, vol. 34, no. 1, pp. 249–258, 2017, doi: 10.1007/s11814-016-0249-5.
[44] B. M. Omar, M. Bita, I. Louafi, and A. Djouadi, "Esterification process catalyzed by ZSM-5 zeolite synthesized via modified hydrothermal method," *MethodsX*, vol. 5, pp. 277–282, 2018, doi: 10.1016/j.mex.2018.03.004.

[45] D. R. Fernandes, A. S. Rocha, E. F. Mai, C. J. A. Mota, and V. Teixeira Da Silva, "Levulinic acid esterification with ethanol to ethyl levulinate production over solid acid catalysts," *Appl. Catal. A Gen.*, vol. 425–426, pp. 199–204, 2012, doi: 10.1016/j.apcata.2012.03.020.
[46] J. A. Melero, G. Morales, J. Iglesias, M. Paniagua, B. Hernández, and S. Penedo, "Efficient conversion of levulinic acid into alkyl levulinates catalyzed by sulfonic mesostructured silicas," *Appl. Catal. A Gen.*, vol. 466, pp. 116–122, 2013, doi: 10.1016/j.apcata.2013.06.035.
[47] Y. Wang, J. You, and B. Liu, "Preparation of mesoporous silica supported sulfonic acid and evaluation of the catalyst in esterification reactions," *React. Kinet. Mech. Catal.*, vol. 128, pp. 493–505, 2019, doi: 10.1007/s11144-019-01645-2.
[48] D. E. López, J. G. Goodwin, D. A. Bruce, and S. Furuta, "Esterification and transesterification using modified-zirconia catalysts," *Appl. Catal. A Gen.*, vol. 339, pp. 76–83, 2008, doi: 10.1016/j.apcata.2008.01.009.
[49] Y. Kaburagi, K. Wako, K. Nemoto, and T. Fujitani, "Esterification of levulinic acid with ethanol over sulfated Si-doped ZrO2 solid acid catalyst: Study of the structure–activity relationships," *Appl. Catal. A Gen.*, vol. 476, pp. 186–196, 2014, doi: 10.1016/j.apcata.2014.02.032.
[50] K. Saravanan, B. Tyag, and H. C. Bajaj, "Sulfated zirconia: an efficient solid acid catalyst for esterification of myristic acid with short chain alcohols," *Catal. Sci. Technol.*, vol. 2, pp. 2512–2520, 2012, doi: 10.1039/c2cy20462b.
[51] K. Srilatha, N. Lingaiah, P. S. S. Prasad, B. L. A. P. Devi, R. B. N. Prasad, and S. Venkateswar, "Influence of Carbon Chain Length and Unsaturation on the Esterification Activity of Fatty Acids on Nb2O5 Catalyst," *Ind. Eng. Chem. Res.*, vol. 48, pp. 10816–10819, 2009, doi: 10.1021/ie900864z.
[52] L. D. T. Câmara and D. A. G. Aranda, "Reaction Kinetic Study of Biodiesel Production from Fatty Acids Esterification with Ethanol," *Ind. Eng. Chem. Res.*, vol. 50, pp. 2544–2547, 2011, doi: 10.1021/ie1005806.
[53] Y. M. Sani, W. M. A. W. Daud, and A. R. A. Aziz, "Activity of solid acid catalysts for biodiesel production: A critical review," *Appl. Catal. A, Gen.*, vol. 470, pp. 140–161, 2014, doi: 10.1016/j.apcata.2013.10.052.
[54] T. Komoń, P. Niewiadomski, P. Oracz, and Małgorzata E. Jamróz, "Esterification of acrylic acid with 2-ethylhexan-1-ol: Thermodynamic and kinetic study," *Appl. Catal. A Gen.*, vol. 451, pp. 127–136, 2013, doi: 10.1016/j.apcata.2012.11.018.
[55] A. Corma, H. Garcia, S. Iborra, and J. Primo, "Modified Faujasite Zeolites as Catalysts in Organic Reactions: Esterification of Carboxylic Acids in the Presence of HY Zeolites," *J. Catal.*, vol. 120, pp. 78–87, 1989, doi: 10.1016/0021-9517(89)90252-2.
[56] K.-J. Lin, "SMTP-1: The First Functionalized Metalloporphyrin Molecular Sieves with Large Channels," *Angew. Chemie Int. Ed.*, vol. 38, no. 18, pp. 2730–2732, 1999, doi: 10.1002/(SICI)1521-3773(19990917)38:18<2730::AID-ANIE2730>3.0.CO;2-9.
[57] L. Zhang *et al.*, "One-step synthesis of mesoporous nanosized sulfated zirconia via liquid-crystal template (LCT) method," *Mater. Res. Bull.*, vol. 47, no. 11, pp. 3931–3936, 2012, doi: 10.1016/j.materresbull.2012.02.014.
[58] S. Suganuma *et al.*, "Hydrolysis of Cellulose by Amorphous Carbon Bearing SO3H, COOH, and OH Groups," *Am. Chem. Soc.*, vol. 130, no. 38, pp. 12787–12793, 2008, doi: 10.1021/ja803983h.
[59] T. Okuhara, "Water-Tolerant Solid Acid Catalysts," *Chem. Rev.*, vol. 102, pp. 3641–3666,

2002, doi: 10.1021/cr0103569.
[60] L. J. Konwar, J. Boro, and D. Deka, “Review on the latest developments in biodiesel production using carbon-based catalysts.,” *Renew. Sustain. Energy Rev.*, vol. 29, pp. 546–564, 2014, doi: 10.1016/j.rser.2013.09.003.
[61] M. Hara, “Biodiesel production by amorphous carbon bearing SO3H, COOH and phenolic OH groups, a solid Brønsted acid catalyst,” *Top. Catal.*, vol. 53, no. 11–12, pp. 805–810, 2010, doi: 10.1007/s11244-010-9458-z.
[62] M. Hara, “Biomass conversion by a solid acid catalyst,” *Energy Environ. Sci.*, vol. 3, pp. 601–607, 2010, doi: 10.1039/b922917e.
[63] L. J. Konwar, J. Wärnå, P. Mäki-Arvela, N. Kumar, and J.-P. Mikkola, “Reaction kinetics with catalyst deactivation in simultaneous esterification and transesterification of acid oils to biodiesel (FAME) over a mesoporous sulphonated carbon catalyst,” *Fuel*, vol. 166, pp. 1–11, 2016, doi: 10.1016/j.fuel.2015.10.102.
[64] F. Su and Y. Guo, “Advancements in solid acid catalysts for biodiesel production,” *Green Chem.*, vol. 16, no. 6, pp. 2934–2957, 2014, doi: 10.1039/c3gc42333f.
[65] S. Niu, Y. Ning, C. Lu, K. Han, H. Yu, and Y. Zhou, “Esterification of oleic acid to produce biodiesel catalyzed by sulfonated activated carbon from bamboo,” *Energy Convers. Manag.*, vol. 163, pp. 59–65, 2018, doi: 10.1016/j.enconman.2018.02.055.
[66] L. H. Tamborini, M. E. Casco, M. P. Militello, J. Silvestre-Albero, C. A. Barbero, and D. F. Acevedo, “Sulfonated porous carbon catalysts for biodiesel production: Clear effect of the carbon particle size on the catalyst synthesis and properties,” *Fuel Process. Technol.*, vol. 149, pp. 209–217, 2016, doi: 10.1016/j.fuproc.2016.04.006.
[67] I. Ogino, Y. Suzuki, and S. R. Mukai, “Esterification of levulinic acid with ethanol catalyzed by sulfonated carbon catalysts: Promotional effects of additional functional groups,” *Catal. Today*, vol. 314, pp. 62–69, 2018, doi: 10.1016/j.cattod.2017.10.001.
[68] T. Liu, Z. Li, W. Li, C. Shi, and Y. Wang, “Preparation and characterization of biomass carbon-based solid acid catalyst for the esterification of oleic acid with methanol,” *Bioresour. Technol.*, vol. 133, pp. 618–621, 2013, doi: 10.1016/j.biortech.2013.01.163.
[69] S. K. Sangar, C. S. Lan, S. M. Razali, M. S. A. Farabi, and Y. H. Taufiq-Yap, “Methyl ester production from palm fatty acid distillate (PFAD) using sulfonated cow dung-derived carbon-based solid acid catalyst,” *Energy Convers. Manag.*, vol. 196, pp. 1306–1315, 2019, doi: 10.1016/j.enconman.2019.06.073.
[70] S. De, A. M. Balu, J. C. van der Waal, and R. Luque, “Biomass-Derived Porous Carbon Materials: Synthesis and Catalytic Applications,” *ChemCatChem Rev.*, vol. 7, pp. 1608–1629, 2015, doi: 10.1002/cctc.201500081.
[71] L. Liu, Y.-P. Zhu, M. Su, and Z.-Y. Yuan, “Metal-Free Carbonaceous Materials as Promising Heterogeneous Catalysts,” *ChemCatChem Rev.*, vol. 7, pp. 2765–2787, 2015, doi: 10.1002/cctc.201500350.
[72] M. Okamura *et al.*, “Acid-Catalyzed Reactions on Flexible Polycyclic Aromatic Carbon in Amorphous Carbon,” *Chem. Mater.*, vol. 18, no. 5, pp. 3039–3045, 2006, doi: 10.1021/cm0605623.
[73] J. Clohessy and W. Kwapinski, “Carbon-Based Catalysts for Biodiesel Production — A Review,” *Appl. Sci.*, vol. 10, no. 3, p. 918, 2020, doi: 10.3390/app10030918.
[74] M. Hara *et al.*, “A Carbon Material as a Strong Protonic Acid,” *Angew. Chemie Int. Ed.*, vol. 43, pp. 2955–2958, 2004, doi: 10.1002/anie.200453947.
[75] A. Takagaki *et al.*, “Esterification of higher fatty acids by a novel strong solid acid,” *Catal.*

*Today*, vol. 116, pp. 157–161, 2006, doi: 10.1016/j.cattod.2006.01.037.
[76] X. Mo *et al.*, "Activation and deactivation characteristics of sulfonated carbon catalysts," *J. Catal.*, vol. 254, no. 2, pp. 332–338, 2008, doi: 10.1016/j.jcat.2008.01.011.
[77] G. M. A. Bureros *et al.*, "Cacao shell-derived solid acid catalyst for esterification of oleic acid with methanol," *Renew. Energy*, vol. 138, pp. 489–501, 2019, doi: 10.1016/j.renene.2019.01.082.
[78] A. Ghosh, A. Singha, A. Auroux, A. Das, D. Sen, and B. Chowdhury, "A green approach for the preparation of a surfactant embedded sulfonated carbon catalyst towards glycerol acetalization reactions," *Catal. Sci. Technol.*, vol. 10, no. 14, pp. 4827–4844, 2020, doi: 10.1039/d0cy00336k.
[79] A. A. Kiss, A. C. Dimian, and G. Rothenberg, "Solid acid catalysts for biodiesel production – towards sustainable energy," *Adv. Synth. Catal.*, vol. 348, pp. 75–81, 2006, doi: 10.1002/adsc.200505160.
[80] E. J. Anthony, A. P. Iribarne, and J. V. Iribarne, "Fouling in a utility-scale CFBC boiler firing 100% petroleum coke," *Fuel Process. Technol.*, vol. 88, no. 6, pp. 535–547, 2007, doi: 10.1016/j.fuproc.2005.05.004.
[81] J. Wang, E. J. Anthony, and J. C. Abanades, "Clean and efficient use of petroleum coke for combustion and power generation," *Fuel*, vol. 83, no. 10, pp. 1341–1348, 2004, doi: 10.1016/j.fuel.2004.01.002.
[82] J. Chen and X. Lu, "Progress of petroleum coke combusting incirculating fluidized bed boilers—A review and future perspectives," *Resour. Conversat. Recycl.*, vol. 49, no. 3, pp. 203–216, 2007, doi: 10.1016/j.resconrec.2006.03.012.
[83] H. Al-Haj-Ibrahim and B. I. Morsi, "Desulfurization of Petroleum Coke: A Review," *Ind. Eng. Chem. Res.*, vol. 31, no. 8, pp. 1835–1840, 1992, doi: 10.1021/ie00008a001.
[84] X. Yu *et al.*, "Temperature-resolved evolution and speciation of sulfur during pyrolysis of a high-sulfur petroleum coke," *Fuel*, vol. 295, no. December 2020, p. 120609, 2021, doi: 10.1016/j.fuel.2021.120609.
[85] M. Wu *et al.*, "Preparation of porous carbons from petroleum coke by different activation methods," *Fuel*, vol. 84, no. 14–15, pp. 1992–1997, 2005, doi: 10.1016/j.fuel.2005.03.008.
[86] J. Landwehr, H. Steldinger, and B. J. M. Etzold, "Introducing sulphur surface groups in microporous carbons: A mechanistic study on carbide derived carbons," *Catal. Today*, vol. 301, pp. 191–195, 2018, doi: 10.1016/j.cattod.2017.05.027.
[87] A. M. Kern, B. Zierath, T. Fey, and B. J. M. Etzold, "Adsorption of Nickel Ions on OxygenFunctionalized Carbons," *Chem. Eng. Technol.*, vol. 39, no. 4, pp. 715–722, 2016, doi: 10.1002/ceat.201500694.
[88] Z. Zeng, L. Cui, W. Xue, J. Chen, and Y. Che, "Recent Developments on the Mechanism and Kinetics of Esterification Reaction Promoted by Various Catalysts," *Chem. Kinet.*, pp. 255–282, 2012, doi: 10.5772/38106.
[89] M. Berrios, J. Siles, M. A. Martín, and A. Martín, "A kinetic study of the esterification of free fatty acids (FFA) in sunflower oil," *Fuel*, vol. 86, pp. 2383–2388, 2007, doi: 10.1016/j.fuel.2007.02.002.
[90] H. S. Fogler, *Elements of chemical reaction engineering*, 5th ed. Boston: Prentice Hall, 2016.
[91] L. Ma, Y. Han, K. Sun, J. Lu, and J. Ding, "Kinetic and thermodynamic studies of the esterification of acidified oil catalyzed by sulfonated cation exchange resin," *J. Energy Chem.*, vol. 24, pp. 456–462, 2015, doi: 10.1016/j.jechem.2015.07.001.

[92] D. Rattanaphra, A. P. Harvey, A. Thanapimmetha, and P. Srinophakun, “Kinetic of myristic acid esterification with methanol in the presence of triglycerides over sulfated zirconia,” *Renew. Energy*, vol. 36, no. 10, pp. 2679–2686, 2011, doi: 10.1016/j.renene.2011.02.018.
[93] M. G. Kulkarni, R. Gopinath, L. C. Meher, and A. K. Dalai, “Solid acid catalyzed biodiesel production by simultaneous esterification and transesterification,” *Green Chem.*, vol. 8, no. 12, pp. 1056–1062, 2006, doi: 10.1039/b605713f.
[94] B. M. Reddy and M. K. Patil, “Organic Syntheses and Transformations Catalyzed by Sulfated Zirconia,” *Chem. Rev.*, vol. 109, no. 6, pp. 2185–2208, 2009, doi: 10.1021/cr900008m.
[95] Y. H. Hui, “Bailey’s Industrial Oil & Fat Products,” vol. 1, p. 24, 1996.
[96] PubChem, “Methyl octanoate (compound),” *US National Library of Medicine, National Center for Biotechnology Information*, 2020. https://pubchem.ncbi.nlm.nih.gov/compound/Methyl-octanoate (accessed Apr. 16, 2020).
[97] X.-X. Han *et al.*, “Syntheses of novel halogen-free Brønsted–Lewis acidic ionic liquid catalysts and their applications for synthesis of methyl caprylate,” *Green Chem.*, vol. 17, pp. 499–508, 2015, doi: 10.1039/c4gc01470g.
[98] M. J. C. Rezende and A. C. Pinto, “Esterification of fatty acids using acid-activated Brazilian smectite natural clay as a catalyst,” *Renew. Energy*, vol. 92, pp. 171–177, 2016, doi: 10.1016/j.renene.2016.02.004.
[99] B. Liu, P. Jiang, P. Zhang, G. Bian, and M. Li, “Preparation and characterization of SO42−/FexAl1−xPO4 solid acid catalysts for caprylic acid esterification,” *Catal. Commun.*, vol. 99, pp. 49–52, 2017, doi: 10.1016/j.catcom.2017.05.020.
[100] S. Furuta, H. Matsuhashi, and K. Arata, “Biodiesel fuel production with solid superacid catalysis in fixed bed reactor under atmospheric pressure,” *Catal. Commun.*, vol. 5, pp. 721–723, 2004, doi: 10.1016/j.catcom.2004.09.001.
[101] S. Furuta, H. Matsuhashi, and K. Arata, “Biodiesel fuel production with solid amorphous-zirconia catalysis in fixed bed reactor,” *Biomass Bioenergy*, vol. 30, pp. 870–873, 2006, doi: 10.1016/j.biombioe.2005.10.010.
[102] K. Saravanan, B. Tyagi, and H. C. Bajaj, “Esterification of caprylic acid with alcohol over nano-crystalline sulfated zirconia,” *J. Sol-Gel Sci. Technol.*, vol. 62, pp. 13–17, 2012, doi: 10.1007/s10971-011-2671-9.
[103] S. Furuta, H. Matsuhashi, and K. Arata, “Catalytic action of sulfated tin oxide for etherification and esterification in comparison with sulfated zirconia,” *Appl. Catal. A Gen.*, vol. 269, pp. 187–191, 2004, doi: 10.1016/j.apcata.2004.04.017.
[104] R. Rennie and J. Law, *A Dictionary of Chemistry*, 7th ed. Cambridge: Oxford University Press, 2016.
[105] G. C. Bond, M. A. Keane, H. Kral, and J. A. Lercher, “Compensation Phenomena in Heterogeneous Catalysis: General Principles and a Possible Explanation,” *Catal. Rev.*, vol. 42, no. 3, pp. 323–383, 2007, doi: 10.1081/CR-100100264.
[106] A. Patel and V. Brahmkhatri, “Kinetic study of oleic acid esterification over 12-tungstophosphoric acid catalyst anchored to different mesoporous silica supports,” *Fuel Process. Technol.*, vol. 113, pp. 141–149, 2013, doi: 10.1016/j.fuproc.2013.03.022.
[107] J. Haber, J. H. Block, and B. Delmon, “Manual of methods and procedures for catalyst characterization,” 1995.
[108] G. C. Bond, “Heterogeneous catalysis: principles and applications,” in *Oxford Chemistry Series 34*, 2nd ed., Oxford: Clarendon Press, 1987, p. 176.

[109] M. D. Koretsky, *Engineering and Chemical Thermodynamics*, 2nd ed. Hoboken, N.J.: Wiley, 2012.
[110] P. N. Dange and V. K. Rathod, "Equilibrium and thermodynamic parameters for heterogeneous esterification of butyric acid with methanol under microwave irradiation," *Resour. Technol.*, vol. 3, pp. 64–70, 2017, doi: 10.1016/j.reffit.2016.11.012.
[111] J. B. Ott and J. Boerio-Goates, *Chemical Thermodynamics: Principles and Applications*, 1st ed. Burlington: Elsevier Science & Technology, 2000.
[112] Q. Huang, A. S. Schafranski, M. J. Hazlett, Y. Xiao, and J. M. Hill, "Nitric Acid Functionalization of Petroleum Coke to Access Inherent Sulfur," *Catalysts*, vol. 10, no. 2, pp. 259–272, 2020, doi: 10.3390/catal10020259.
[113] Agilent Technologies, "Fundamentals of Gas Chromatography," Wilmington, Delaware, G1176-90000, 2002. [Online]. Available: https://www.agilent.com/cs/library/usermanuals/Public/G1176-90000_034327.pdf.
[114] E. Stauffer, J. A. Dolan, and R. Newman, "Gas Chromatography and Gas Chromatography-Mass Spectrometry," in *Fire Debris Analysis*, 1 ed., Boston, MA: Elsevier Science & Technology, 2008, p. 683.
[115] L. Geng, G. Yu, Y. Wang, and Y. Zhu, "Ph-SO3H-modified mesoporous carbon as an efficient catalyst for the esterification of oleic acid," *Appl. Catal. A Gen.*, vol. 427–428, pp. 137–144, 2012, doi: 10.1016/j.apcata.2012.03.044.
[116] M. Boudart, "Turnover Rates in Heterogeneous Catalysis," *Chem. Rev.*, vol. 95, no. 3, pp. 661–666, 1995, doi: 10.1021/cr00035a009.
[117] Q. Zhang, X. Liu, T. Yang, C. Yue, Q. Pu, and Y. Zhang, "Facile synthesis of polyoxometalates tethered to post Fe-BTC frameworks for esterification of free fatty acids to biodiesel," *RSC Adv.*, vol. 9, no. 14, pp. 8113–8120, 2019, doi: 10.1039/c8ra10574j.
[118] R. D. Cortright and J. A. Dumesic, "Kinetics of Heterogeneous Catalytic Reactions: Analysis of Reaction Schemes," in *Advances in Catalysis*, vol. 46, 2001, pp. 161–264.
[119] J. W. Harris, A. A. Verma, J. W. Arvay, A. J. Shih, W. N. Delgass, and F. H. Ribeiro, "Consequences of product inhibition in the quantification of kinetic parameters," *J. Catal.*, vol. 389, pp. 468–475, 2020, doi: 10.1016/j.jcat.2020.06.014.
[120] A. M. Helmenstine, "ThoughtCo.," *Random Error vs. Systematic Error*, 2020. https://www.thoughtco.com/random-vs-systematic-error-4175358 (accessed Oct. 14, 2020).
[121] A. Kolski-Andreaco, A. Wilkens, and A. Manocchi, "Internal Standards," *University of Virginia*. www.jove.com/t/10225/internal-standards (accessed Oct. 18, 2020).
[122] D. M. Levine, P. P. Ramsey, and R. K. Smidt, *Applied Statistics for Engineers and Scientists*. New Jersey: Prentice Hall, 2001.
[123] Y. Liu, E. Lotero, and J. G. J. Goodwin, "A comparison of the esterification of acetic acid with methanol using heterogeneous versus homogeneous acid catalysis," *J. Catal.*, vol. 242, pp. 278–286, 2006, doi: 10.1016/j.jcat.2006.05.026.
[124] RESTEK®, "Guide to GC Column Selection and Optimizing Separations," *Pure Chromatography*. p. 16, 2013, doi: GNBR1724-UNV.
[125] K. Kelly, "Phenomenex®," *Choosing an Internal Standard*, 2014. https://www.phenomenex.com/ (accessed Oct. 18, 2020).
[126] WOLFRAM, "WolframAlpha," 2020. https://www.wolframalpha.com/ (accessed Oct. 11, 2020).
[127] Y. Zou, "A comparison study of the analysis of volatile organic acids and fatty acids,"

Shanghai, 2018. doi: 5991-9223EN.
[128] P. R. S. Dos Santos, F. Wypych, F. A. P. Voll, F. Hamerski, and M. L. Corazza, “Kinetics of ethylic esterification of lauric acid on acid activated montmorillonite (STx1-b) as catalyst,” *Fuel*, vol. 181, pp. 600–609, 2016, doi: 10.1016/j.fuel.2016.05.026.
[129] M. Banchero and G. Gozzelino, “Nb2O5-catalyzed kinetics of fatty acids esterification for reactive distillation process simulation,” *Chem. Eng. Res. Des.*, vol. 100, pp. 292–301, 2015, doi: 10.1016/j.cherd.2015.05.043.
[130] N. Asikin-Mijan, H. V. Lee, and Y. H. Taufiq-Yap, “Synthesis and catalytic activity of hydration–dehydration treated clamshell derived CaO for biodiesel production,” *Chem. Eng. Res. Des.*, vol. 102, pp. 368–377, 2015, doi: 0.1016/j.cherd.2015.07.002.
[131] M. S. A. Farabi, M. L. Ibrahim, U. Rashid, and Y. H. Taufiq-Yap, “Esterification of palm fatty acid distillate using sulfonated carbon-based catalyst derived from palm kernel shell and bamboo,” *Energy Convers. Manag.*, vol. 181, pp. 562–570, 2019, doi: 10.1016/j.enconman.2018.12.033.
[132] Aspen Plus®, “Aspen Plus User Guide.” Aspen Technology, Inc., Cambridge, MA, p. 936, 2000, [Online]. Available: www.aspentech.com.
[133] S. Z. Hassan and M. Vinjamur, “Analysis of Sensitivity of Equilibrium Constant to Reaction Conditions for Esterification of Fatty Acids with Alcohols,” *Ind. Eng. Chem. Res.*, vol. 52, pp. 1205–1215, 2013, doi: 10.1021/ie301881g.
[134] A. Alsalme, E. F. Kozhevnikova, and I. V. Kozhevnikov, “Heteropoly acids as catalysts for liquid-phase esterification and transesterification,” *Appl. Catal. A Gen.*, vol. 349, no. 1–2, pp. 170–176, 2008, doi: 10.1016/j.apcata.2008.07.027.
[135] L. Geng, Y. Wang, G. Yu, and Y. Zhu, “Efficient carbon-based solid acid catalysts for the esterification of oleic acid,” *Catal. Commun.*, vol. 13, no. 1, pp. 26–30, 2011, doi: 10.1016/j.catcom.2011.06.014.
[136] L. H. O. Pires *et al.*, “Esterification of a waste produced from the palm oil industry over 12-tungstophosforic acid supported on kaolin waste and mesoporous materials,” *Appl. Catal. B Environ.*, vol. 160–161, no. 1, pp. 122–128, 2014, doi: 10.1016/j.apcatb.2014.04.039.
[137] A. E. R. S. Khder, “Preparation, characterization and catalytic activity of tin oxide-supported 12-tungstophosphoric acid as a solid catalyst,” *Appl. Catal. A Gen.*, vol. 343, no. 1–2, pp. 109–116, 2008, doi: 10.1016/j.apcata.2008.03.027.
[138] D. E. López, J. G. Goodwin Jr, D. A. Bruce, and E. Lotero, “Transesterification of triacetin with methanol on solid acid and base catalysts,” *Appl. Catal. A Gen.*, vol. 295, pp. 97–105, 2005, doi: 10.1016/j.apcata.2005.07.055.
[139] I. Sádaba, M. López Granados, A. Riisager, and E. Taarning, “Deactivation of solid catalysts in liquid media: the case of leaching of active sites in biomass conversion reactions,” *Green Chem.*, vol. 17, no. 8, pp. 4133–4145, 2015, doi: 10.1039/c5gc00804b.
[140] D. R. Lathiya, D. V. Bhatt, and K. C. Maheria, “Synthesis of sulfonated carbon catalyst from waste orange peel for cost effective biodiesel production,” *Bioresour. Technol. Reports*, vol. 2, pp. 69–76, 2018, doi: 10.1016/j.biteb.2018.04.007.
[141] J. M. Fraile, E. García-Bordejé, E. Pires, and L. Roldán, “New insights into the strength and accessibility of acid sites of sulfonated hydrothermal carbon,” *Car*, vol. 77, pp. 1157–1167, 2014, doi: 10.1016/j.carbon.2014.06.059.
[142] T. E. Souza, M. F. Portilho, P. M. T. G. Souza, P. P. Souza, and L. C. A. Oliveira, “Modified Niobium Oxyhydroxide Catalyst: An Acetalization Reaction to Produce Bio-additives for Sustainable Use of Waste Glycerol,” *ChemCatChem Full Pap.*, vol. 6, pp. 2961–2969,

2014, doi: 10.1002/cctc.201402322.
[143] X. Mo, E. Lotero, C. Lu, Y. Liu, and J. G. Goodwin, "A Novel Sulfonated Carbon Composite Solid Acid Catalyst for Biodiesel Synthesis," *Catal. Letters*, vol. 123, pp. 1–6, 2008, doi: 10.1007/s10562-008-9456-y.
[144] S. Ebnesajjad, "Surface and Material Characterization Techniques," in *Surface Treatment of Materials for Adhesion Bonding*, William Andrew Applied Science, 2006, pp. 43–75.
[145] J. R. Kastner, J. Miller, D. P. Geller, J. Locklin, L. H. Keith, and T. Johnson, "Catalytic esterification of fatty acids using solid acid catalysts generated from biochar and activated carbon," *Catal. Today*, vol. 190, no. 1, pp. 122–132, 2012, doi: 10.1016/j.cattod.2012.02.006.
[146] W. O. Haag, "Zeolites and Related Microporous Materials: State of the Art 1994," in *Studies in Surface Science and Catalysis*, 1st ed., vol. 84B, no. 1, Amsterdam, 1994, p. 1375.
[147] K. Sun *et al.*, "Polar and aliphatic domains regulate sorption of phthalic acid esters (PAEs) to biochars," *Bioresour. Technol.*, vol. 118, pp. 120–127, 2012, doi: 10.1016/j.biortech.2012.05.008.
[148] E. T. Özer and Ş. Güçer, "Determination of Some Phthalate Acid Esters in Artificial Saliva by Gas Chromatography-Mass Spectrometry after Activated Carbon Enrichment," *Talanta*, vol. 84, no. 2, pp. 362–367, 2011, doi: 10.1016/j.talanta.2011.01.003.
[149] Y. Liu, E. Lotero, and J. G. Goodwin Jr, "Effect of water on sulfuric acid catalyzed esterification," *J. Mol. Catal. A Chem.*, vol. 245, pp. 132–140, 2006, doi: 10.1016/j.molcata.2005.09.049.
[150] J. F. G. Oliveira *et al.*, "Biodiesel production from waste coconut oil by esterification with ethanol: The effect of water removal by adsorption," *Renew. Energy*, vol. 35, no. 11, pp. 2581–2584, 2010, doi: 10.1016/j.renene.2010.03.035.
[151] L. P. Fallavena *et al.*, "Ultrasound technology and molecular sieves improve the thermodynamically controlled esterification of butyric acid mediated by immobilized lipase from Rhizomucor miehei," *RSC Adv.*, vol. 4, pp. 8675–8681, 2014, doi: 10.1039/c3ra47315e.
[152] I. L. Lucena, G. F. Silva, and F. A. N. Fernandes, "Biodiesel Production by Esterification of Oleic Acid with Methanol Using a Water Adsorption Apparatus," *Ind. Eng. Chem. Res.*, vol. 47, no. 18, pp. 6885–6889, 2008, doi: 10.1021/ie800547h.
[153] I. L. Lucena *et al.*, "Oleic acid esterification with ethanol under continuous water removal conditions," *Fuel*, vol. 90, pp. 902–904, 2011, doi: 10.1016/j.fuel.2010.10.022.
[154] I. E.I. du Pont de Nemours & Co., "Molecular Sieves," *Sigma-Aldrich*, 2021. https://www.sigmaaldrich.com/chemistry/chemical-synthesis/learning-center/technical-bulletins/al-1430/molecular-sieves.html (accessed May 11, 2021).
[155] P. N. Dwivedi and S. N. Upadhyay, "Particle-Fluid Mass Transfer in Fixed and Fluidized Beds," *Ind. Eng. Chem. Process Des. Dev.*, vol. 16, no. 2, pp. 157–165, 1977, doi: 10.1021/i260062a001.
[156] C. J. King, L. Hsueh, and K. W. Mao, "Liquid Phase Diffusion of Nonelectrolytes at High Dilution," *J. Chem. Eng. Data*, vol. 10, no. 4, pp. 348–350, 1965, doi: 10.1021/je60027a014.
[157] I. E. Maloka, "Generalized liquid molar volume at the normal boiling point correlation," *Pet. Sci. Technol.*, vol. 23, no. 2, pp. 133–136, 2005, doi: 10.1081/LFT-200028058.
[158] NIST, "National Institute of Standards and Technology," *Methyl Alcohol*, 2018. https://webbook.nist.gov/cgi/cbook.cgi?ID=C67561&Type=HVAP (accessed Oct. 30,

2020).
[159] A. P. Toor, M. Sharma, G. Kumar, and R. K. Wanchoo, “Kinetic study of esterification of acetic acid with n-butanol and isobutanol catalyzed by ion exchange resin,” *Bull. Chem. React. Eng. Catal.*, vol. 6, no. 1, pp. 23–30, 2011, doi: bcrec_017_2010_665.
[160] H. J. Klimisch, M. Andreae, and U. Tillman, “Robust Summary of Information on Petroleum Coke,” 2000.
[161] L. Zhao and Q. Sun, “Calculations of effectiveness factors and the criteria of mass transfer effect for high-temperature methanation (HTM) catalyst,” *Int. J. ofLow-Carbon Technol.*, vol. 10, pp. 288–293, 2015, doi: 10.1093/ijlct/ctu005.
[162] K. Ountaksinkul, S. Wannakao, P. Praserthdam, and S. Assabumrungrat, “Intrinsic kinetic study of 1-butene isomerization over magnesium oxide catalyst via a Berty stationary catalyst basket reactor,” *RSC Adv.*, vol. 10, pp. 36667–36677, 2020, doi: 10.1039/d0ra05453d.
[163] P. B. Weisz and C. D. Prater, “Interpretation of Measurements in Experimental Catalysis,” *Adv. Catal.*, vol. 6, no. C, pp. 143–196, 1954, doi: 10.1016/S0360-0564(08)60390-9.
[164] M. Ternan, “The diffusion of liquids in pores,” *Can. J. Chem. Eng.*, vol. 65, no. 2, pp. 244–249, 1987, doi: 10.1002/cjce.5450650208.
[165] F. Jiménez-Cruz and G. C. Laredo, “Molecular size evaluation of linear and branched paraffins from the gasoline pool by DFT quantum chemical calculations,” *Fuel*, vol. 83, pp. 2183–2188, 2004, doi: 10.1016/j.fuel.2004.06.010.
[166] C. E. Webster, R. S. Drago, and M. C. Zerner, “A Method for Characterizing Effective Pore Sizes of Catalysts,” *J. Phys. Chem. B*, vol. 103, no. 8, pp. 1242–1249, 1999, doi: 10.1021/jp984055n.
[167] H. H. Funke, A. M. Argo, C. D. Baertsch, J. L. Falconer, and R. D. Noble, “Separation of close-boiling hydrocarbons with silicalite zeolite membranes,” *Faraday Trans.*, vol. 92, no. 13, pp. 2499–2502, 1996, doi: 10.1039/FT9969202499.
[168] Z. Ziyang, K. Hidajat, and A. K. Ray, “Determination of adsorption and kinetic parameters for methyl tert-butyl ether synthesis from tert-butyl alcohol and methanol,” *J. Catal.*, vol. 200, no. 2, pp. 209–221, 2001, doi: 10.1006/jcat.2001.3180.
[169] G. D. Yadav and M. B. Thathagar, “Esterification of maleic acid with ethanol over cation-exchange resin catalysts,” *React. Funct. Polym.*, vol. 52, no. 2, pp. 99–110, 2002, doi: 10.1016/S1381-5148(02)00086-X.
[170] N. Ozbay, N. Oktar, G. Dogu, and T. Dogu, “Activity comparison of different solid acid catalysts in etherification of glycerol with tert-butyl alcohol in flow and batch reactors,” *Top. Catal.*, vol. 56, no. 18–20, pp. 1790–1803, 2013, doi: 10.1007/s11244-013-0116-0.
[171] AlfaAesar, “89079 Amberlyst® 15(H), ion exchange resin,” *Thermo Fisher Scientific*, 2021. https://www.alfa.com/en/catalog/089079/ (accessed Mar. 20, 2021).

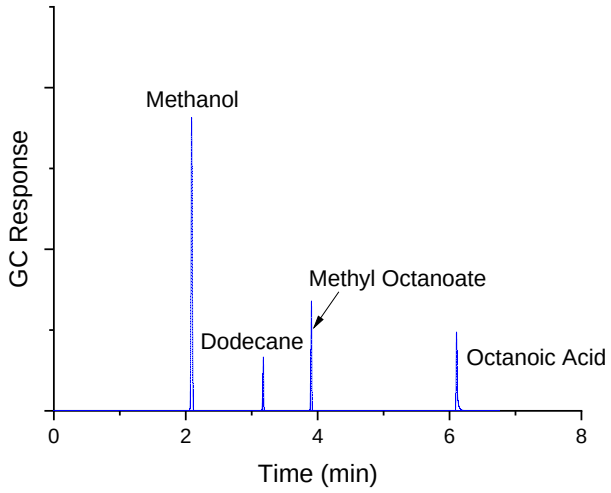


Figure A-1. GC analysis using the column DB-FATWAX UI for a sample of the model reaction (esterification of octanoic acid with methanol using dodecane as the internal standard) at around 50% ester yield.

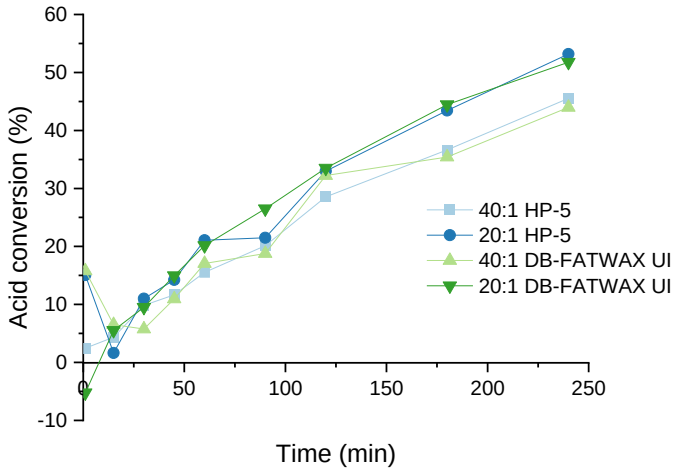


Figure A-2. Results of acid conversion analyzed by GC columns HP-5 and DB-FATWAX UI; reactions with Amberlyst-15 at same conditions (60 °C, 600 rpm, 4 h, catalyst loading of 5 wt%) and methanol-to-acid ratio equal to 40:1 or 20:1.

*Mass Transfer Limitations*

*External Mass Transfer Limitation*

To confirm the absence of external transfer limitation using catalyst loading of 2 wt%, Mears Criterion ($MR$) was also applied [90], Equation 31. When $MR$ < 0.15, the same concentration in the bulk solution and external surface of the catalyst is expected, which means that no limitations due to external mass transfer exist.

$$MR = \frac{-r'_A \rho_c r_p n}{k_c C_{A0}} < 0.15 \qquad 31$$

where $-r'_A$ is the reaction rate per unit mass of catalyst (mol/g-cat·s); $\rho_c$ is the density of catalyst (g/mL); $r_p$ is the catalyst particle radius (m); $n$ is the reaction order (assumed as 1); $k_c$ is the mass transfer coefficient (m/s); $C_{A0}$ is the bulk reactant concentration (mol/mL) at the beginning of the reaction (octanoic acid, in this case). Experimental results are still necessary for this analysis since the Mears criterion depends on the observed reaction rate at a specific stirring speed.

The mass transfer coefficient ($k_c$) necessary for Equation 31, was estimated by Dwidevi-Upadhyay mass transfer correlation [155], Equation 32, which is adequate for small particles with diameter < 0.6 mm, suspended in agitated liquids.

$$k_c = \frac{2D_{AB}}{d_p} + 0.31 N_{SC}^{-\frac{2}{3}} \left(\frac{\Delta\rho \mu_s g}{\rho_s^2}\right)^{1/3} \qquad 32$$

where $D_{AB}$ is the diffusivity of the limiting reactant (octanoic acid) in the solvent (methanol) ($m^2/s$); $d_p$ is the diameter of the catalyst (m); $N_{SC}$ is the Schmidt number, defined as $\frac{\mu_c}{\rho_c D_{AB}}$; $\Delta\rho$ is

the absolute differential density of the catalyst and solution (kg/m$^3$); $\mu_s$ is the viscosity of the solution (Pa·s); $g$ is the gravitational acceleration (m/s$^2$); and $\rho_s$ is the density of solution (kg/m$^3$).

Likewise, an appropriate expression for the diffusivity of octanoic acid in methanol ($D_{AB}$) must be chosen. Being a liquid dilute solute (< 10 mol%) in a non-aqueous solvent, the expression of King, Hsueh, and Mao applies correctly [156], Equation 33,

$$D_{AB} = 4.4 \times 10^{-8} \frac{T}{\mu_B} \left(\frac{V_B}{V_A}\right)^{1/6} \left(\frac{\Delta H_{vap,B}}{\Delta H_{vap,A}}\right)^{1/2} \quad 33$$

where $T$ is the system temperature (K); $\mu_B$ is the viscosity of solvent (methanol) (Pa·s); $V_i$ is the molar volume of component i (octanoic acid or methanol) at normal boiling point (m$^3$/kmol); $\Delta H_{vap,i}$ is the enthalpy of vaporization of those components at normal boiling point (J/kmol).

Functionalized petcoke P-N-3 was chosen as a reference for petcoke-derived catalysts. Data used to calculate the parameters given by Equations 31 - 33 for both Amberlyst-15 and P-N-3 catalysts are presented in Table A-1 and Table A-2. Due to the lack of data in the literature at specific conditions of temperature (normal boiling point of compounds and reaction temperature), some parameters were simulated by Aspen Properties. The thermodynamic model chosen was UNIQUAC – Hayden-O'Connell, a good predictive model for strongly nonideal liquid solutions (combination of polar and non-polar compounds) and liquid-liquid equilibria [132]. Additional parameters were the system temperature at reaction condition of 60 °C and gravitational acceleration equal to 9.81 m/s$^2$.

Table A-1. Physico-chemical properties of methanol, octanoic acid, and mixture of reagents at reaction conditions for calculation of diffusivity and mass transfer coefficient.

| **Properties** | | **Reference** |
|---|---|---|
| Viscosity of methanol at 60 °C, $\mu_B$ (Pa·s) | 3.60 x $10^{-4}$ | Aspen |
| Molar volume of methanol at 64.7 °C, $V_B$ ($cm^3$/mol) | 42.5 | [157] |
| Molar volume of octanoic acid at 237 °C, $V_A$ ($cm^3$/mol) | 19.9 | Aspen |
| Heat of vaporization of methanol, $\Delta H_{vap,B}$ (J/kmol) | 3.52 x $10^7$ | [158] |
| Heat of vaporization of octanoic acid, $\Delta H_{vap,A}$ (J/kmol) | 5.38 x $10^7$ | Aspen |
| Viscosity of solution at 60 °C, $\mu_s$ (Pa·s) | 3.93 x $10^{-4}$ | Aspen |
| Density of solution at 60 °C, $\rho_s$ (g/mL) | 0.776 | Aspen |
| Initial concentration of octanoic acid in solution, $C_{A0}$ (mol/mL) | 1.0 x $10^{-3}$ | Calculated |

Particle sizes of catalysts were measured in the laboratory using a set of stainless-steel standard sieves (W.S. Tyler, ON, Canada). The reaction rates corresponded to experiments at the following conditions: 60 °C, 600 rpm, methanol-to-acid ratio of 20:1, and catalyst loading of 2 wt% (0.1 g), using data below 10% conversion.

Table A-2. Physical properties for the catalysts Amberlyst-15 and P-N-3, and initial rate of reaction (at 60 °C, 600 rpm, methanol-to-acid ratio of 20:1, catalyst loading of 2 wt%) catalyzed by these materials for calculation of mass transfer coefficient and Mears criterion.

| **Properties** | | **Reference** |
|---|---|---|
| Amberlyst-15 | | |
| Density, $\rho_b$ ($kg/m^3$) | 1410 | [159] |
| Particle size, $d_p$ (m) | 5.0 x $10^{-4}$ | Measured |
| Reaction rate, $-r'_A$ (mol/g-cat·s) | 1.3 x $10^{-5}$ | Measured |
| Functionalized Petcoke, P-N-3 | | |
| Density, $\rho_b$ ($kg/m^3$) | 2110 | [160] |
| Particle size, $d_p$ (m) | < 5.0 x $10^{-5}$ | Measured |
| Reaction rate, $-r'_A$ (mol/g-cat·s) | 1.9 x $10^{-6}$ | Measured |

The diffusivity of octanoic acid in methanol, the mass transfer coefficient, and the Mears criterion are presented in Table A-3.

Table A-3. Calculated parameters to evaluate the existence of external mass transfer limitation in reactions catalyzed by Amberlyst-15 and P-N-3 at 60 °C, 600 rpm, methanol-to-acid ratio of 20:1, catalyst loading of 2 wt%.

| **Parameter** | **Amberlyst-15** | **P-N-3** |
|---|---|---|
| Diffusivity of octanoic acid, $D_{AB}$ ($m^2/s$) | 2.5 x $10^{-9}$ | 2.5 x $10^{-9}$ |
| Mass transfer coefficient, $k_c$ (m/s) | 1.6 x $10^{-4}$ | 2.9 x $10^{-4}$ |
| Mears criterion, $MR$ | 0.029 | < 0.001 |

Mears criterion was satisfied for both catalysts ($MR$< 0.15), meaning no external mass transfer limitation should be present in the reaction system. Calculating for the P-S-3 sample, the Mears criterion resulted in 0.003, which was also satisfied. This way, no external mass transfer limitation was assumed for the reactions at 60 °C catalyzed by Amberlyst-15 and functionalized petcoke.

The same calculation using the appropriate reaction rates at 60 °C for the masses of 0.2 g (4.5 wt%) resulted in values equal to 0.027 and 3 x $10^{-4}$ for Amberlyst-15 and P-N-3, respectively. The Mears criterion was again satisfied, contradicting the behavior observed in Table 4-5 of diffusion limitation using a loading of 4.5 wt% for Amberlyst-15.

*Internal Mass Transfer Limitation*

For first-order reactions, the internal-diffusion-limited reaction rate is given by Equation 34, which is proportional, among other parameters, to the catalyst particle size, $-r_A \propto \frac{1}{d_p}$, when internal diffusion prevails.

$$-r_A = \frac{3}{r_p}\sqrt{D_{eff}k_1}\,C_{A0} \qquad 34$$

where $-r_A$ is the volumetric rate of reaction (mol/mL·s); $r_p$ is the catalyst particle radius (m); $D_{eff}$ is the effective diffusivity inside the catalyst particle ($m^2/s$); $k_1$ is the rate constant of the forward reaction ($min^{-1}$); and $C_{A0}$ is the bulk reactant concentration (mol/mL) at the beginning of the reaction. Therefore, a common practice in the literature [11], [15] is reporting the test of reactions at identical conditions, just separating the particles according to their different particle sizes (diameters). Nevertheless, those tests were not possible in this study since the catalysts employed have a narrow range of particle size, e.g., for P-N-3, $d_p$ < 50 μm.

Another preferable approach taken by many kinetic studies [67], [91], [161], [162] is the calculation of Weisz-Prater criterion ($WP$). This parameter, according to Equation 35, considers that the Thiele modulus (φ) and the effectiveness factor ($\eta$) are both related to internal diffusion behavior.

$$WP = \varphi^2\eta < 1 \qquad 35$$

Large Thiele modulus values are commonly associated with internal diffusion limitations; meanwhile, for small values, the surface reaction is usually the limiting step [90]. The effectiveness factor ($\eta$), ranging from 0 to 1, is a measurement between the actual overall rate of reaction and the expected rate if the entire inner surface was exposed to the external conditions of temperature and concentration [90]. Therefore, in the absence of diffusion limitations, this value is expected to be $\eta$ > 0.95.

However, as long as it is difficult to estimate with accuracy the effectiveness factor $\eta$, the Weisz-Prater criterion based only on measurable quantities is a more practical parameter [163], Equation

36. When $WP < 1$, there is no concentration gradient within the particle, and no limitations of internal mass transfer exist.

$$WP = \frac{-r_A {r_p}^2}{D_{eff} C_{A0}} < 1 \qquad 36$$

where $-r_A$ is the volumetric rate of reaction (mol/mL·s); $r_p$ is the catalyst particle radius (cm); $D_{eff}$ is the effective diffusivity inside the catalyst particle (cm$^2$/s); and $C_{A0}$ is the bulk reactant concentration (mol/mL) at the beginning of the reaction.

Some parameters necessary for Equation 36 are already known from the calculation of external mass transfer limitation. For calculating the effective diffusivity, there are some expressions in the literature, like the one proposed by Ternan [164] for the diffusion of liquids inside pores, Equation 37.

$$D_{eff} = D_{AB} \frac{(1-\lambda)^2}{1+P\lambda} \qquad 37$$

where $D_{eff}$ is the effective diffusivity inside the catalyst particle (cm$^2$/s); $D_{AB}$ is the diffusivity of octanoic acid in methanol (cm$^2$/s); and $\lambda$ is the ratio 'radius of solute molecule (nm)'/'pore radius (nm)'. The parameter *P* has values in the range [2-16] fitted by empirical data of several catalysts. In this calculation, a value of 2 was a good approximation for small values of $\lambda$ and solvents of low viscosity [164]. The value of 16 was also tested in the calculation, not affecting the final result much.

Data used to calculate the effective diffusivity are presented in Table A-4. The radius of the solute molecule (octanoic acid) was not found in the literature. Therefore, the value presented in Table A-4 is an estimation based on work developed by Jiménez-Cruz & Laredo [165]. They

reported the kinetic molecular diameter of isooctane as 6.547 Å, considering the mean between width and height of the molecule. According to Webster *et al.*, this value is the effective minimum dimension of the molecule to access pores [166]. Another reference reported the isooctane diameter as 6.2 Å [167]. As long as the carboxylic group is a bit more voluminous than the paraffinic chain, the value 7.0 Å was used as an estimation for the octanoic acid diameter. The pore radius of Amberlyst-15 was taken from a study made by Ziyang *et al.* [168]. The pore radius of functionalized petcoke was considered as the higher value presented by Huang *et al.* [112], resulting in the largest estimation for the Weisz-Prater criterion.

Table A-4. Physical properties of catalysts Amberlyst-15 and P-N-3 and diffusivity parameter for calculation of effective diffusivity of reagents inside these materials.

| **Parameter** | **Amberlyst-15** | **P-N-3** |
|---|---|---|
| Diffusivity of octanoic acid, $D_{AB}$ ($cm^2/s$) | $2.5 \times 10^{-5}$ | $2.5 \times 10^{-5}$ |
| Radius of solute molecule (nm) | 0.35 | 0.35 |
| Pore radius (nm) | 12 [168] | 0.40 [112] |
| Ratio 'solute radius'/'pore radius', $\lambda$ | 0.029 | 0.875 |
| Effective diffusivity, $D_{eff}$ ($cm^2/s$) | $1.6 \times 10^{-5}$ | $2.7 \times 10^{-8}$ |

Values used for the calculation of the Weisz-Prater criterion are listed in Table A-5. Some parameters, such as the reaction rate, particle radius, and initial concentration of octanoic acid in solution, were taken from the previous analysis and tables.

Table A-5. Calculated parameters to evaluate the existence of internal mass transfer limitation in reactions catalyzed by Amberlyst-15 and P-N-3 at 60 °C, 600 rpm, methanol-to-acid ratio of 40:1, catalyst loading of 2 wt%, through the Weisz-Prater criterion.

| **Parameter** | **Amberlyst-15** | **P-N-3** |
|---|---|---|
| Volumetric rate of reaction, $-r_A$ (mol/mL·s) | 4.2 x $10^{-8}$ | 6.2 x $10^{-9}$ |
| Particle radius, $r_p$ (cm) | 2.5 x $10^{-2}$ | 2.5 x $10^{-3}$ |
| Initial concentration of octanoic acid in solution, $C_{A0}$ (mol/mL) | 1.0 x $10^{-3}$ | 1.0 x $10^{-3}$ |
| Effective diffusivity, $D_{eff}$ ($cm^2/s$) | 1.6 x $10^{-5}$ | 2.7 x $10^{-8}$ |
| Weisz-Prater criterion, $WP$ | 0.002 | 0.002 |

In conclusion, the Weisz-Prater criterion was satisfied for both catalysts ($WP < 1$). For P-S-3, the calculation resulted in a value equal to 0.012, satisfying the Weisz-Prater criterion as well. Therefore, internal mass transfer limitations should not be present for the experimental conditions tested, and the experiments were assumed to be in the kinetic region at 60 °C. Nevertheless, many parameters were estimated with uncertainties as for the calculation of external mass transfer resistance. Thus, these results should be accepted with caution, especially because the pore size of the petcoke samples is not significantly larger than the estimated diameter of the octanoic acid molecule. On the other hand, the small pore size of those petcoke samples might infer that the "true" active sites for reaction are mostly on the external surface of the catalyst, not suffering diffusion limitation.

Table A-6. Simulated values for Gibbs free energy and enthalpy of formation of reaction compounds using UNIQUAC – Hayden-O'Connell model in Aspen Plus®.

| **Temperature (°C)** | **Gibbs Free Energy of Formation (kJ/mol)** | | | |
|---|---|---|---|---|
| | Octanoic Acid | Methanol | Methyl Octanoate | Water |
| **25** | -354.4 | -166.8 | -300.9 | -237.2 |
| **60** | -322.1 | -158.4 | -266.9 | -231.6 |
| **80** | -304.2 | -153.7 | -248.0 | -228.5 |
| **100** | -286.6 | -149.1 | -229.5 | -225.5 |
| **120** | -269.4 | -144.6 | -211.3 | -222.6 |
| **140** | -252.6 | -140.2 | -193.4 | -219.8 |
| **160** | -236.2 | -135.8 | -175.9 | -217.0 |
| **180** | -220.1 | -131.5 | -158.7 | -214.2 |
| **200** | -204.3 | -127.2 | -141.8 | -211.5 |
| **Temperature (°C)** | **Enthalpy of Formation (kJ/mol)** | | | |
| | Octanoic Acid | Methanol | Methyl Octanoate | Water |
| **25** | -634.6 | -238.4 | -595.7 | -285.8 |
| **60** | -622.8 | -234.9 | -585.3 | -283.2 |
| **80** | -615.9 | -232.6 | -579.0 | -281.6 |
| **100** | -608.7 | -230.1 | -572.4 | -280.0 |
| **120** | -601.4 | -227.4 | -565.4 | -278.3 |
| **140** | -593.9 | -224.4 | -558.1 | -276.6 |
| **160** | -586.2 | -221.1 | -550.5 | -274.7 |
| **180** | -578.4 | -217.5 | -542.6 | -272.8 |
| **200** | -570.3 | -213.3 | -534.2 | -270.8 |

## APPENDIX B: SUPPLEMENTARY INFORMATION FOR CHAPTER 5

*Strong Acidity of Amberlyst-15*

Amberlyst-15 is a strongly acidic material: a macroreticular resin with -$SO_3H$ species attached to its surface. The strong acidity of Amberlyst-15 was questionable using the standard procedure described in Section 3.2.5, since it is a specific parameter for the calculation of catalytic activity. Thereby, the titration method was modified for Amberlyst-15 to provide an adequate exchange procedure with excess ions. Table B-1 shows the strong acidity values determined for different NaCl solution concentrations employing Equation 15. The NaCl solution volume for the ion exchange was kept constant as 5 mL, except in the last analysis. The equivalent mass of catalyst in solution was the mass used for ion exchange divided by the dilution volume (5 or 10 parts). The NaCl solution was standardized with KHP (potassium hydrogen phthalate) before the titrations.

$$[H^+] = \frac{V_{NaOH} \times C_{NaOH}}{m_{c,eq}} \qquad 15$$

Table B-1. Experiment results for the determination of strong acidity of Amberlyst-15 by the ion-exchange titration method.

| $C_{NaCl}$ (Molarity) | $C_{NaOH}$ (Molarity) | $V_{NaOH,1}$ (mL) | $V_{NaOH,2}$ (mL) | $V_{NaOH,3}$ (mL) | $m_{cat}$ (g) | $[H^+]$ (mmol/g) | $s$ (mmol/g) |
|---|---|---|---|---|---|---|---|
| 0.1 | 0.005 | 12.10 | 12.10 | 12.25 | 0.02 | 3.01 | 0.02 |
| 0.2 | 0.005 | 14.45 | 14.45 | 14.40 | 0.02 | 3.58 | 0.00 |
| 0.4 | 0.005 | 16.30 | 16.40 | 16.30 | 0.02 | 4.02 | 0.01 |
| 1.0 | 0.010 | 8.95 | 8.95 | 9.00 | 0.02 | 4.42 | 0.01 |
| 2.0 | 0.010 | 9.35 | 9.20 | 9.28 | 0.02 | 4.62 | 0.02 |
| 2.0* | 0.010 | 4.85 | 4.87 | 4.82 | 0.01 | 4.70 | 0.00 |

* Using 10 mL of solution instead of 5 mL.

Therefore, the strong acidity of Amberlyst-15 was determined as 4.70 mmol/g. This result is in agreement with other studies [169], [170]. Moreover, the total exchange capacity of Amberlyst-15 reported by the manufacturer is 4.70 eq/kg [171].

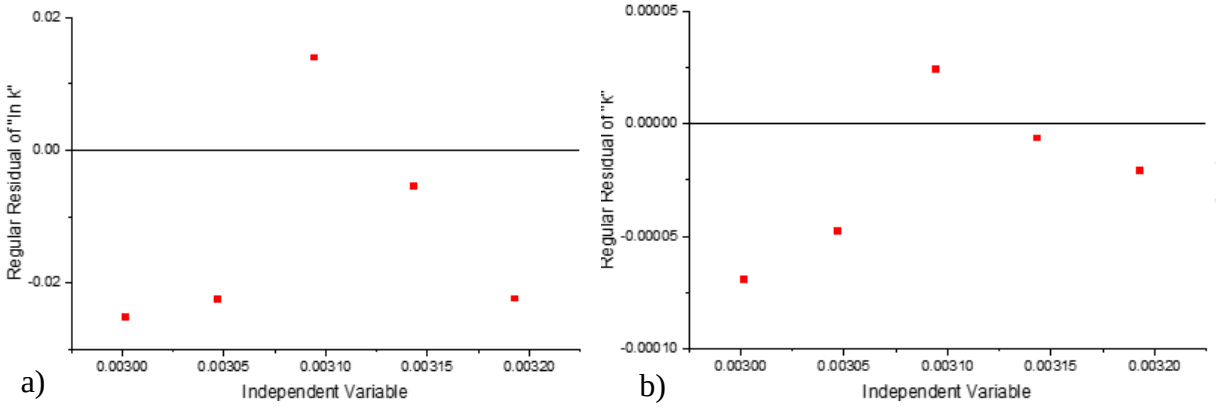


Figure B-1. Residual plots of the fitted curves for determination of activation energy of the model reaction catalyzed by Amberlyst-15 in the range of 40 - 60 °C; using a) linearized and b) exponential Arrhenius equation.

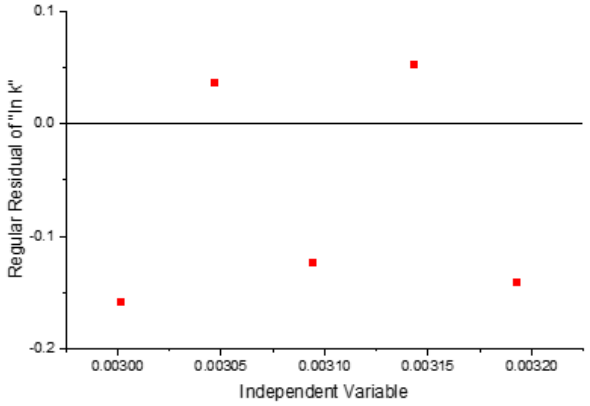


Figure B-2. Residual plot of the fitted curve for determination of activation energy of the model reaction catalyzed by P-S-3 in the range of 40 - 60 °C; using linearized Arrhenius equation.

APPENDIX C: PERMISSION LETTERS FOR REPRINTED CONTENT

## Permission for Table 2-1

JOHN WILEY AND SONS LICENSE
TERMS AND CONDITIONS

May 17, 2021

---

This Agreement between Annelisa Schemberger Schafran ("You") and John Wiley and Sons ("John Wiley and Sons") consists of your license details and the terms and conditions provided by John Wiley and Sons and Copyright Clearance Center.

| | |
|---|---|
| License Number | 5071641302221 |
| License date | May 17, 2021 |
| Licensed Content Publisher | John Wiley and Sons |
| Licensed Content Publication | Canadian Journal of Chemical Engineering |
| Licensed Content Title | Characterization, gasification, activation, and potential uses for the millions of tonnes of petroleum coke produced in Canada each year |
| Licensed Content Author | Maryam Malekshahian, Arash Karimi, Josephine M. Hill |
| Licensed Content Date | Aug 17, 2014 |
| Licensed Content Volume | 92 |
| Licensed Content Issue | 9 |
| Licensed Content Pages | 9 |

| | |
|---|---|
| Type of use | Dissertation/Thesis |
| Requestor type | University/Academic |
| Format | Print and electronic |
| Portion | Figure/table |
| Number of figures/tables | 2 |
| Will you be translating? | No |
| Title | Esterification of Octanoic Acid over Solid Acid Catalysts derived from Petroleum Coke |
| Institution name | University of Calgary |
| Expected presentation date | Jun 2021 |
| Portions | Table 1. Proximate and ultimate analysis of petcoke and char, and ash analysis [10,13,14]; Table 2. Surface areas and pore volumes of petcoke and char. |
| Requestor Location | Annelisa Schemberger Schafran<br>Calgary<br><br>Calgary, AB [redacted]<br>Canada<br>Attn: Annelisa Schemberger Schafran |
| Publisher Tax ID | EU826007151 |
| Total | 0.00 CAD |

## Permission for Figure 2-1

Copyright Clearance Center | Marketplace™

**Order Number:** 1119661
**Order Date:** 17 May 2021

### Payment Information

Annelisa Schemberger Schafran
[redacted]@ucalgary.ca
**Payment method:** Invoice

**Billing Address:**
Annelisa Schemberger Schafran
[redacted]
Calgary, AB [redacted]
Canada

[redacted]@ucalgary.ca

**Customer Location:**
Annelisa Schemberger Schafran
[redacted]
Calgary, AB [redacted]
Canada

### Order Details

1. Green chemistry

**Billing Status:** Open

| | |
|---|---|
| **Order license ID** | 1119661-1 |
| **Order detail status** | Completed |
| **ISSN** | 1463-9270 |
| **Type of use** | Republish in a thesis/dissertation |
| **Publisher** | ROYAL SOCIETY OF CHEMISTRY |
| **Portion** | Chart/graph/table/figure |

**0.00 CAD**
Republication Permission

#### LICENSED CONTENT

| | | | |
|---|---|---|---|
| **Publication Title** | Green chemistry | **Country** | United Kingdom of Great Britain and Northern Ireland |
| **Author/Editor** | Royal Society of Chemistry (Great Britain) | **Rightsholder** | Royal Society of Chemistry |
| **Date** | 12/31/1998 | **Publication Type** | e-Journal |
| **Language** | English | **URL** | http://firstsearch.oclc.org/journal=1463-9262;screen=info;ECOIP |

#### REQUEST DETAILS

| | | | |
|---|---|---|---|
| **Portion Type** | Chart/graph/table/figure | **Distribution** | Worldwide |
| **Number of charts / graphs / tables / figures requested** | 1 | **Translation** | Original language of publication |
| | | **Copies for the disabled?** | No |
| **Format (select all that apply)** | Print,Electronic | **Minor editing privileges?** | Yes |
| **Who will republish the content?** | Academic institution | **Incidental promotional use?** | No |
| | | **Currency** | CAD |
| **Duration of Use** | Life of current edition | | |
| **Lifetime Unit Quantity** | Up to 499 | | |
| **Rights Requested** | Main product | | |

#### NEW WORK DETAILS

| | | | |
|---|---|---|---|
| **Title** | Esterification of Octanoic Acid over Solid Acid Catalysts derived from Petroleum Coke | **Institution name** | University of Calgary |
| | | **Expected presentation date** | 2021-06-21 |
| **Instructor name** | Dr. Josephine M. Hill | | |

#### ADDITIONAL DETAILS

| | |
|---|---|
| **The requesting person / organization to appear on the license** | Annelisa Schemberger Schafranski |

#### REUSE CONTENT DETAILS

| | | | |
|---|---|---|---|
| **Title, description or numeric reference of the portion(s)** | Scheme 1 | **Title of the article/chapter the portion is from** | Solid acid catalyzed biodiesel production by simultaneous esterification and transesterification |
| **Editor of portion(s)** | N/A | | |
| **Volume of serial or monograph** | 8 | **Author of portion(s)** | Mangesh G. Kulkarni, Rajesh Gopinath, Lekha C. Meher and Ajay K. Dalai |
| **Page or page range of portion** | page 1059 | | |
| | | **Publication date of portion** | 2006-09-15 |

**Total Items: 1**

Subtotal: 0.00 CAD
**Order Total: 0.00 CAD**

**Permission for Figure 2-2**



Available from: https://www.intechopen.com/books/chemical-kinetics/recent-developments-on-the-mechanism-and-kinetics-of-esterification-reaction-promoted-by-various-cat

## Permission for Figure 2-3

JOHN WILEY AND SONS LICENSE
TERMS AND CONDITIONS

May 17, 2021

---

This Agreement between Annelisa Schemberger Schafran ("You") and John Wiley and Sons ("John Wiley and Sons") consists of your license details and the terms and conditions provided by John Wiley and Sons and Copyright Clearance Center.

| | |
|---|---|
| License Number | 5070500555354 |
| License date | May 15, 2021 |
| Licensed Content Publisher | John Wiley and Sons |
| Licensed Content Publication | Wiley Books |
| Licensed Content Title | Principles of Heterogeneous Catalysis |
| Licensed Content Author | Michel Boudart, George W. Huber, James A. Dumesic |
| Licensed Content Date | Mar 15, 2008 |
| Licensed Content Pages | 15 |
| Type of use | Dissertation/Thesis |
| Requestor type | University/Academic |
| Format | Print and electronic |
| Portion | Figure/table |

| | |
|---|---|
| Number of figures/tables | 1 |
| Will you be translating? | No |
| Title | Esterification of Octanoic Acid over Solid Acid Catalysts derived from Petroleum Coke |
| Institution name | University of Calgary |
| Expected presentation date | Jun 2021 |
| Portions | Figure 1. General effects of temperature on catalytic activity. The intrinsic activation energy is equal to Ea, and R is the gas constant. |
| Requestor Location | Annelisa Schemberger Schafran<br>Calgary<br><br>Calgary, AB [redacted]<br>Canada<br>Attn: Annelisa Schemberger Schafran |
| Publisher Tax ID | EU826007151 |
| Total | 0.00 CAD |

## Permission for Figure 3-2

ELSEVIER LICENSE
TERMS AND CONDITIONS

May 17, 2021

---

This Agreement between Annelisa Schemberger Schafran ("You") and Elsevier ("Elsevier") consists of your license details and the terms and conditions provided by Elsevier and Copyright Clearance Center.

| | |
|---|---|
| License Number | 5070510334598 |
| License date | May 15, 2021 |
| Licensed Content Publisher | Elsevier |
| Licensed Content Publication | Elsevier Books |
| Licensed Content Title | Fire Debris Analysis |
| Licensed Content Author | Eric Stauffer,Julia A. Dolan,Reta Newman |
| Licensed Content Date | Jan 1, 2008 |
| Licensed Content Pages | 59 |
| Start Page | 235 |
| End Page | 293 |
| Type of Use | reuse in a thesis/dissertation |
| Portion | figures/tables/illustrations |
| Number of figures/tables/illustrations | 1 |
| Format | both print and electronic |
| Are you the author of this Elsevier chapter? | No |

| | |
|---|---|
| Will you be translating? | No |
| Title | Esterification of Octanoic Acid over Solid Acid Catalysts derived from Petroleum Coke |
| Institution name | University of Calgary |
| Expected presentation date | Jun 2021 |
| Portions | FIGURE 8-7 A gas chromatograph and its main components. |
| Requestor Location | Annelisa Schemberger Schafran<br>Calgary<br><br>Calgary, AB T[redacted]<br>Canada<br>Attn: Annelisa Schemberger Schafran |
| Publisher Tax ID | GB 494 6272 12 |
| Total | 0.00 CAD |